Impairment of cAMP Response Element Binding Protein (CREB) signaling in Alzheimer's disease: Implication for neurodegeneration

BY

YANG HE

A Thesis

Submitted to the Faculty of Graduate Studies

in partial fulfillment of the requirements

for the degree of

MASTER OF SCIENCE

Department of Biochemistry and Medical Genetics

Faculty of Medicine

University of Manitoba

Winnipeg, Manitoba, Canada

THE UNIVERSITY OF MANITOBA

FACULTY OF GRADUATE STUDIES

*****

COPYRIGHT PERMISSION

Impairment of cAMP Response Element Binding Protein (CREB) signaling in Alzheimer's disease: Implication for neurodegeneration

BY

Yang He

A Thesis/Practicum submitted to the Faculty of Graduate Studies of The University of Manitoba in partial fulfillment of the requirement of the degree

OF

MASTER OF SCIENCE

ABSTRACT

Alzheimer's disease (AD) is characterized by cognitive dysfunction and neuronal loss, believed to be due to excess amyloid-β peptide (Aβ). The prevailing hypothesis is that Aβ reduces cAMP response element binding protein (CREB) phosphorylation and impairs its signaling, leading to synaptic dysfunction and neuronal degeneration. However, this hypothesis has not been examined in AD. Here, we report that there is no significant change in CREB phosphorylation status in a familial Alzheimer's mouse model (TgCRND8) and AD brain, relative to Non-Tg (C3H/C57 genetic background mouse) and Non-AD (patients who did not die of neurological diseases), respectively. Surprisingly, CREB is expressed predominantly in cytoplasm of the TgCRND8 mice and AD brain cells, in contrast to their nuclear localization in controls. Consistently, CREB-DNA binding activity and cAMP response element (CRE) dependent transcription is suppressed in primary cortical neuronal cultures from the TgCRND8 mice, indicating impairment in CREB signaling. Coimmunoprecipitation identifies a novel interaction between the carboxy-terminal fragment (CTF) of amyloid precursor protein (APP-CTF_{100}) and CREB, leading to cytosolic anchorment of CREB and inhibition of its nuclear translocation. This interaction is significantly ($P<0.05$) higher in the TgCRND8 mice and AD brain compared to controls. Although CREB overexpression results in its nuclear accumulation and reduction in Aβ-induced neurotoxicity, there is no

significant difference between this neuroprotective activity of CREB and phospho-CREBSer133. Co-expression of N-but not C-terminal deletion APP mutant and CREB, leads to a marked reduction in nuclear CREB levels and increased Aβ-induced neurotoxicity. Furthermore, it has been shown a significant increase of cell apoptosis in the TgCRND8 mice and AD brains, compared with Non-Tg mice and Non-AD brains. Apoptotic cells in TgCRND8 mice and AD brains express markedly reduced nuclear CREB levels. These new findings suggest that reduction in nuclear CREB, but not phospho-CREB levels could sensitize neurons to Aβ-toxicity, and likely contributes to neurodegeneration in AD.

TABLE OF CONTENTS

LIST OF FIGURES

LIST OF TABLES

LIST OF ABBREVIATION

AC	adenylyl cyclase
AD	Alzheimer's disease
AICD	APP intracellular domain fragment
AMPA	alpha-amino-3-hydroxy-5-methyl-4-isoxazolepropionic acid
ApoE	apolipoprotein E
APP	amyloid precursor proteins
APP-BP1	APP-binding protein 1
ATF	activating transcription factor
Aβ	amyloid-beta
BDNF	brain-derived neurotrophic factor
BTA	2-(4′-Methylaminophenyl) benzothiazole
bZip	basic leucine zipper
CaMK	calcium calmodulin-dependent protein kinase
cAMP	cyclic adenosine monophosphate
CBP	CREB-binding protein
CK-I	casein kinase I
CTF	carboxyl terminal fragment
CNS	central nervous system
CRE	cAMP response element
CREB	cAMP response element binding protein
CREM	cAMP-responsive element modulator
DAPI	4′, 6-diamidino-2-phenylindole
DIG	digoxigenin
DMSO	dimethyl sulfoxide
ECL	enhanced chemiluminescence
EMSA	electrophoretic mobility shift assay
ER	endoplasmic-reticulum
Erk	extracellular signal-regulated kinase
FAD	familial Alzheimer's disease
FBS	fetal bovine serum
GAP	GTPase activating protein
GluR1Rs,	glutamate receptor subunit homomeric AMPA receptors
GSK-3	glycogen synthase kinase 3

GST	gluthathione S-transferase
G_0	guanine 5'-triphosphate GTP binding protein
G418	gentamycin (Geneticin® antibiotic)
HAT	histone acetyl transferase
LSF	late simian virus 40 transcription factor
LTP	long-term potentiation
MAPK	mitogen-activated protein kinase
MCN	mouse cortical neurons
MEKK	MAPK kinase kinases
MSK	mitogen- and stress-activated protein kinases
NFTs	neurofibrillary tangles
NIH 3T3 cell	mouse embryonic fibroblast cell line
NMDA	N-Methyl-D-aspartate receptor
PARP	poly-A DP-ribose polymerase
PC12 cell	rat adrenal pheochromocytoma cell line
PDE	phosphodiesterase
PID	phosphotyrosine-interaction domain
PI3-K	phosphoinositol-3-kinase
PKA	protein kinase A
PKC	protein kinase C
PLC,	phospholipase C
PS	presenilin
RAGE	The receptor for advanced glycation end-products
RSK	ribosomal S6 kinases
snRNP	small nuclear ribonucleoparticle
Tip60	the histone acetyl transferase
TNF-α	tumor necrosis factor alpha
TrkB	neurotrophin tyrosine kinase receptor type 2
TUNEL	terminal deoxynucleotidyl transferase mediated UTP-end labelling
VSCC	voltage-sensitive calcium channels

1. INTRODUCTION

1.1. Alzheimer's disease (AD)

Alzheimer's disease (AD) is a progressive neurodegenerative disorder with learning and memory deficits as well as difficulties in language, behaviour and visual perception, which was first identified by German neurologist Alois Alzheimer in 1907 [1]. It has been characterized pathologically by the overproduction and accumulation of β-amyloid peptide (Aβ), neurofibrillary tangles (Figure 1), massive neurons' loss in the cerebral cortex and hippocampus. Recently granulovacuolar degeneration and Hirano bodies have been observed in the hippocampus of Alzheimer's brains.

a

(Eliminated for Copyright Reasons)

b

(Eliminated for Copyright Reasons)

Figure 1. a. Pathological and anatomical changes in AD brain, compared to normal. Brain Atrophy reveals the damage caused by AD. Certain regions of the brain-including the hippocampus and cortex-lose neurons, and the normally convoluted surface of the brain ultimately wastes away. **b.** Two hallmarks of AD, amyloid plaques and hyperphosphorylation of tau induced neurofibrillary tangles, occurs in the later stages of AD. The A β core of the plaque appears brown and is surrounded by a halo of nerve endings containing black tau filaments.

The manifestation of AD is defined by different stages: the initial mild stage, where the patient show short-term memory impairment often accompanies by symptoms of anxiety and depression; the moderate stage where symptoms appear to abate as neuropsychiatric manifestations such as visual hallucinations, false beliefs and reversal of sleep patterns; and the severe stage, where the patients become more sedentary and are no longer able to take care for themselves [2]. Additionally, two lesions in particular were described, which now define AD: dense fiber-like tangles (later termed neurofibrillary tangles) and darkly staining amyloid plaques [3].

After 76 years from Alois Alzheimer first characterized AD, Allsop *et al.* identified biochemically the major constituent of these amyloid plaques as a peptide, amyloid-β (Aβ) [3]. And another group determined that this peptide fragment originated from a precursor protein, amyloid precursor protein (APP) in 1987 [4]. The subsequent genetic studies have revealed that four different genes are involved in the pathogenesis of AD: APP itself, apolipoprotein E (ApoE), presenilin 1 (PS1) and presenilin 2 (PS2) [5, 6].

Neurofibrillary tangles, the other hallmark of AD, are composed of hyperphosphorylated tau protein which is a microtubule-associated protein that normally maintains the structural integrity and stabilization of microtubules. Hyperphosphorylated forms of tau, which is mutated in AD brains, do not bind to

microtubules and loose the structural function, resulting in neuronal microtubule disruption [6]. The hyperphosphorylated tau proteins wound around each other to form neurofibrillary tangles (NFTs), which disorganize microtubules. This would lead to blockage of axonal and dendrite transport of micronutrients which are dependent on microtubules [7, 8, 9, 10, 11], such as the anterograde transport of mitochondria and synaptic vesicles from the neuronal cell bodies to the synaptic endings and the retrograde transport of neurotrophic signals in a reversed way, resulting in synaptic degeneration and neuronal cell death progressively.

Interestingly, when APP transgenic mice were crossed with mutant tau transgenic mice, the offspring developed the significantly increased neurofibrillary tangles [12]. Another *in vitro* study has shown that Aβ induced phosphorylation of tau in rat primary septal cultures [13]. All these evidences have indicated that Aβ has become the central focus to investigate the pathogenesis of AD. Therefore, APP, from which Aβ is generated, has been widely accepted as a critical feature of the neurodegenerative changes in AD.

Because of a major therapeutic target of Aβ, many efforts are underway to either reduce the production of Aβ or enhance its clearance by using both active and passive Aβ immunization [14]. Regulation of APP processing has also become a potential targets for AD treatment through inhibition of β-secretase or activation of

α-secretase [15]. Antioxidants (such as vitamins C and E), estrogens and non-steroidal anti-inflammatory drugs are suggested to possess beneficial effects in AD patients [15].

1.2. Amyloid precursor protein (APP)

APP is a type I transmembrane glycoprotein, including a large extracellular/intraluminal domain and a small cytosolic domain [4]. Its gene is localized to chromosome 21 (21q21.2-3) and is expressed ubiquitously in almost all tissues and cell types, including endothelia, glia and neurons of the brain [16]. At least three major APP isoforms (APP695, APP751 and APP770) arise from the alternative splicing of its pre-mRNA (Figure 2) [17]. APP751 and APP770 are present in both neuronal and non-neuronal cells, but APP695 is expressed in high levels only in brain [18]. Some fragments (APP intracellular domain fragment (AICD) and C31) are generated by the extensively post-translational glycosylation and specific proteolytic cleavage. APP and its fragments have been shown to participate widely in adhesion, neurotrophic and neuroproliferative activity, intercellular communication, neurodegeneration and membrane-to-nucleus signaling [19, 20].

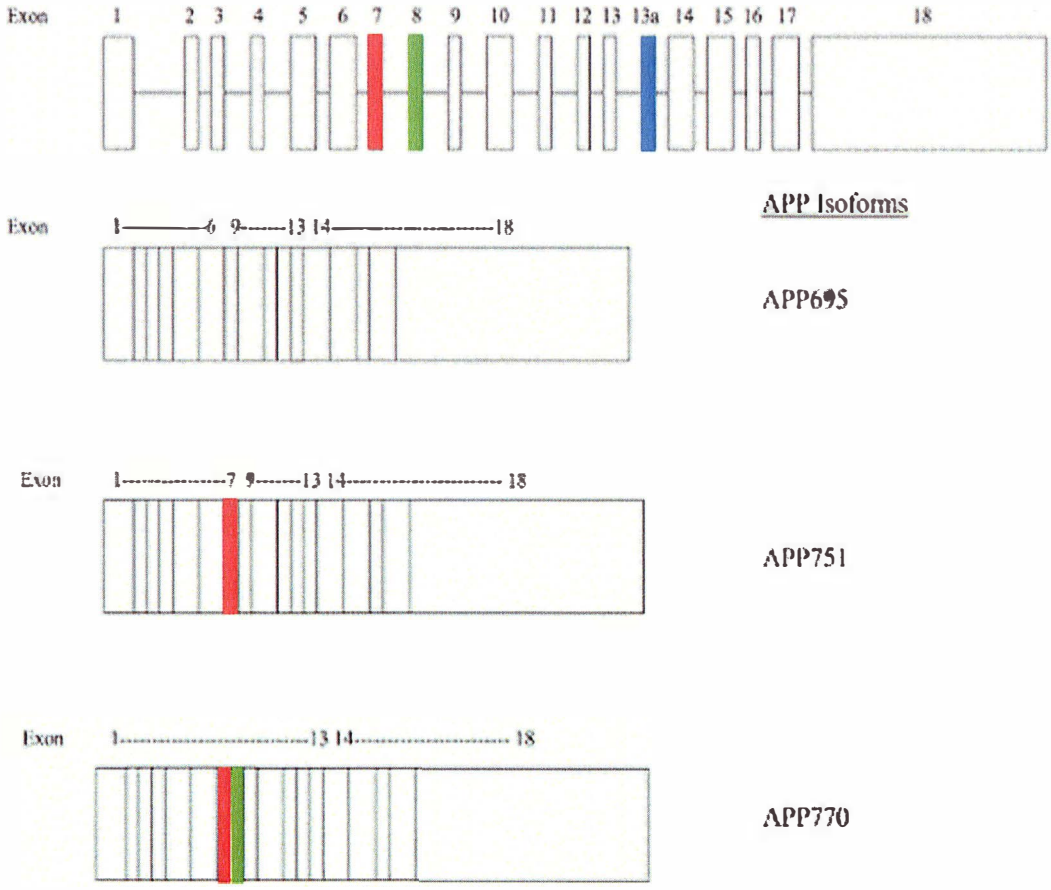

Figure 2. Schematic representation of the APP gene and its three major isoforms. The human APP gene contains 19 exons. Multiple isoforms exist generated by alternative splicing of APP pre-mRNA. The predominant transcripts are APP695 (exons 1-6, 9–18), APP751 (exons 1–7, 9–18), and APP770 (exons 1-18). APP695 is the predominant form in neuronal tissue, whereas APP751 is the predominant variant elsewhere. APP751 and APP770, but not APP695, contain exon 7 which encodes a serine protease inhibitor (KPI, Kunitz proteinase inhibitor) [17].

1.2.1. Aβ generation from APP and their roles in neurodegeneration of AD

The Aβ accumulation and $A\beta_{42}$ itself have been characterized to lead to subsequent events, such as an inflammatory response, neuritic injury, formation of fibrillary tangles and ultimately neuronal dysfunction in the pathogenesis of AD. Aβ peptide fragments, such as $A\beta_{40}$, $A\beta_{41}$, $A\beta_{42}$, and various C-terminal fragments are the resulting products from APP proteolytic processes [21]. There are three cleavage sites on APP, which are recognized by three different proteases: α-secretase, β-secretase (BACE) and γ-secretase (Figure 3). BACE aberrantly cleaves APP to release a APP NH_2-terminal fragment (sAPPβ) and leave a carboxy-terminal fragment CTF (C99/100) remaining membrane-bound, which exists in both normal condition and AD. Subsequently, the γ-secretase cleaves the remained C99/100, predominantly generating $A\beta_{40}/A\beta_{42}$ and CT59/CT57 (AICD: APP intracellular domain fragment), sometimes $A\beta_{41}$ and $A\beta_{43}$. However, in the conventional APP secretary process, the α-secretase, instead of β-secretase, cleaves APP within the Aβ region first in most of conditions, which produces an extracellular fragment and a remaining CTF (C83). C83 is processed by the γ-secretase to release a shortened fragment p3 and the same AICD [22]. Furthermore, the mutations near β- and γ-cleavage sites on APP in AD will increase the

production of Aβ fragments [23, 24, 25]. These Aβ fragments ($A\beta_{40}$ and mostly $A\beta_{42}$) pathologically accumulate and aggregate into dense plaques, usually containing degenerating axons and dendrites of neurons as well as microglial and astrocytes [26].

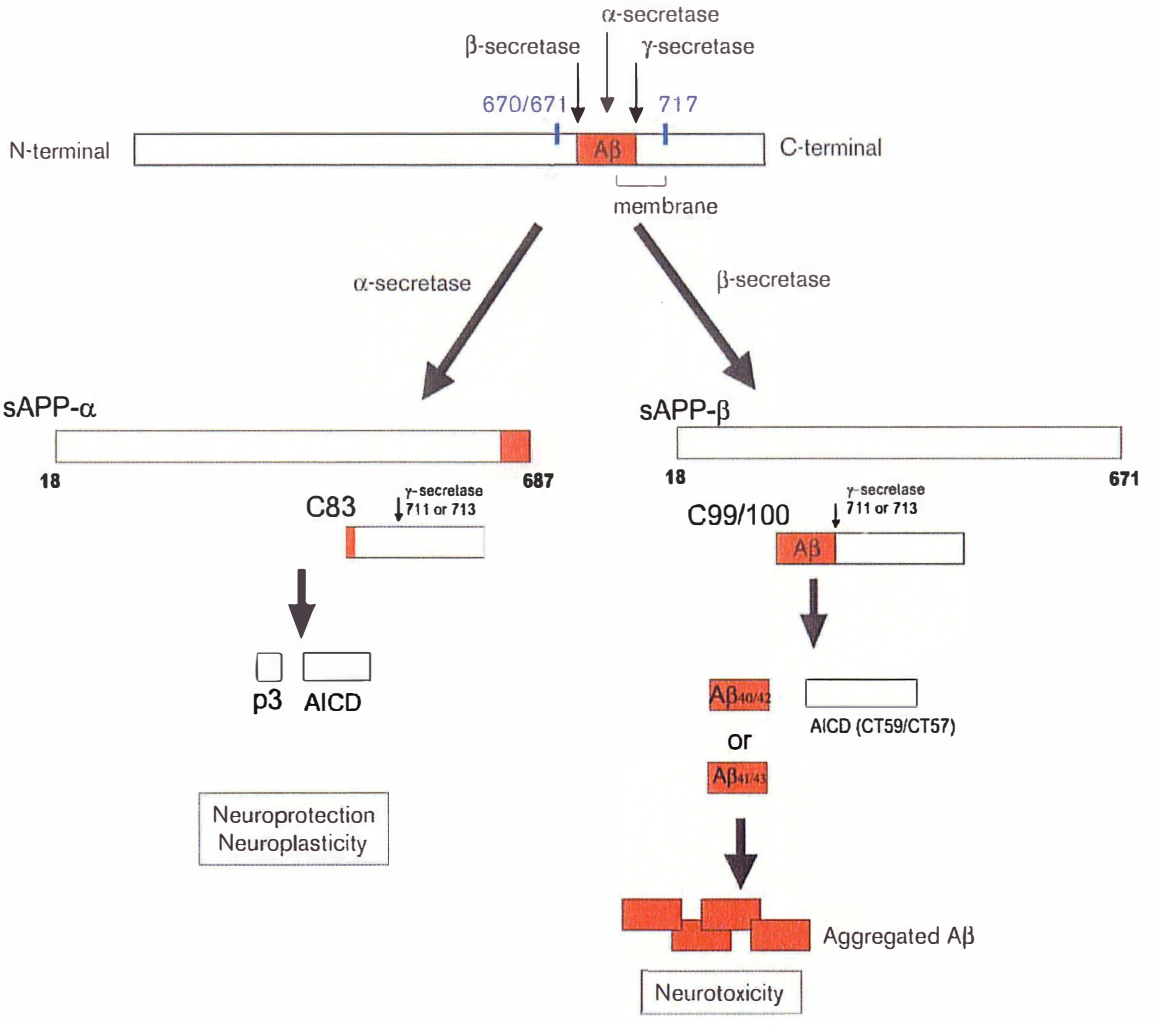

Figure 3. Cleavage sites on APP. The location of familial Alzheimer's disease (AD) mutations (highlighted in blue) is indicated. These sites are recognized by α-secretase, secretase (BACE), and γ-secretase. BACE aberrantly cleaves APP to release a APP NH_2-terminal fragment (sAPPβ) and leave a carboxy-terminal fragment CTF (C99/100) remaining membrane-bound, which exists in both normal condition and AD. Subsequently, the γ-secretase cleaves the remained C99/100, predominantly generating $Aβ_{40}$/$Aβ_{42}$ and CT59/CT57 (AICD: APP intracellular domain fragment), sometimes $Aβ_{41}$ and $Aβ_{43}$. However, α-secretase cleavage breaks the Aβ production. The soluble extracellular domains of APP may serve a neuroprotective role or facilitate processes of synaptic plasticity. Aβs undergo aggregation over time to form protofibrils and eventually larger plaque aggregates [27].

.

The central role of amyloid β peptides in AD is supported by the finding that Aβ can cause neuronal toxicity in vitro and in vivo [28, 29, 30]. The mechanisms of Aβ neurotoxicity are unclear, but Aβ has been demonstrated to induce oxidative stress and elevate the concentration of intracellular Ca^{2+} [30, 31, 32]. The increased concentration of Ca^{2+} might activate calpain proteases which activate the tau protein kinase (Cdk5), resulting in formation of neurofibrillary tangles and finally cell death. Furthermore, several pathways of neuronal apoptosis induced by Aβ have been investigated. Aβ may interact with neuronal receptors, such as the receptor for advanced glycation endproducts (RAGE), which can mediate the formation of free radicals [32], and the p75 neurotrophin receptor, which can induce neuronal cell death [33]. When interacting with Aβ, these neuronal cell-surface receptors can activate caspases like caspase-2 and caspase-12 which may be involved in apoptosis of neuronal cells [34, 35]. Additionally, Aβ induces activation of microglial cells in AD brains [36]. This is a prominent feature of inflammatory response in the brains leading to neuronal cell death. The activated microglial cells would secrete TNF-α and other pro-inflammatory cytokines [37] that induce neuronal apoptosis through the generation of reactive oxygen species in cells [38]. Thus abnormal neuronal degeneration is a consequence of Aβ toxicity involving microglial activation, oxidative stress, and hyperphosphorylation of tau.

In addition, AICD fragments generated along with Aβ have been believed to contribute to the neurodegenerative process. Some evidences showed that AICD ccould interact with FE65, LSF and the histone acetyl transferase Tip60 to activate some gene transcription, which may be able to trigger the cell apoptotic process [39]. Taken together, fragments produced from APP and APP itself plays important roles in neurodegeneration of AD, in association with other proteins.

1.2.2. APP functions as a cell membrane protein

1.2.2.1. APP in cell adhesion and mobility

Various studies have explored the roles of APP in cell adhesion and motility [40, 41, 42, 43]. Some domains in the extracellular portion of APP have been observed to bind some matrix proteins including heparin, collagen and laminin [44, 45, 46], as well as some cell adhesion molecules including β-1-integrin and telencephalin [47, 48]. These evidences have suggested a potential role of APP in cell adhesion and mobility.

1.2.2.2. APP as a signaling receptor

Although very little is known about the APP functions as a signaling receptor and the ligands binding to its extracellular domain, the cloning and characterization studies have revealed the APP features in signaling transduction. In 1995, it was found that full-length APP could function as a typical cell surface G-protein-coupled receptor by using reconstituted vesicles [49]. But this APP situation *in vivo* is more complicated and has not been clearly elucidated. Some other studies have shown an interesting process, which at least demonstrated that APP itself has the ability to modulate its processing by receiving extracellular signaling. In this self-modulating process, the secreted Aβ fragments interact with the full-length APP, forming a proteins complex, in cortical neurons [50]. Further investigations found that APP bound to a variety of fibrillar peptides containing Aβs, which induce lipid peroxidation and subsequent neuronal cell death via the alteration of Cu^{2+} reduction and the generation of toxic free radicals, OH^{-} from Cu^{+}. This extracellular $A\beta_{42}$ interaction with APP leads to the alteration of APP proteolysis resulting in more Aβ aggregation and accumulation [51]. These evidences suggested that both APP and Aβ fragments play a role in signaling transduction as a cell-membrane receptor.

1.2.3. APP interaction with other proteins

Many investigations have revealed a complex network of APP interacting proteins through the short C-terminal domain of APP. In particular, a YENPTY motif, lying between a.a. 682 and 687 (in APP 695 numbering), has been identified, which interacts with several adaptor proteins [21, 52]. By associating with different proteins, this APP proteins complex is involved in various cell biological processes, such as neuronal proliferation and differentiation, intracellular trafficking, protein degradation and cell survival and apoptosis.

1.2.3.1. Fe65, LSF/CP2 and Mena

Fe65, a brain-specific snRNP (small nuclear ribonucleoparticle)-associated protein [53], is characterized as an adaptor protein in several regions of the mammalian nervous system [54, 55]. Fe65 is expressed at high levels in neurons. In adult mouse brain Fe65 is highly expressed in neurons in the hippocampus, cerebellum, thalamus, and midbrain, with some expression in a subset of astrocytes in the hippocampus [56]. Three domains have been identified to participate in protein-protein interaction: a WW domain (two tryptophan (W) residues are one of the prominent features of this sequence

motif) and two phosphotyrosine interaction/phosphotyrosine binding domains (PID1 and PID2) (Figure 4) [57].

The most C-terminal of PID domains (PID2) is required to bind APP, and the other (PID1) binds to a late simian virus 40 transcription factor /α-globin CCAAT-binding protein (LSF/CP2) [58, 59]. It has been suggested that LSF/CP2 may have a protective function against the risk of AD [60]. It has been shown that Fe65 can interact with C-terminal fragments of amyloid precursor protein (APP-CT) and LSF/CP2 to form a ternary complex in nuclear fraction of neuronal cells, which upregulates the transcription of GSK-3β, followed by increased phosphorylation of tau and reduced β-catenin level, subsequently inducing neuronal degeneration [61]. In addition, FE65 has been shown to interact with APP intracellular tail (C-terminal domain) in Alzheimer mouse model (TgCRND8) and Alzheimer brain samples by our unpublished studies. These suggest that Fe65 plays a role through associating with fragments of APP to block the activation of LSF/CP2 in neuronal survival. It may be also a novel pathway to regulate the LSF/CP2 in contributing to neuronal degeneration of Alzheimer's disease.

In addition, the WW domain in FE65 is shown to bind to Mena, the mammalian homologue of the Drosophila Enabled protein, which is found in

actin remodelling, such as lammellipodia, and the tips of axonal growth cone flipodia [62]. Mena, in turn, binds to profilin and enhances actin filament formation, which bridges APP to the cell cytoskeleton. As well, it has been reported that overexpression of both APP and FE65 can increase cell motility *in vitro* [43]. Taken together, these results suggest that APP interaction with Mena via FE65 is involved in cell adhesion, cytoskeleton dynamics and axon guidance [63].

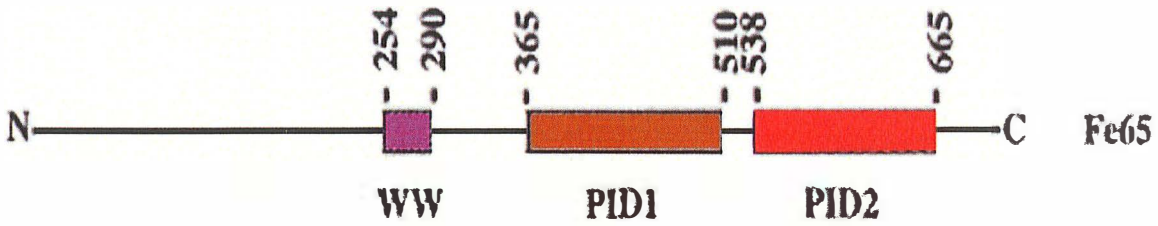

Figure 4. Schematic representation of the domains of Fe65. Three domains are indicated. The WW domain is shown to bind to Mena, the mammalian homologue of the Drosophila Enabled protein. The PID1 domain binds to LSF/CP2 and the PID2 domain is required to interact with C-terminal of APP [57].

1.2.3.2. Some other binding partners

There are lots of proteins binding to APP cytoplasmic domain (Figure 5), not only associating with the YENPTY motif but other parts of the APP C-terminal domain. The GTP-binding protein G_0 has been identified to bind the His657-Lys676 sequence in the APP cytoplasmic tail [64]. G_0 protein was found in neuronal cells involved in propagating signals for cell adhesion [65], neurite ourgrowth [66] and locomotion [67]. APP signaling through G_0 has been investigated physiologically in AD. FAD mutation in APP activates G_0 via the $G_{\beta\gamma}$ subunit dissociated from the trimeric G-protein complex after ligands binding to G-protein-coupled receptor [49, 68, 69, 70]. The activated G_0 by FAD mutant APP may suppress the cAMP response element (CRE) to induce cell apoptosis [68, 71].

Another protein, named PAT1 (protein interacting with the APP tail 1) which is a microtubule-interacting protein, recognizes a specific a.a. site, Tyr653, in the APP cytoplasmic domain [72]. The APP interaction with PAT1 provides a potential link to microtubules, which may mediate the translocation of APP along microtubules toward the cell surface. However, the precise functions of PAT1 remain undefined. An APP-BP1 (APP-binding protein 1) has also been suggested to bind to the APP cytoplasmic domain by screening a cDNA

expression library with the APP C-terminus, but the exact binding site and the functions have not been identified [73].

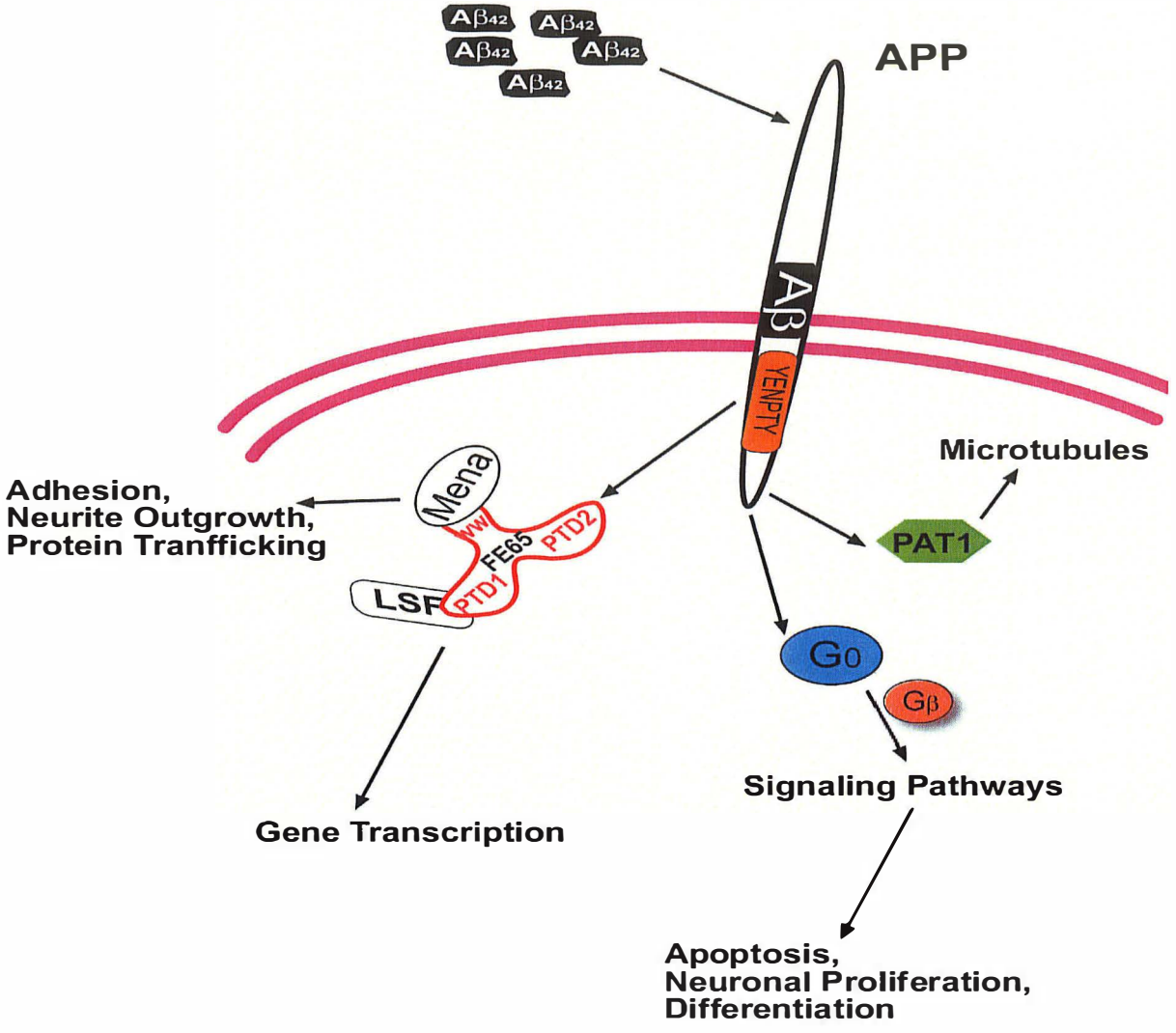

Figure 5. The reprentation of APP interationwith ither prioteins through the intracellular domain. APP interacts with Aβs through extracellular domain, and other proteins, such as FE65, G_0 protein and PAT1, through the intracellular tail. FE65 interacts Mena to regulate cell adhesion, neurite outgrowth and protein tranfficking. FE65 interaction with LSF and AICD could mediate transcription of some genes. APP interaction with G_0 protein stimulates signaling pathways which are involved in cell apoptosis, neuronal proliferation and differentiation. PAT1 is another protein binding to APP intracellular tail and bridging APP to microtubules, which may mediate the translocation of APP along microtubules toward the cell surface.

1.3. cAMP response element binding protein (CREB)

1.3.1. The family of cAMP response element binding protein

CREB is a member of a large family (CREB/ATF) of structurally related transcription factors which bind to the same promoter cAMP responsive element (CRE) consisting of the palindromic consensus sequence TGACGTCA. More than 10 additional members of this family have been identified since CREB was firstly named in 1987 [74], and they show many structural and functional variations in a broad range of tissues and cell types [75, 76]. Most of them have conserved a similar basic leucine zipper (bZip) DNA binding domain (Figure 6 [77]). Based on the similarity of their amino acid, members in the CREB family can be divided into subgroups: CREB/CREM, CRE-BP1 (ATF2), ATF3, ATF4, ATF6 and B-ATF subgroups (Table-1; reviewed in [78]). As well, these members share structural features within their transactivation domains which consist of two regions. The first region, called phosphorylation box (P-box), contains several protein kinases recognition motifs, such as GSK3, PKA, PKC, CaMK, CK-I, etc (Figure 6). The leucine zipper consists of an α-helical coiled-coil structure which is required for homo- and hetero-dimerization. The basic region is responsible for the sequence-specific DNA-binding of CREB to CRE. The activation of

CREB family members can be regulated through phosphorylation by particular kinases in this P-box region. The other region consists of two glutamine-rich motifs, Q1 and Q2, which exist in CREB and CREM [79]. ATF-1 only contains Q1 but not Q2 [80]. This glutamine-rich region is required to interact with other transcription factors or co-activators, which are necessary for CREB transcriptional activity. It has also been suggested that the P-box and at least one of glutamine-rich domains are essential for CREB and CREM transcriptionaql activity [79, 81].

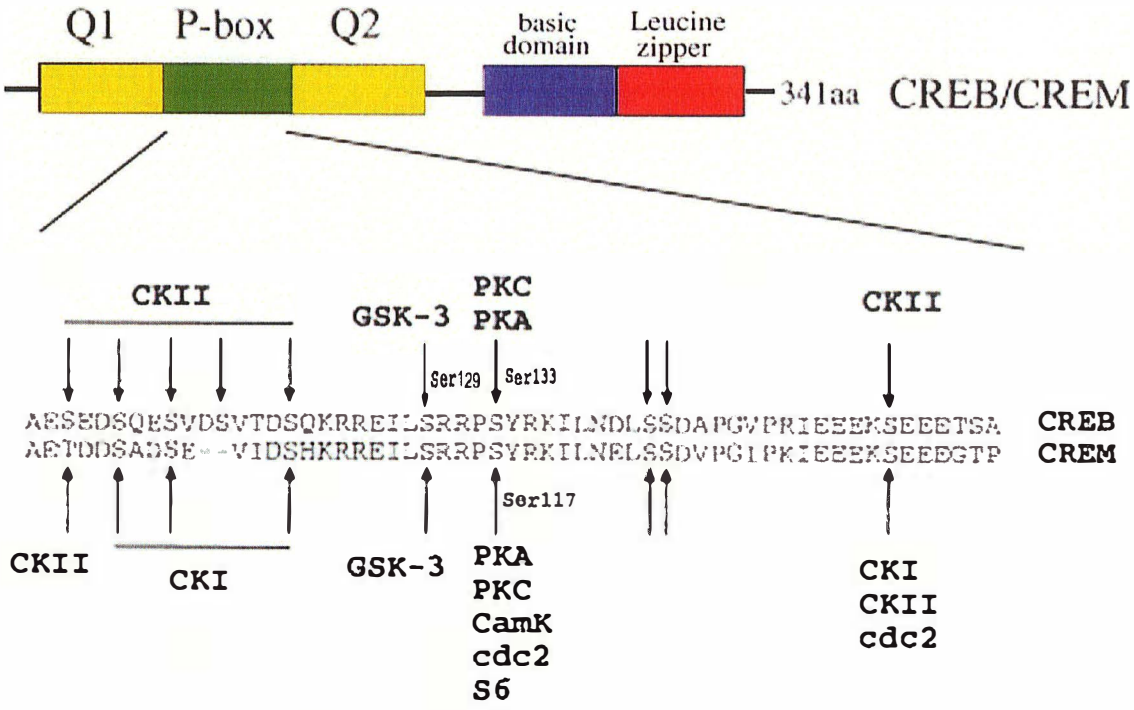

Figure 6. Structures of ATF, CREB and CREM proteins. The bottom panel indicates serine and threonine residues which can be phosphorylated by different kinases (arrows). The P-box, the glutamine-rich domain (Q1 and Q2) and the DNA binding region (leucine zipper and basic domain) are indicated.

Table 1. The mammalian ATF/CREB family of transcription factors (Adapted from [78]).

(Eliminated for Copyright Reasons)

1.3.2. Regulation of CREB activity

1.3.2.1. Activation and repression of CREB

CREB, expressed in all cell types as a transcription factor, performs its function in regulations of gene expression in response of extracellular stimuli. External stimuli initiate numerous intracellular signaling cascades (described in 1.3.2.2.) by interacting with cell membrane receptors. Subsequently, CREB is triggered to mediate its target gene transcription. In this process, some essential events are involved in regulating CRE-dependent gene transcription, including CREB binding at DNA response elements, dimerization, phosphorylation/dephosphorylation and association with other transcription co-factors [82].

In general, two CREB molecules firstly form an inactive dimer which binds to the CRE site under basal conditions. The stimulated intracellular signaling cascades cause the phosphorylation of both molecules of the CREB dimer, followed by recruiting some associated proteins, CREB-binding protein (CBP) and p300, and assembling a large transcription complex. This complex promotes chromatin remodelling via histone acetylation by histone acetyl transferase (HAT), which alters the conformation of the nearby chromatin and

enables the RNA synthesis by RNA polymerase II (Figure 7, [82]). However, the first step has been questioned in this traditional processes, whether the CREB dimer binding to the CRE site provokes the phosphorylation, or sometimes the phosphorylation initiates the interaction and DNA binding [83].

There are numerous phosphorylation sites on the CREB protein, which regulate CREB performance differently. And various kinases are able to phosphorylate CREB at different sites. For instance, PKA, Ca2+/calmodulin-dependent kinase (CaMK) IV and MAPK-activated ribosomal S6 kinases (RSKs) individually phosphorylate CREB at serine 133, which is necessary for CREB transcriptional activity [84]. Although it is generally accepted that the Ser133 phosphorylation of CREB is necessary,

(Eliminated for Copyright Reasons)

Figure 7. CREB transcription complex binding on the target gene. The transcription complex contains phosphorylated CREB dimer, CREB-binding protein (CBP) and p300. Consequently, the chromosome remodelling by a histone acetyl transferase (HAT) promotes the RNA synthesis through RNA polymerase II.

more and more studies have proposed that it is not always sufficient for activation of CREB. It has been suggested that some events in addition to CREB Ser133 phosphorylation are required for the CREB transcription activity [85]. CaMKII is able to phosphorylate CREB at serine 142 to dissociate the CREB dimer and reduce CREB-mediated gene transcription [86, 87]. GSK-3α/β is able to phosphorylate CREB at serine 129 following the phosphorylation at serine 133, and it remains undefined whether this further phosphorylation at 129 activates or represses the CREB transcription activity.

On the other hand, CREB can be regulated through dephosphorylation by several protein phosphatases. The serine-threonine protein phosphatase 1 (PP1) and 2A (PP2A) have been found in directly removing the Ser133 phosphate added by PKA [88, 89, 90]. Some *in vitro* studis has shown that PP1 and PP2A also dephosphorylate Ser98 of CREB by CaMKIV [90]. Additionally, some phosphatases have been found to indirectly affect the phosphorylation of CREB via inhibition of kinases. For example, calcineurin (also known as PP2B) has been suggested to play an indirect role in CREB dephosphorylation in rat hippocampal neurons through potentiating the activity of PP1 [91]. Another example is the tumor suppressor PTEN, which diminishes phosphorylation of CREB by inhibiting the activation of Akt/PKB [92]. However, what is the significance of dephosphorylation of CREB remains

poorly understood. Whether or not the dephosphorylation of CREB positively or negatively regulates its activity still remains unclear.

1.3.2.2. Phosphorylation of CREB via various signaling pathways

There are more than 300 different stimuli described in the literature that can provoke the phosphorylation at Ser133 on CREB through numerous intracellular signaling pathways (Figure 8, [82]). The cAMP-dependent PKA signaling pathway was firstly identified to phosphorylate CREB by *in vitro* studies in 1987 [74]. G-protein coupled receptors are activated by some external stimuli like neurotransmitters, followed by stimulation of adenylyl cyclase (AC). AC causes the accumulation of cAMP and the release of catalytic subunits of cAMP-dependent PKA, which subsequently phosphorylate CREB at Ser133. Additionally, GSK-3α/β is also a downstream target activated by PKA. The activated GSK-3 has been revealed to phosphorylate CREB at Ser129 following the PKA-dependent phosphorylation at Ser133 [93]. Presently there are two conversed views about whether the further phosphorylation at Ser129 increases the CREB transcription activity or negatively regulates its function. Substitution of serine 129 by alanine strongly impaired forskolin-induces CREB-dependent transcription in neuronal PC12 cell, but not in NIH 3T3 cell [93, 94]. And

what this dual-phosphorylation contributes to the CREB activities *in vivo* remains unclear.

Since the crucial role of CREB in most biological processes, various signaling pathways have been characterized to play roles in regulating CREB by phosphorylation. Ras/Erk and p38/MAPK signaling pathways have been reported to phosphorylate CREB. In response to some neuron growth factors like neurotrophins, the MAPK pathways are triggered and the members of RSK and MSK families are activated by MAPK to ultimately phosphorylate CREB at Ser133 (Figure 8) [95, 96]. The PI3-kinase/Akt pathway has also been documented to activate CREB under some circumstances. Recent studies in neurons have implicated the PI3-kinase/Akt pathway as a regulator in CREB phosphorylation and activation [97, 98]. However, whether Akt directly phosphorylates CREB remains undefined. Although some of kinases have not been precisely identified to directly phosphorylate CREB, these studies have indicated that various intracellular signaling pathways contribute to CREB phosphorylation leading to the regulation of its activity.

(Eliminated for Copyright Reasons)

Figure 8. General signaling pathways focusing on CREB. Various signaling pathways are provoked by cell membrane receptors (TrkB, AMPA receptors, NMDA receptors and G-protein-coupled receptors) in response to extracellular stimuli. CREBs are activated by phosphorylation via the pathways depicted in the figure, MAPK/RSK, CaM/CaMKIV and PKA signaling cascades. In contrast, CaMKII induces the dephosphorylation of CREB. Gi-linked receptor might reduce CREB phosphorylation via inhibition of adenylyl cyclase, but in some cell types it has been observed to promote CREB phosphorylation via MAPK pathways. Abbreviations not defined before: CaM, calmodulin; GluR1Rs, glutamate receptor subunit GluR1 homomeric AMPA receptors; PDE, phosphodiesterase; PLC, phospholipase C; TrkB, neurotrophin tyrosine kinase receptor type 2.

1.3.2.3. Ca^{2+} regulation on CREB

Ca^{2+} level has been demonstrated to be an important contributor to CREB activities as well. Early work has found that CREB can be activated by Ca^{2+} [99, 100, 101]. Subsequent studies have revealed that Ca^{2+} interacts with a large number of intracellular molecules and initiate many signaling pathways to mediate CREB functions. For example, in neurons, Ca^{2+} influx appears through voltage-sensitive calcium channels (VSCC), L-type Ca^{2+} channels, because of the membrane depolarization or through glutamate-activated NMDA receptors. Intracellular Ca^{2+} interacts with Ca^{2+} binding protein calmodulin (CaM), which activates CaMK-I, CaMK-II and CaMK-IV. CaMK-II and CaMK-IV can phosphorylate CREB *in vitro* and *in vivo* [100, 102, 103, 104, 105, 106, 107]. This CaMK-IV dependent CREB activation is necessary for long-term synaptic plasticity in the hippocampus [108, 109]. Additionally, Ca^{2+} can also activate the additional pathways, like the Ras/Erk pathway which signals to an independent set of CREB kinases [110, 111, 112].

1.3.3. CREB functions

As extensively demonstrated by the literature, CREB performs functions in the cellular processes in response to physiological stimuli, such as cell

proliferation, differentiation, cell survival and death. In the following sections, I will focus on its functions involved in memory loss and neuronal apoptosis relevant to Alzheimer's disease.

1.3.3.1. CREB in learning, memory and plasticity

A large amount of studies explore the importance of CREB in central nervous system (CNS) functions, especially in memory, by using different animal models, such as the mollusc *Aplysia*, the fruitfly *Drosphila melanogaster*, and the mouse. In these species, disruption of CREB functions in neurons by dominant-negative mutation or deletion of key CREB isoforms has been shown to block the long-term memory [113], and up-regulation of CREB-dependent transcription significantly enhances long term potentiation (LTP) which is a cellular model for memory formation [114, 115, 116].

LTP has been extensively studied as a candidate memory mechanism, which reflects the synaptic efficacy of the long-lasting enhancements with high frequency stimulation. Various studies have revealed that LTP is important in memory formation [117, 118]. Upon stimulation, post-synaptic receptors, such as N-methy-D-asparatate (NMDA) receptors, are activated and leads to Ca^{2+} influx. The Ca^{2+} influx activates several protein kinases, consequently

inducing two different types of LTP, i) an early and short lasting LTP (E-LTP, between 1-2hr); ii) a late but longer lasting cAMP-dependent LTP (L-LTP, >7hr). Both the E-LTP and L-LTP are considered analogous to the processes of memory consolidation [113].

The critical studies have been performed in the transgenic mice (CREB-αΔ knockout), lacking the two predominant CREB isoforms α and Δ, as a model to assess the importance of CREB in learning and memory [119]. In these knockout mice, studies have demonstrated that there are learning and long-term memory deficits in the following learning and memory performances: contextual fear conditioning, the Morris water maze and the social transmission of food preferences [120, 121]. These results support the view that CREB is important in the acquisition of learning and memory. Considering the important involvement of cAMP-PKA pathway and its capacity to activate CREB, CREB-dependent gene transcription could be affected by alteration of the cAMP-PKA pathway and CREB phosphorylation. Consistent with this hypothesis, it has been shown that the phosphorylation of CREB and CRE-reporter gene expression are increased in cortical neurons during development plasticity [122] and in hippocampal neurons [111, 123, 124, 125, 126]. Another related study has found that the intra-hippocampal infusion of CREB antisense oligoes produces deficits in spatial learning in rats

[127]. Collectively, these findings suggest that CREB and CREB-dependent gene transcription play a crucial role in the long-term memory. However, the precise mechanisms about how CREB facilitates memory and how the regulation of CREB transcription activity contributes to the long-term memory need to be further investigated.

1.3.3.2. CREB in neuronal survival and neurodegeneration: implication for AD

Memory deficit is the best identified manifestation of AD, and pathologically extensive neuronal loss is believed to contribute to the memory disorder. CRE-dependent gene expression has been indicated to be necessary for multiple neuronal subtypes' survival as a protective response against cell death stress [128, 129, 130]. In fact, some studies have revealed that induced CREB phosphorylation via activation of CaMK-IV acts as a neuroprotective response to glutamate excitotoxicity *in vitro* and by ischemia stress *in vivo* [131]. It has been shown that disruption of CREB function specifically induces neuronal apoptosis [132]. Another group has found that CREB overexpression inhibits hippocampal neuronal apoptosis induced by staurosporine, glutamate excitotoxicity and ischemia stress *in vitro* [133]. CREB also exerts the activation of the Bcl-2 promoter via the CRE, producing a protective effect in response to hypoxia stress in PC12 neuronal cells [134].

These evidences implicate that the alteration of CREB activation would compromise CREB anti-apoptotic neuronal function through disruption of downstream gene expressions and the CREB-regulated pathway may play a protective role in neurodegeneration of AD.

More recently, it has been reported that $A\beta_{42}$ at sublethal concentrations that do not induce cell death in primary cortical neuronal cell, can nevertheless suppress CREB activity and the activation of the CRE-containing brain-derived neurotrophic factor (BDNF) [135]. Furthermore, the inhibition of Aβ-induced apoptosis in cultured neurons is associated with increased CREB phosphorylation through MAPK and PI3-kinase signaling pathways [136], indicating that Aβ-induced apoptosis results in impairment of CREB activation. In the other hand, depending on the different concentration, Aβ can induce CREB phosphorylation and provoke different response on CRE-directed transcription [137, 138].

In additional, APP, another key protein in AD, negatively influences CREB activity and CREB-dependent gene expression. Familial Alzheimer's mutants of APP suppress the transcriptional activity of CREB by a G_0-dependent mechanism, but the wild type APP has no effect on CREB [71]. Considering of the essential role of CREB in the long-term memory formation, it is

implicated that the CREB deficiency potentially contributes to memory loss in AD. As discussed above, it has been generally suggested that Aβ alters CREB phosphorylation, contributing to neuronal degeneration in AD. However, very few *in vivo* studies provide direct evidences to prove that whether CREB expression and phosphorylation are altered in AD, whether those alterations are directly due to the effects of Aβ fragments and whether altered CREB phosphorylation contributes to neuronal apoptosis in AD.

1.3.4. CREB responsive target genes

It is believed that CREB family members, as transcription factors, perform their functions through regulating their target gene expression. Over 100 putative CREB-dependent genes have been identified, which function in neurotransmission, cell structure, signal transduction, transcription, and metabolism. All CREB target genes share one or more conserved sequences (CRE) in their promoter regions, which response to CREB-mediated regulation.

CREB-dependent genes have been shown to involve in different biological processes. Among them, *c-fos* is an important immediate-early gene in response to a wide variety of stimuli [139]. It has been found that c-fos

transcription peaks within minutes of stimulation, but invariably returns to baseline after 1hr [140]. And some stimuli which activate CREB induce the c-fos expression in a CRE-dependent manner [141, 142, 143, 144]. Upon synaptic stimulation, the expression of brain-derived neurotrophic factor (BDNF), another CREB target gene, requires the CREB activation, which is induced specifically in hippocampal neurons but not in some other types of neurons [145, 146]. The expression of the anti-apoptotic Bcl-2 gene is up-regulated in neuronal cells as a protective response to hypoxia. A CRE site locates in the Bcl-2 promoter and the phosphorylation of CREB has been induced rapidly by hypoxia, indicating the importance of CREB in the induction of Bcl-2 expression against the damage stimulus [134]. Thus, the decreased Bcl-2 expression in AD may be due to the impaired CREB activity by APPs or Aβ. To this end, we have analyzed the link between the altered CREB signaling and the decreased Bcl-2 expression in the transgenic AD mouse model (TgCRND8).

1.4. Caspases in AD

The apoptotic cell death is observed extensively in Alzheimer brain. Caspases activation, a critical step in apoptosis, has been reported to lead to the proteolytic cleavage of several neuronal proteins in either AD brain or AD

mice models. One of key protein in AD, $A\beta_{42}$, has been shown to trigger the activation of caspase-3 [147, 148, 149]. The activated caspase-3 subsequently cleave tau protein, the main component of neurofibrillary tangles (another hallmarks of AD), resulting in accelerating tau aggregation *in vitro* [150, 151, 152, 153, 154, 155]. In addition, the pro-apoptotic caspase-cleaved tau co-localizes with both intracellular Aβ and activated caspase-3 in AD brain [151]. These evidences have suggested that caspases may provide links for both of the hallmarks in AD, ultimately leading to the neuronal death.

Furthermore, the full-length APP has been identified to be the substrate of caspases, besides its cleavage by α-, β-, γ-secretases [156, 157, 158, 159]. This caspase-cleavage produces the neurotoxic APP C-terminal fragments that favor Aβ production. The overproduced Aβ in turn leads to additional caspase-3 activation, resulting in cell death. Additionally, caspases are carried out to degrade some proteins required for survival during neuronal apoptosis, such as poly-ADP-ribose polymerase (PARP) [160] and actin-severing protein gelsolin [161], and anti-apoptotic signal transduction molecules, such as Ras-GAP, Raf-1, MEKK1, and Akt [162, 163]. An *in vitro* study has revealed that the activation of the caspase-3 cause the degradation of CREB [164], suggesting a possible CREB regulation mechanism in neuronal apoptosis.

1.5. Bcl-2 in neuronal apoptosis

Among the CREB-dependent genes, Bcl-2 has been reported to be one of well-characterized candidates involving neuronal survival and neurodegeneration. Bcl-2 (B-cell CLL/lymphoma 2) is a member of Bcl family which consists of anti-death members [Bcl-2, Bcl-X_L, and myeloid cell leukemia sequence (Mcl)-1] and pro-death members [BCL2-associated X protein (Bax), BCL2-antagonist/killer (Bak), BCL2-antagonist of cell death (Bad), BCL2-interacting killer (Bik), BCL2-related ovarian killer (Bok), and Bcl-X_S] [165]. Indeed, neurotrophic deprivation-induced apoptosis of neuronal cells is inhibited by Bcl-2 overexpression *in vitro*, and overexpressed Bcl-2 in transgenic mice increases the population of neurons in many brain regions by inhibiting naturally occurring neuronal cell death [166, 167, 168, 169, 170]. These evidences indicate that Bcl-2 may play a potential protective role against neuronal apoptosis.

Bcl-2 has been shown locating on the outer mitochondrial membrane, endoplasmic-reticulum (ER) membrane and the nuclear envelope [171]. Some possible mechanisms have been proposed on the Bcl-2 suppressing apoptosis, although the exact processes are undefined. Bcl-2 locating on mitochondria may alter mitochondrial functions and the release of mitochondrial

cytochrome c, Bcl-2 on ER membrane may control the efflux of Ca^{2+} from ER stores, and Bcl-2 may inhibit production of oxygen free-radicals [172]. Since a CRE site exists in the promoter of Bcl-2, CREB has been indicated to mediate the expression of Bcl-2 significantly in neuronal cells. These would present a view that CREB exerts its protective effect in response to death stimuli by mediating the increased Bcl-2 expression in neurons.

2. RESEARCH HYPOTHESIS AND SPECIFIC OBJECTIVES

In this study, we focused on CREB signaling and investigated the possibility that impairment in CREB signaling is due to changes in its expression, phosphorylation and transcriptional activity, resulting in neuronal apoptosis *in vivo*.

We hypothesised that impairment in CREB signaling is associated with neuronal cell death in Alzheimer's disease.

To address this hypothesis, the following specific objectives will be examined:

(I) To examine impairment of CREB signaling in AD, including expression, distribution, phosphorylation levels and CREB-dependent transcriptional activity by performing immunofluorescence staining, Westernblotting, PKA assay, electrophoretic mobility shift assay and CRE luciferase assay in a familiar Alzheimer disease mouse model (TgCRND8);

(II) To determine neurodegeneration caused by neuronal apoptosis in AD by using TUNEL and Annexin-V apoptosis tests;

(III) To examine the relationship between CREB signaling and neuronal apoptosis in AD by performing co-immunoprecipitation assay, *in vitro* GST bind assay and siRNA assays.

3. MATERIALS

3.1. Regents and chemicals

All chemicals and solvents were of reagent or analytical grade, and were obtained from one of the following sources: GE Health Care-Amersham Biosciences (Baie d'Urfe, Quebec), Bio-Rad Laboratories (Mississauga, ON), Sigma-Aldrich (Oakville, ON), VWR Canlab (Mississauga, ON) and Roche Diagnostics (Indianapolis, IN).

Neurobasal-A medium, fetal bovine serum (FBS), G418, N-2 supplement and other cell culture products were purchased from Gibco-BRL (Burlington, ON). Digoxigenin (DIG) DNA gel shift kit and *in situ* cell death detection kits were obtained from Roche Diagnostics (Indianapolis, IN). The CRE consensus wild type and mutant double stranded oligonucleotides were from Santa Cruz Biotechnology (Santa Cruz, CA) or synthesised by the DNA Synthesis Lab (University of Calgary, AB)

3.2. Transgenic and gene-targeted mouse lines

The non-transgenic and transgenic mice, TgCRND8 (65% C57BL/6J and

35% CH3 background) overexpressing a double mutant form of hAPP695Swe/Ind (KM670/671NL, Swedish mutation + V717F, Indiana mutation) under control of the prion gene promoter used in this study, have been described previously [173]. This mouse model exhibits excess $A\beta_{42}$ deposits and robust cognitive dysfunction at 3 months of age. The double transgenic mice generated from crosses of transgene heterozygotes were identified using the REDExtract-N-AMP Tissue PCR kit (Sigma), including specific hAPP695 forward and reverse primers. The use of animals in this study was in accordance with the University of Manitoba Animal Care and Ethics Committee.

3.3. Human brain cortical and hippocampal tissues

Protocols for experimental use of human brain tissues were reviewed and approved by the Institutional Review Board of the Health Sciences Center, University of Manitoba. Ten cases of sporadic AD (age range, 77-83 years) and ten age-matched/sex-matched control cases (Non-AD; age range, 77 to 86 years) were used in this study (Table 2). Sporadic AD cases were diagnosed according to the Consortium to Establish a Registry for AD (CERAD) and were scored Braak's stages V (n=4) or VI (n=6). Control cases were non-demented patients who died without any known neurological disorders.

Samples encompassing the parietal, frontal and temporal cortex, and hippocampus exhibited no significant differences in age (80.6 versus 80.3, $P<$ 0.85), postmortem interval (5.29 versus 5.92., $P<$ 0.93), control versus AD, respectively.

3.4. Primary mouse cortical neurons (MCN)

Enriched primary mouse cortical neurons (MCN) from embryonic day 16 mouse fetuses were prepared as described [174]. Briefly, cortices were dissected and freed from meninges. The cells were dissociated by trituration with a fire-polished Pasteur pipette. The cell suspension plated at 2.0 X 10^4 cells/cm^2 were cultured in poly-D-lysine in borate treated-plates and maintained in 10% fetal bovine serum optimal neurobasal medium (Invitrogen) at 37^0C overnight. The next day, the cells were maintained in serum-free optimal neurobasal medium supplemented with B27 components (Invitrogen) and 10 μM of cytosine arabinoside to inhibit proliferation of non-neuronal cells. Cultures were maintained for 10 d before treatments. Experiments were performed on neuronal cultures.

3.5. Antibodies, DAPI and BTA

The following antibodies were used for western blotting (WB) or Immunofluorescence staining (IF) or immunoprecipitation (IP). From Cell Signaling Technology (Beverly, MA): CREB (Rabbit, 1:2000, WB; 1:100, IF) and pCREB (Ser133) (Rabbit, 1:1000, WB; 1:100, IF), From Abcam: pCREB (Ser133/129) (Rabbit; 1: 1000, WB; 1:200, IF). From Sigma: APP-C terminal (Rabbit, 1:4000, WB; 1:1000 IF) and actin (20-33; 1:2000, WB). From Santa Cruz Biotechnology: Histone-1 (FL-219; 1:500) and Bcl-2 (Mouse; 1:500, WB). From Upstate Biotechnology: pGSK3 (Tyr279/Tyr216) (Mouse monoclonal; 1:1000, WB). From BD-PharMingen (San Diego, CA): Active caspase-3 (Rabbit; 1:1000, WB). From Chemicon International: MAP2-neuron specific (Rabbit; 1:200, IF). Calbiochem: $A\beta_{1-42}$ (Rabbit; 1:400, WB; 1:500, IF).

4′, 6-diamidino-2-phenylindole (DAPI; excitation is 358 nm when bound to dsDNA, emission max is 461 nm; blue fluorescence), was used for nuclear counterstaining. Briefly, 5 mg/mL stock solution was made in dimethylformamide. The DAPI stock solution was diluted to 300 μM in PBS before use. 2-(4′-Methylaminophenyl) benzothiazole (BTA-1) (Sigma) was used to counterstain Aβ deposits in brain tissues for multicolor fluorescence. BTA was dissolved in DMSO at 400 μM stock solution of BTA was made in DMSO (to yield <1% DMSO in the final assay). The stock solution was

diluted to 100 nM in PBS, pH 7.0 for future use. BTA is characterized by violet blue fluorescence using a UV filter set: excites 360-370 nm, DM400, 420 long-pass filter).

3.6. Plasmids, Promoter Constructs and siRNA

The pBcl-2 was obtained from Upstate Biotech. All siRNAs were duplexed, desalted, and protected. CRE- pTAL Luc, pTAL-Luc, pCREB and p-KCREB were from Clontech. The pBcl-2 wt and mut promoter-Luc have been described [134]. All oligonucleotides (150 nM) were transfected into cultures using HiPerFect Reagent, according to the manufacturer's instructions (Qiagen).

3.7. Equipment

The following equipment was used for the experimental methods carried out in this study. Biochrom Novaspec II spectrophotometer, Fisher Scientific Accumet Basic pH meter, Mettler Toledo AG104 balance, Eppendorf 5317C centrifuge, IEC Centra CL3R centrifuge, Beckman J2-HS centrifuge, Beckman TL-100 ultracentrifuge, Beckman LS6500 scintillation counter, E-C apparatus Corporation EC250-90 power supply, VWR Scientific 2300

incubator, Bio-Rad Mini-PROTEAN3 gel electrophoresis equipment, Bio-Rad PROTEAN II xi electrophoresis equipment, Bio-Rad Trans-Blot electrophoretic transfer apparatus, Nikon Eclipse. E600 Fluorescence microscope.

4. EXPERIMENTAL PROCEDURES

4.1. Cell culture

Human neuroblastoma SK-N-SH cells and Rat B103 cells lacking expression of endogenous APP and APP-like protein were cultured in Neurobasal-A medium containing N-2 supplement and 10% fetal bovine serum at 37°C in a 5% CO2 humidified atmosphere. After 40-50% confluence, cells were maintained, in the same condition but without FBS, to differentiate for 5days. The SK-N-SH cells or B103 cells stably transfected with neo-vector/wtAPP/mutAPP by Miss Teralee Burton (a previous Master student) were cultured in the same conditions with 50μg/ml G418. The N-2 supplement is an optimized serum substitute currently used routinely for the long-term growth and survival of primary neurons and differentiated cultures, without the need for exogenous growth factors. In some experiments, differentiated cells were exposed to appropriate concentration of $A\beta_{42}$ for 72 hrs. In this study, all experiments performed on differentiated SK-N-SH cells or B103 cells were under the above conditions, unless otherwise specified.

4.2. Aβ exposures

Solution of fribrillar amyloid-β peptides ($A\beta_{1-42\ /42-1}$; Sigma-Aldrich) was prepared as described (Lesné et al., 2005). Briefly, Aβs were dissolved in sterile deoinized water to obtain a stock solution of 2 mM, which was kept at 37 °C for 48 h and stored at 4 °C until use. The presence of fribrillar Aβ was confirmed by SDS-PAGE. Aβ induced apoptosis was performed in the presence of MK-801, non-competitive NMDA receptor antagonist (10 μM) to prevent cell death.

4.3. Assessment of cell/tissue damage and viability

Apoptosis in fixed primary cultures or paraffin- embedded brain tissues was measured using the terminal deoxynucleotidyl transferase-mediated fluorescein dUTP nick end labeling (TUNEL assay) *In Situ cell detection Kit* reagents, according to the manufacturer's procedure (Roche Molecular Biochemicals). Cells were then observed under an epifluorescence microscope/analyzed by flow cytometry (FACS analysis). Annexin V-FLUOS binding test (Roche Molecular Biochemicals) on brain tissues evaluated by fluorescence microscopy, according to the manufacturer's protocol, was also used for the detection of apoptosis. The number of TUNEL/Annexin positive cells in five random fields was counted in three separate experiments, and the results were normalized as percentage ratios to the total number of cells

stained per field. One-way analysis ANOVA and *post hoc* unpaired *t* tests with the Bonferroni multiple comparisons tests were used for data analysis.

4.4. Tissue and Cellular Protein Processing

Tissues and cells prepared for experiments were the cortices of mice/human brains, and primary cortical cells of mice. Frozen tissues or cell pellets were homogenized in ice-cold hypotonic buffer (1.5 mM $MgCl_2$, 10 mM KCl, 0.2 mM PMSF, 20 μg/mL aprotinin, 1mM leupetin, 10 mM DTT and 10 mM Hepes, ph 7.9). Homogenates were incubated for 20 min on ice and centifriged (25,000 *g*, 15 min. 4 ^{o}C). Cytoplasmic proteins were collected from the supernatant and nuclear proteins from the pellets. Briefly, pellets were washed once with the hypotonic buffer and centrifuged at 10,000 *g* for 15 min at 4 ^{o}C after which pellets were suspended in ice-cold low-salt buffer (25% v/v glycerol, 1.5 mM $MgCl_2$, 0.2 mM EDTA, 0.2 mM PMSF, 1.0 mM DTT, 20 mM KCl, 20 mM Hepes, pH 7.9). Nuclear proteins were released by adding a high-salt buffer (25% v/v glycerol, 1.5 mM $MgCl_2$, 0.2 mM EDTA, 0.2 mM PMSF, 1.0 mM DTT, 1.2 M KCl, 20 mM Hepes, pH 7.9) drop by drop at a final concentration of 0.4 M KCl, followed by sonication at 67 Hz (Sonicator, Branson 1510 model) for 2 h at 4 ^{o}C. Soluble nuclear proteins were recovered by centrifugation (25,000 *g*, for 30 min at 4 ^{o}C) and proteins

were stored at -80 ^{0}C. The concentrations of total protein, cytoplasmic, or nuclear proteins were measured using Bicinchoninic acid (BCA) Protein Assay Reagent Kit (Pierce)

4.5. Western blotting Analysis and Co-immunoprecipitation assay

To examine protein expression levels or the size of cleavage products, the prepared tissue or cell lysates were analysed by gel electrophoresis as described previously [173]. Briefly, samples were boiled for 3 min is SDS-sample buffer and separated on 10-20 % Tricine gradient gels (Novex). Thereafter the gels were transferred to Nytran membranes, and the membranes were blocked in 5% non-fat milk and probed with appropriate antibodies. Blots were finally developed with an enhanced chemiluminescence (ECL) western blotting detection system, according to the manufacture's instructions (Amersham Pharmacia). Co-immunoprecipitation experiments were performed using the *Immunocatcher System* (CytoSignal, Irvine, CA, USA) the protein lysates (600μg) were precleared with pre-immune serum and protein G agarose beads, after which appropriate antibodies were added, and the mixture was incubated overnight at 4 ^{o}C with gentle shaking. 50% slurry of protein-G agarose beads was then added to precipitate the immune complexes. The beads were incubated with the

reaction mixture for 6 h at 4 °C with rotation and then collected by centrifugation. The beads were washed with lysis buffer and resuspended in 0.1mL of SDS-sample buffer. 30 μl of the protein solutions were resolved on SDS-PAGE and detected by immunoblotting with appropriate antibodies. Measurment of protein levels was performed by densitometric analysis. Briefly, the autoradiograms were acquired from a Bio-Rad densitometer (Model GS-700). Western blot signals were quantified by two-dimension densitometry analysis with Quantity One (Bio-Rad).

4.6. Immunocyto and Immunohisto fluorescence staining

Immunofluorescence on MCN was performed as described [43]. Briefly, Primary mouse neuronal cell cultures grown on poly-D-lysine-coated coverslips were washed with cold-PBS, fixed for 30 min in freshly made 4% paraformaldehyde at 4 °C, rinsed with PBS, blocked for 30 min at room temperature in 5% normal goat serum. The fixed cells were then washed once with cold-PBS and permeabilized in 0.1% Triton X-100 for 15 min at 4 °C. After three washes, cells were incubated with the appropriate primary antibody in PBS with 5% normal goat serum for 2 h. Cells or sections were rinsed with PBS and incubated with the corresponding secondary antibody (anti-biotinylated antibody, Texas red conjugated secondary antibody)

(Amershampharmacia Biotech) for 1 h at room temperature, followed by washing twice with PBS,. For the Cells or sections incubated with anti-biotinylated secondary antibody, those were subsequently incubated in streptavidin Fluorescein (1:100) for 1 h at room temperature. Cells or sections were counterstained with DAPI or BTA, to visualize nuclei and Aβ plaque deposits, respectively. After a final rinse in PBS, cells on coverslips were mounted onto glass slides using Prolong anti-fade (Molecular Probes, OR).

Immunohisto-fluorescent staining was performed as described previously [175] with slight modifications. Cortical tissue samples were fixed in 4% paraformaldehyde and used for preparing paraffin embedded blocks, before serial sectioning to thickness ranging from 2 to 8 μm. To reduce autofluorescence at FITC and Texas red channels, a combination of quenching procedure was used with slight modifications. Briefly, dewaxed and rehydrated tissue slides were incubated in 0.1% $KMnO_4$ for 10 sec, washed with water, and then treated with a solution of 1% $K_2S_2O_5$ and 1% oxalic acid until the brown color was removed from the tissue (around 10 sec). After washing with water, a solution of 0.5% sodium borohydride was applied on the slides for 5 min. Slides were then washed with PBS. Antigens were retrieved by incubating the slides in an Antigen Unmasking Solution at 1:100 dilutions (No. H-3300; Vector Laboratories, Burlingame, CA) with

microwaving (100% power) for 2 min, followed by a second microwaving (30% power level) for 10 min, and washed twice with PBS. Then the sections were subjected to conventional immunofluorescence staining. The sections were blocked in and permeabilized in 0.4 % Triton X-100, 2% BSA, and 5% goat serum in PBS for 2 h at room temperature. After washing, the sections were incubated with the appropriate primary antibody diluted in 2% BSA in PBS, overnight at 4 ^{o}C. The sections were then rinsed in PBS twice for 5 min each time, and incubated in the appropriate secondary antibody (typically, anti-biotinylated conjugated or Texas red conjugated, both at 1:100) for 1 h. Sections that were incubated with the anti-biotinylated secondary antibody, after washing twice with PBS, were incubated in streptavidin Fluorescein (1:100) for 1 h at room temperature. In some sections, the order of the primary antibodies was reversed in double-labeling experiments to control for possible effects of some antibodies on altering access to subsequent antibody binding. After washing, sections were counterstained with DAPI or BTA, to visualize nuclei and Aβ plaque deposits, respectively. After a final rinse in PBS, sections were mounted with coverslips using Prolong anti-fade (Molecular Probes, OR).

4.7. Image analysis

Immunofluorescence was examined by epifluorescence microscopy (Nikon Eclipse. E600) for immunocytochemistry and immunohistochemistry. In double and triple-labeling immunoflurorescence experiments, bleed-through was controlled by observing the absence of fluorescence of a given fluorochrome-labeled secondary antibody when it was illuminated using the alternative fluorochrome excitation wavelength. In addition, for co-localization experiments, each channel was imaged separately, eliminating the "bleed-through."

Fluorescent images were captured using a Nikon digital camera interfaced with a computer equipped with Compix AIC software (PA, USA), and were presented in Adobe Photoshop CS. Image processing and measurements of relative fluorescence intensity, colocalization, scatter plot, and 3D-topographic imaging were performed with *the Image Space Analysis Tools, Version 3.10* (Molecular Dynamics, CA, USA) on Silicon Graphics operating system. Fluorescence intensities were independently determined in several randomly selected fields from different sections (> 300 cells). Investigators were blinded to the type of sections, cultures, or treatment. The mean pixel intensity for each image was determined, and each image was thresholded at the mean plus at least 2 standard deviations above the mean. The thresholded images were then multiplied. At any pixel intensity where intensity=0 (i.e., no

fluorescence) for either image, the product=0; therefore, non-zero pixel intensities correspond to colocalization. The colocalization between CREB/pCREB (Ser133)/pCREB (Ser129/133) and MAP2 was evaluated by calculating the cross correlation coefficient (r_{cc}) as described previously [43]. Briefly, images from several optical slices from the top and bottom of the double-labeled cells were captured. The mean pixel intensities for the image pairs as well as the fluorescence signal levels at individual pixels in the image pairs were recorded. In the summation to determine the *r* value, all pixels inside the cells were included.

4.8. *In vitro* APP binding assay

In vitro APP-glutathione S-transferase (GST) linked protein binding assay was performed as described [73] with modifications. Briefly, plasmids containing full length and subregions of APP fused with GST in pGEX-6P-1(Amersham biosciences, Piscataway, NJ) were constructed by PCR amplification of the corresponding cDNA sequences with oligonucleotides containing the appropriate restriction sites for in-frame fusion. Recombinant proteins from *E. coli* were easily purified from bacterial lysates by affinity chromatography using glutathione sepharose beads, according to the manufacturer's instructions (Amersham biosciences).

The pCMV-CREB cDNA (Clontech) was used as a template for complimentary PCR primers. The resulting CREB-PCR fragments were cloned into the corresponding multiple cloning sites in the pGEM-T (Promega, Madison, WI) and used for linked in *vitro* transcription-translation using the PROTEINscript II linked transcription-translation system (Ambion, Austin, TX). These plasmid constructs were generated by our laboratory technicians. Subsequently, [^{35}S] Methionine-labeled CREB was incubated with control GST or APP-GST fusion proteins on glutathionine sepharose beads in the presence and absence of competitor proteins for 1 h at room temperature. Complexes were washed with 5 x 1 ml of PBS containing 0.5% Nonidet P-40, immediately boiled in SDS sample buffer, and analyzed by PAGE. The gels were dried and exposed directly to film overnight. The quantity of fusion protein on beads and competitor proteins was estimated by SDS-PAGE followed by Coomasie blue staining. The amounts of GST-fusion proteins used in each reaction were normalized to the quantity of beads added to each reaction.

4.9. Electrophoretic mobility shift assay (EMSA) and Cre-Luc reporter gene assay.

EMSAs were performed using the digoxigenin (DIG) reagent kit according to

the manufacturer's protocol (Roche Biochemicals). The optimal wt/mut CREB binding site and Bcl-2 promoter sequence oligonucleotides were used as probe. Primary mouse cortical neuronal cultures were transiently transfected with the pBcl-2 CRE-Luc [134], or with pTAL Luc/ pCRE TAL Luc (Clontech). Briefly, cultures in six-well plates were transfected with 3 μg of CRE-luc and 0.5 μg of pCMV-β galactosidase plasmid (p-βgal) as an internal control for transfection efficiencies, in the presence of Effectene Transfection Reagents (Qiagen). At 48 h post transfection, some of the cultures received 20 μM $A\beta_{42}$, then the cells were lysed with 200 μL lysis buffer. Subsequently, luciferase and β-gal assays were performed according to the manufacturer's instructions (Promega).

4.10. Protein kinase A assay

Basal Protein kinase A (PKA) activity was measured as described [176]. Briefly, mouse cortical tissues were homogenized in radioimmunoprecipitation assay buffer (50 mM Tris HCl, pH 7.4, 1% Nonidet P-40, 0.35% sodium deoxycholate, 125 mM NaCl, 0.5 mM EDTA, I mM PMSF, 1 μM pepstatin and 1 μM sodium vanadate) containing 80 mM β-glycerophosphate, and the homogenate was centrifuged for 15 min at 30,000 $X\,g$ at 4°C. The supernatants were then used to measure basal PKA

activity by using the heptapeptide Leu-Arg-Arg-Ala-Ser-Leu-Gly (10 μg/μl kemptide, Sigma) as substrate, in the presence of 0.1 μCi/μl [γ^{-32}P]ATP (1 Ci = 37 GBq) and 50 μM ATP with or without the PKA inhibitor amide fragment 6-12 (PKI, Sigma) for 20 min at 30 °C. The reaction mixtures were then spotted on to phopsphocellulose filters (Whatman) for 10 min, washed twice in orthophosphoric acid and counted.

4.11. APP siRNA and scrambled oligonucleotides

APP siRNA directed at bp 1754-1772 of mouse APP cDNA (GenBank NM 007471) corresponding to the APP siRNA target sequence at bp 1769-1788 of rat APP cDNA (Gen Bank X07648), ACAUCAAGACGGAAGAGAU and non- silencing scrambled siRNA target sequence, AATTCTCCGAACGTGTCACGT, have been described [177]: APP siRNA sense sequence, ACAUCAAGACGGAAGAGAUdTT; anti sense AUCUCUUCCGUCUUGAUGUdTT. Scrambled siRNA: sense sequence, UUCUCCGAACGUGUCACGUdTT; anti-sense sequence, ACGUGACACGUUCGGAGAAdTT. These siRNAs were obtained from Invitrogen (Carlsbad, CA). The oligonucleotides of the siRNAs were synthesized, and then duplexed, desalted, and protected. Lyophilized siRNAs were reconstituted, according to the instructions of the manufacturer,

condensed with enhancer reagent, mixed with HiPerFect solution (Qiagen), and transfected into cultures, at a final concentration (150 nM).

4.12. Statistical Analysis

Results were analyzed using StatView and Microsoft Excell software. Non-parametric Friedman ANOVA for relative fluorescence was used to evaluate differences between tissue sections for each experimental group. Densitometric data of western blots were analyzed by ANOVA, followed by Fisher's *Post hoc t* tests for comparisons. Results are expressed as the mean ± S.E.M., unless otherwise indicated. n indicates the number of independent experiments or samples. In all cases, unless otherwise stated, $P<0.05$ was considered significant.

5. RESULTS

5.1. Phosphorylation status of CREB is not altered in AD model brain

Accumulating evidence indicates that $A\beta_{42}$ or familiar Alzheimer disease (FAD) mutant APP (mutAPP) impairs CREB phosphorylation and CRE-dependent signaling, resulting in neuronal apoptosis [71, 136]. However, it remains uncertain whether CREB signaling under conditions of excess $A\beta_{42}$ or overexpression of FAD mutAPP is impaired *in vivo*. We performed studies by using a FAD mouse model (TgCRND8) that overexpresses a double mutant form of hAPP695Swe/Ind (KM670/671NL, Swedish mutation + V717F, Indiana mutation), and more details can be found in *3.2. Transgenic and gene-targeted mouse lines*.

Mice cortical tissues (8 samples from Non-Tg; 10 samples from TgCRND8) were homogenized and processed for protein extraction. Expression levels of total and phosphorylated CREB (t/p-CREB) in cortical region of the TgCRND8 mice brains at various ages were measured by Western blot analyses. As shown in Figure 9, there was no significant difference in the levels of t-CREB (Figure 9a), p-CREBSer133 (Figure 9b) and p-CREBSer-133/129 (Figure 9c) with age, between the Non-Tg and TgCRND8 mice.

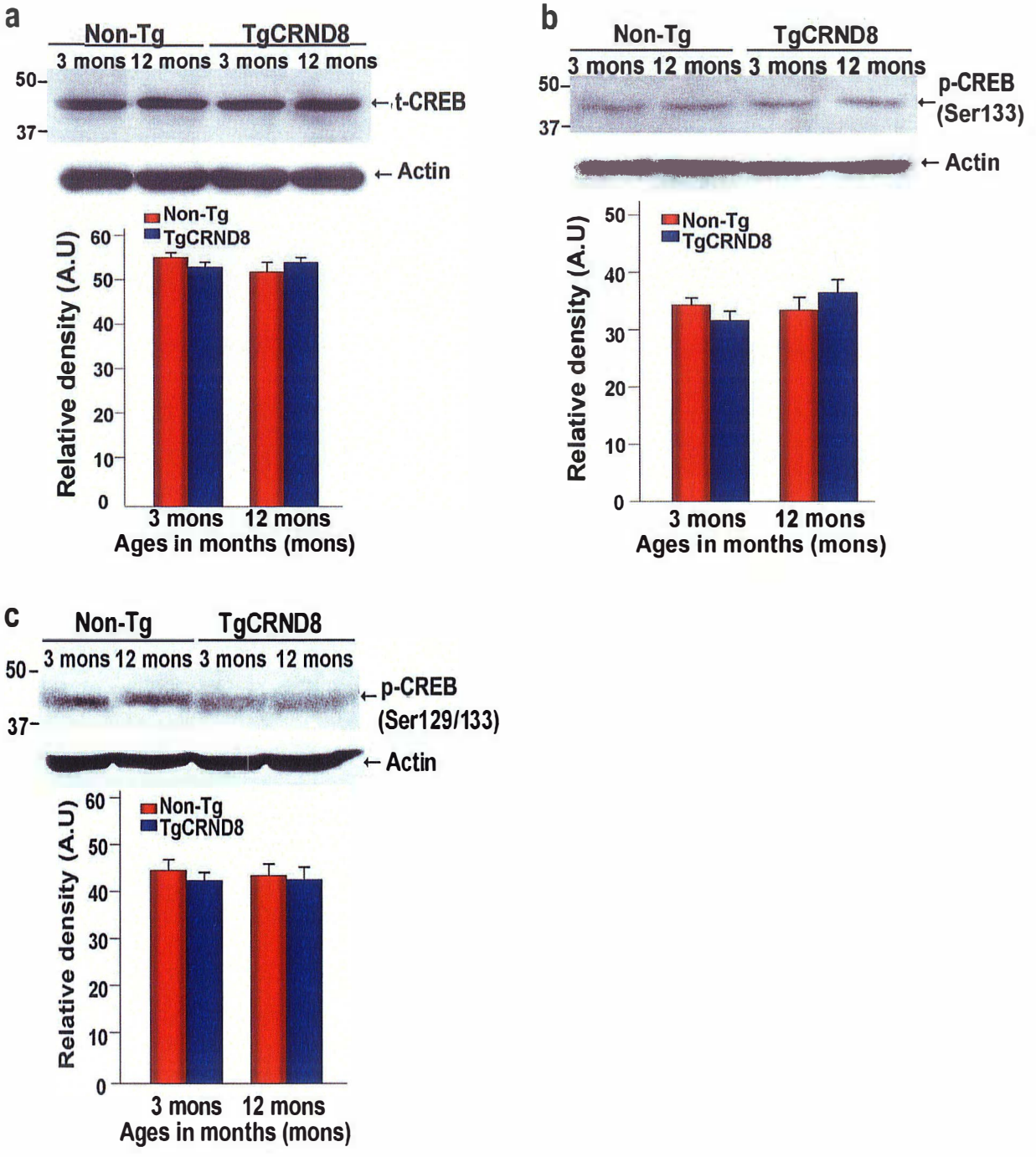

Figure 9. The levels of t-CREB, p-CREB (Ser133) and p-CREB(Ser129/133) from mouse cortical tissue lysates have no changes (p>0.01 *vs* Non-Tg) with age, between the Non-Tg and TgCRND8 mice.

Cortical tissues were fixed and sectioned. Then immunofluorescent staining was performed on the tissue slides, followed by analysis under a fluorescence microscope. t-CREB (Figure 10a) and p-CREB (Ser133/129) (green signals) (Figure 10c) were expressed predominantly in nuclei of the Non-Tg mice, but mainly cytoplasmic in the TgCRND8 mice cortical brain cells, indicating differential localization of these CREBs. In the TgCRND8 mice, there was an age-dependent decrease in nuclear levels of CREB and p-CREBSer-133/129. However, there was no significant difference in cytoplasmic or nuclear p-CREBSer133 staining between the Non-Tg and TgCRND8 mice (Figure 10b); p-CREBSer133 was mainly detected in the cytoplasm with diminished nuclear staining.

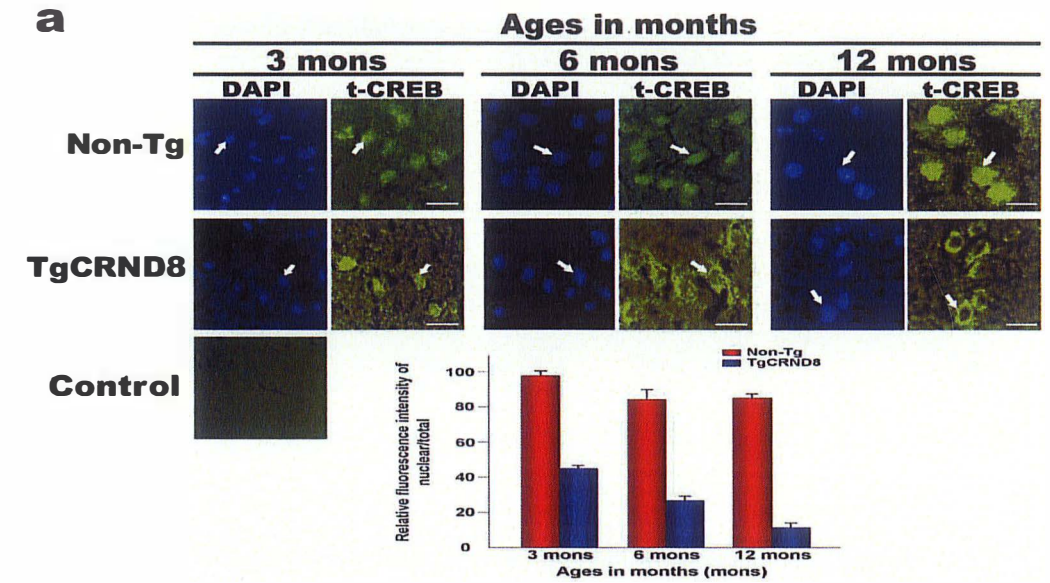
a
Ages in months
3 mons
6 mons
12 mons
DAPI
t-CREB
Non-Tg
TgCRND8
Control
Non-Tg
TgCRND8
Relative fluorescence intensity of nuclear/total
100
80
60
40
20
0
3 mons
6 mons
12 mons
Ages in months (mons)

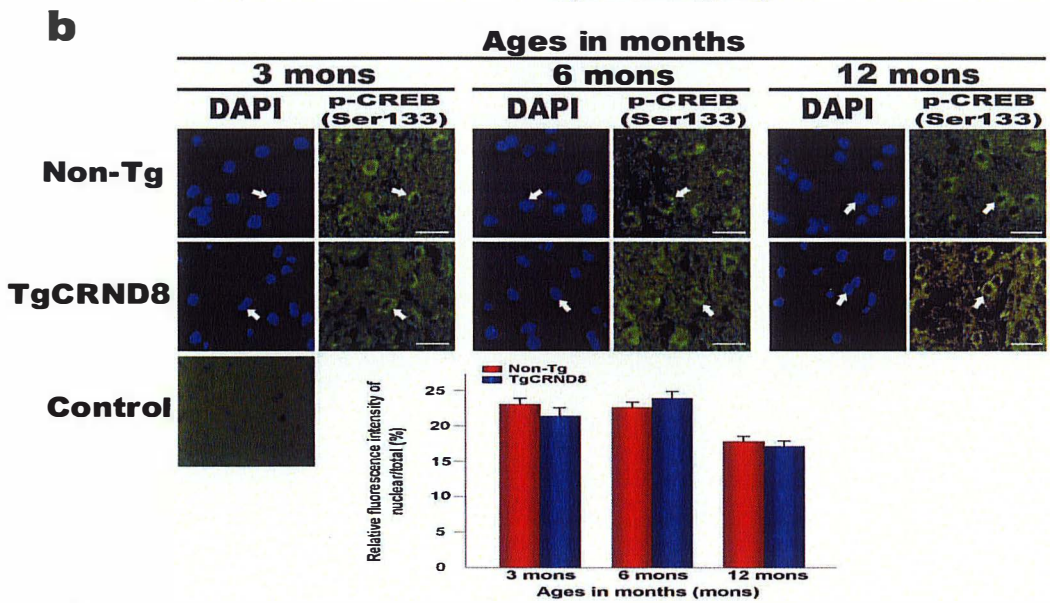
b
Ages in months
3 mons
6 mons
12 mons
DAPI
p-CREB (Ser133)
Non-Tg
TgCRND8
Control
Non-Tg
TgCRND8
Relative fluorescence intensity of nuclear/total (%)
25
20
15
10
5
0
3 mons
6 mons
12 mons
Ages in months (mons)

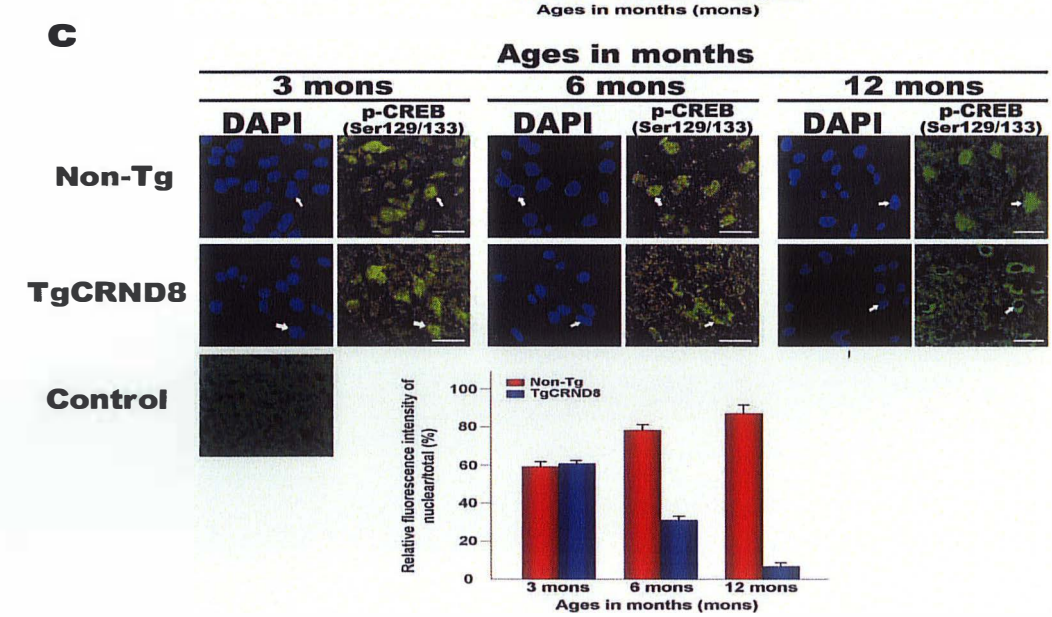
c
Ages in months
3 mons
6 mons
12 mons
DAPI
p-CREB (Ser129/133)
Non-Tg
TgCRND8
Control
Non-Tg
TgCRND8
Relative fluorescence intensity of nuclear/total (%)
100
80
60
40
20
0
3 mons
6 mons
12 mons
Ages in months (mons)

Figure 10. Cortical tissue samples were fixed, embedded by paraffin, and sectioned. Following immunofluorescence staining were performed on these sectioned tissue slides. **a.** t-CREB (green) is expressed predominantly in nuclei of the Non-Tg mice, but mainly cytoplasmic in the TgCRND8 mice cortical brain cells. DAPI staining indicated nuclear location. The graph showed relative fluorescence intensity of nuclear/total protein of CREB. For all three groups of age, there are more percentages of nuclear CREB in Non-Tg than TgCRND8 mice. $p<0.01$ *vs* Tg **b.** p-CREBSer133 (green) is mainly detected in the cytoplasm with diminished nuclear staining in both Non-Tg and TgCRND8 mice. As shown in graph, there was no significant difference in percentages of nuclear p-CREBSer133 between the Non-Tg and TgCRND8 mice. **c.** p-CREB (Ser133/129) (green) has been also shown predominantly in nuclei of the Non-Tg mice, but mainly cytoplasmic in the TgCRND8 mice cortical brain cell. For groups of age 6 & 12 months, more nuclear p-CREB (Ser133/129) is detected in Non-Tg than TgCRND8 mice, $p<0.01$ *vs* Tg. Absorption of the antibodies strongly diminishes immunoreactivity (Control). Scale bar, 50μm.

To further emphasize and demonstrate the differential localization of CREB that we have observed, we measured the colocalization ratio (r_{cc}) between CREBs and the nuclear marker, DAPI (blue signals), from immunofluorescent data of cortical samples at 12 months in Figure 10. The results showed that t-CREB immunoreactivity (Figure 11a) was significantly reduced in the nuclei (r_{cc}=0.0257), but was localized predominantly and homogenously in the cytoplasm of the TgCRND8 mice. In contrast, it was localized mainly in the nuclei (r_{cc}= 0.7858) of the Non-Tg mice. There was no significant difference in nuclear staining of p-CREBSer133 (Figure 11b) between the Non-Tg (r_{cc}= 0.2476) and TgCRND8 mice (r_{cc}= 0.2110), suggesting the cytoplasmic expression of p-CREBSer133 in both the Non-Tg and TgCRND8 mice. However, p-CREBSer-133/129 immunoreactivity (Figure 11c) was markedly reduced in the nuclei (r_{cc}= 0.1021) of the TgCRND8 mice, whereas it was mainly located in nuclei (r_{cc}= 0.7532) of the Non-Tg mice. Furthermore, there were no significant differences in the total intensities of CREB immunoreactivities between the Non-Tg and TgCRND8 mice.

Co-immunofluorescence staining was performed on mouse cortical sections by using CREBs and neuron specific microtubule associated protein-2 (MAP2) antibodies. Interestingly, t-CREB (Figure 12a) and p-CREBs (Figure 12b and c) were expressed primarily in neurons (red) with minimal staining in non-neuronal cells (no red signals).

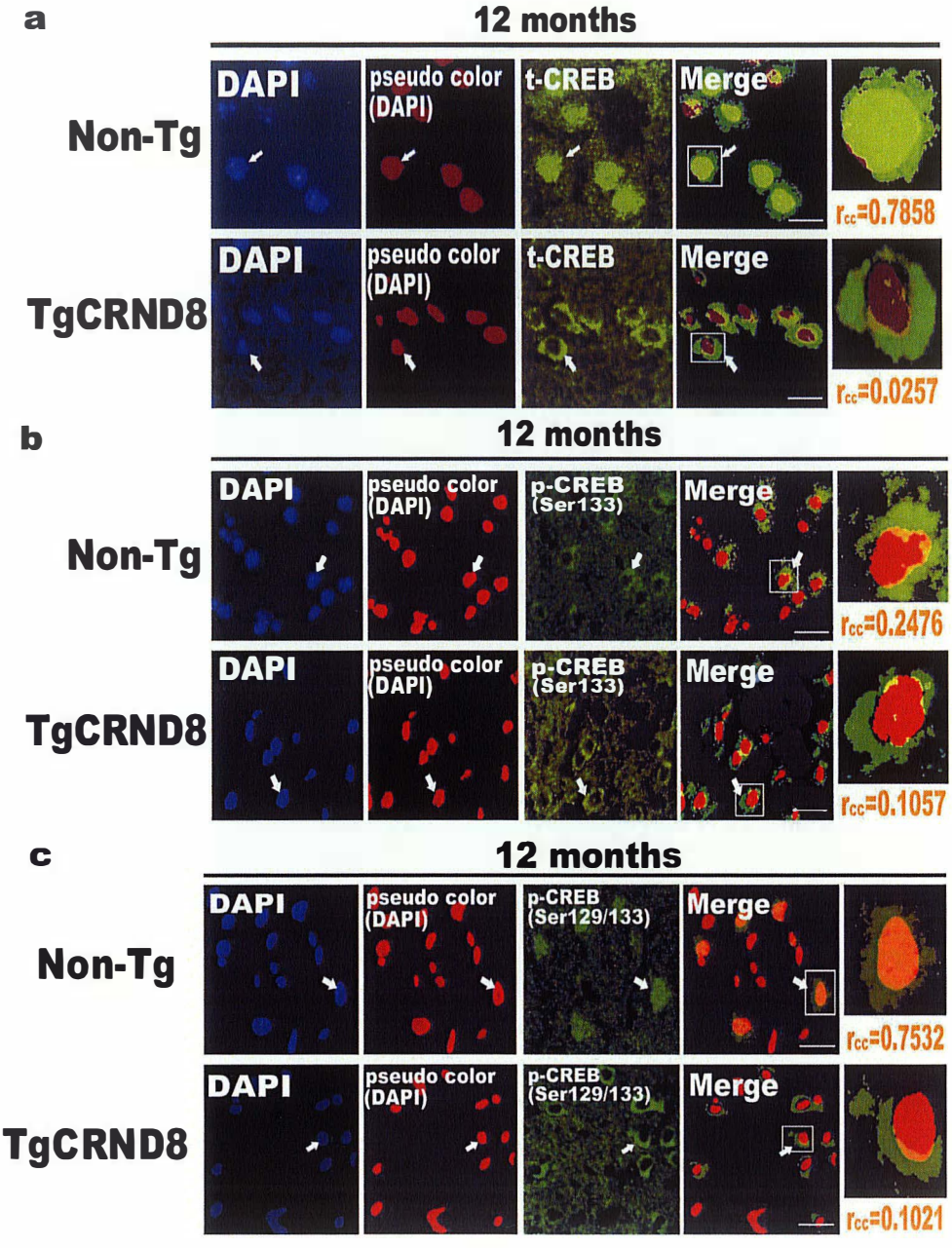

Figure 11. From the sections in Figure 10, cortical tissues of 12 months mice were presented. The blue DAPI stainings were converted to the red pseudo colors for purpose of viewing colocalized colors. **a.** The nulear localization of t-CREB (green, arrows) is shown in Non-Tg, but in the cytoplasm of TgCRND8 mice. **b.** p-CREB (Ser133) (green, arrows) is expressed mainly in cytoplasm of both Non-Tg and Tg CRND8 mice. **c.** p-CREB (Ser129/133) (green, arrows) have been shown mainly in the nuclei of Non-Tg mouse cortical sections, but in the cytoplasm of TgCRND8. Cross co-localization coefficients (rcc) are measured (see Experimental Procedures 4.7). Scale bar, 50μm.

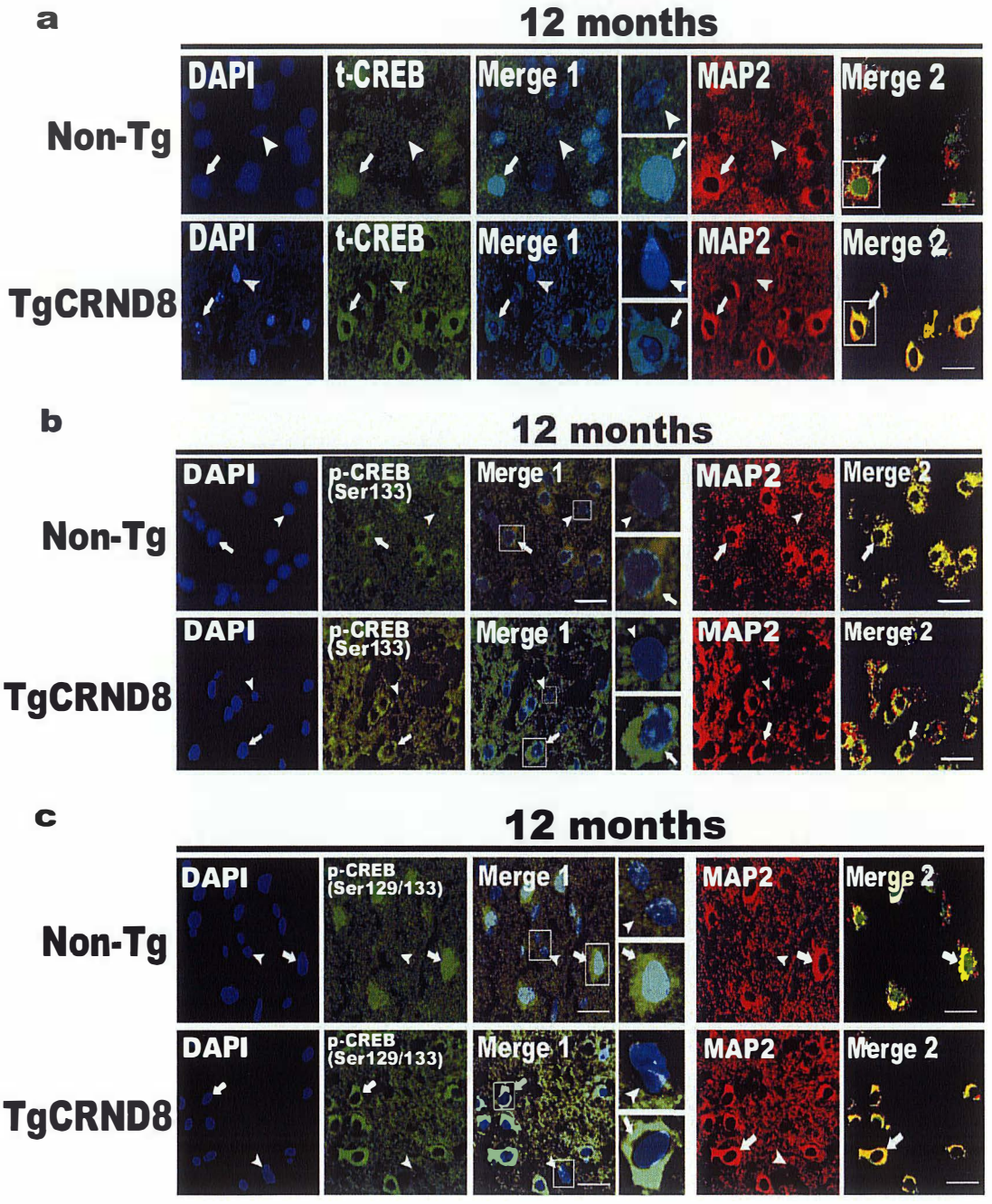

Figure 12. The co-localization of CREBs and neurons in mice brains. Co-immunofluorescence staining was performed on mouse cortical sections by using CREBs and neuron specific microtubule associated protein-2 (MAP2) antibodies. CREBs (green) is overlayed with nuclear DAPI staining (blue) in "Merge1" and with MAP2 staining (red) in "Merge 2". **a., b. and c.** CREB and p-CREBs immunostainings are presented in neuronal cells identified by MAP2 (arrows) but not in MAP2 unstained cells that are non-neurons (arrow heads). Scale bar, 50μm.

To confirm the immunofluorescent staining showing differential distribution of CREBs, we examined subcellular expression of CREBs in cortical tissue extracts by Western blotting. Consistent with the immunofluorescent data shown above, there was a significant increase in cytoplamic t-CREB (Figure 13a, left) and p-CREBSer-133/129 (Figure 13b, left) levels in the TgCRND8 mice. Higher levels of t-CREB (Figure 13a, right) and p-CREBSer-133/129 (Figure 13b, right) were observed in nuclear fractions from the Non-Tg compared with the TgCRND8 mice. As expected, there was no difference in nuclear or cytoplasmic levels of p-CREBSer-133 between the Non-Tg and TgCRND8 mice (results not included). Consistantly, Western blot analyses on hippocampal tissue extracts revealed that t-CREB and p-CREBSer-133/129 were expressed predominantly in nuclei of the Non-Tg mice in contrast to mainly cytoplasmic expression in the TgCRND8 mice. In addition, there was no significant difference in p-CREBser133 expression and localization, indicating that phosphorylation of CREB on Ser133 is not altered in the TgCRND8 mice.

We also examined the expression level and localization of CREBs in mouse primary neuronal cortical cultures (MCN) from the TgCRND8 and Non-Tg mice. There was no difference between the Non-Tg and TgCRND8 mice relating to the expression levels of t-CREB, p-CREBSer133 and p-CREBSer133/129. However, t-CREB and p-CREBSer133/129 were expressed predominantly in nuclei of the

Non-Tg mice and mainly in cytoplasm of the TgCRND8 mice. However, pCREBSer133 was expressed predominantly in cytoplasm of both the Non-Tg and TgCRND8 mice (Figure 14). These results showed that the level and distribution of CREBs in the MCN reflect those observed *in vivo*.

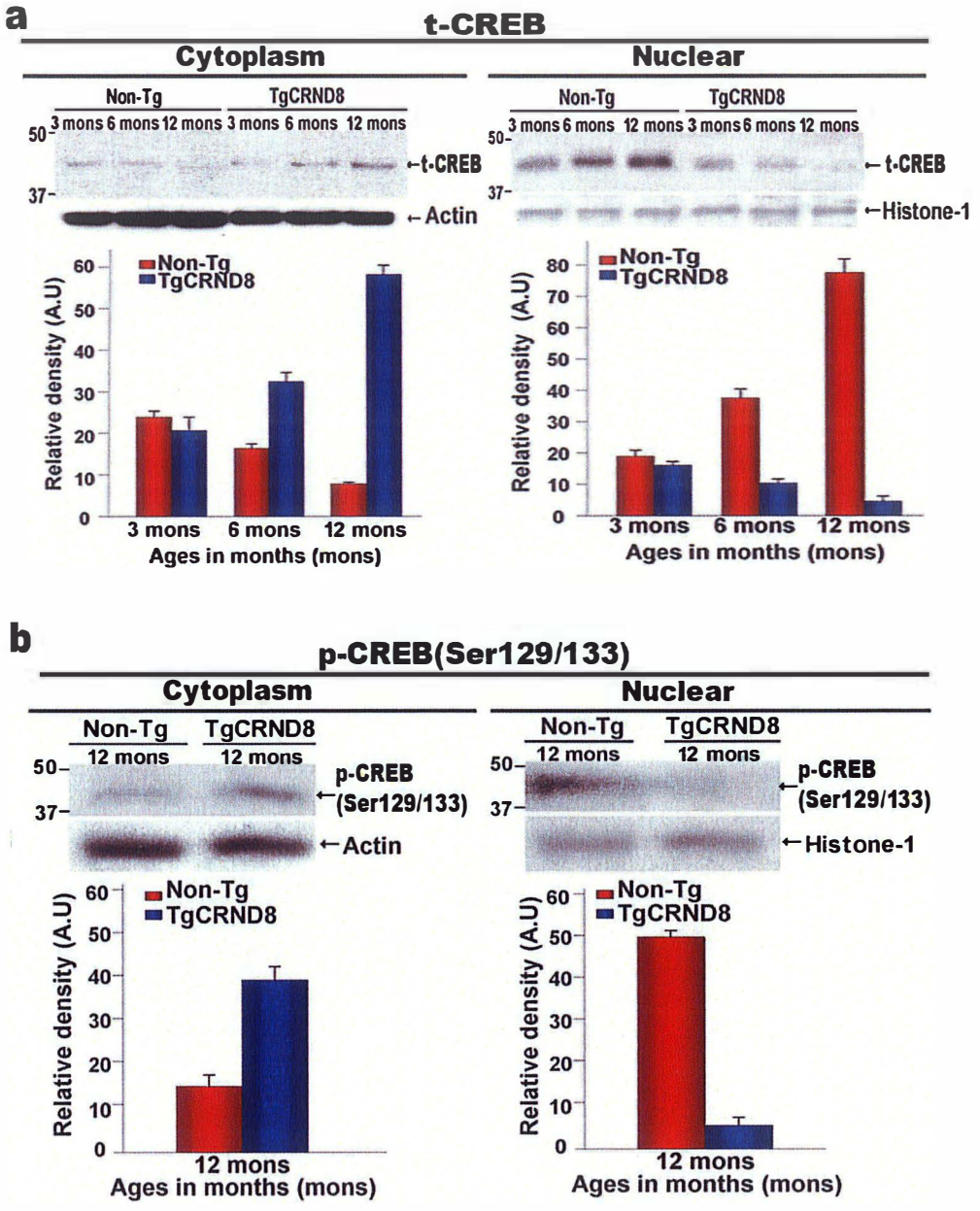

Figure 13. The expression levels of t-CREB and p-CREB (Ser129/133). The cytoplasmic and nuclear fractions of cortical tissue lysis from Non-Tg and TgCRND8 mice were analyzed by western blotting. **a.** There was a significant increase in cytoplamic t-CREB (left) and a decrease in nuclear t-CREB protein levels between the Non-Tg and TgCRND8 mice. **b.** The cytoplasmic p-CREBSer129/133 (left) level is higher in TgCRND8 mice, relative to the Non-Tg mice (left). higher levels of nuclear p-CREBSer129/133 (right) were observed in the Non-Tg compared with the TgCRND8 mice. The relative density of CREBs protein levels [t-CREB and p-CREB(Ser129/133): cytoplasmic, $p<0.05$ *vs* Non-Tg, nuclear, $p<0.05$ vs Tg].

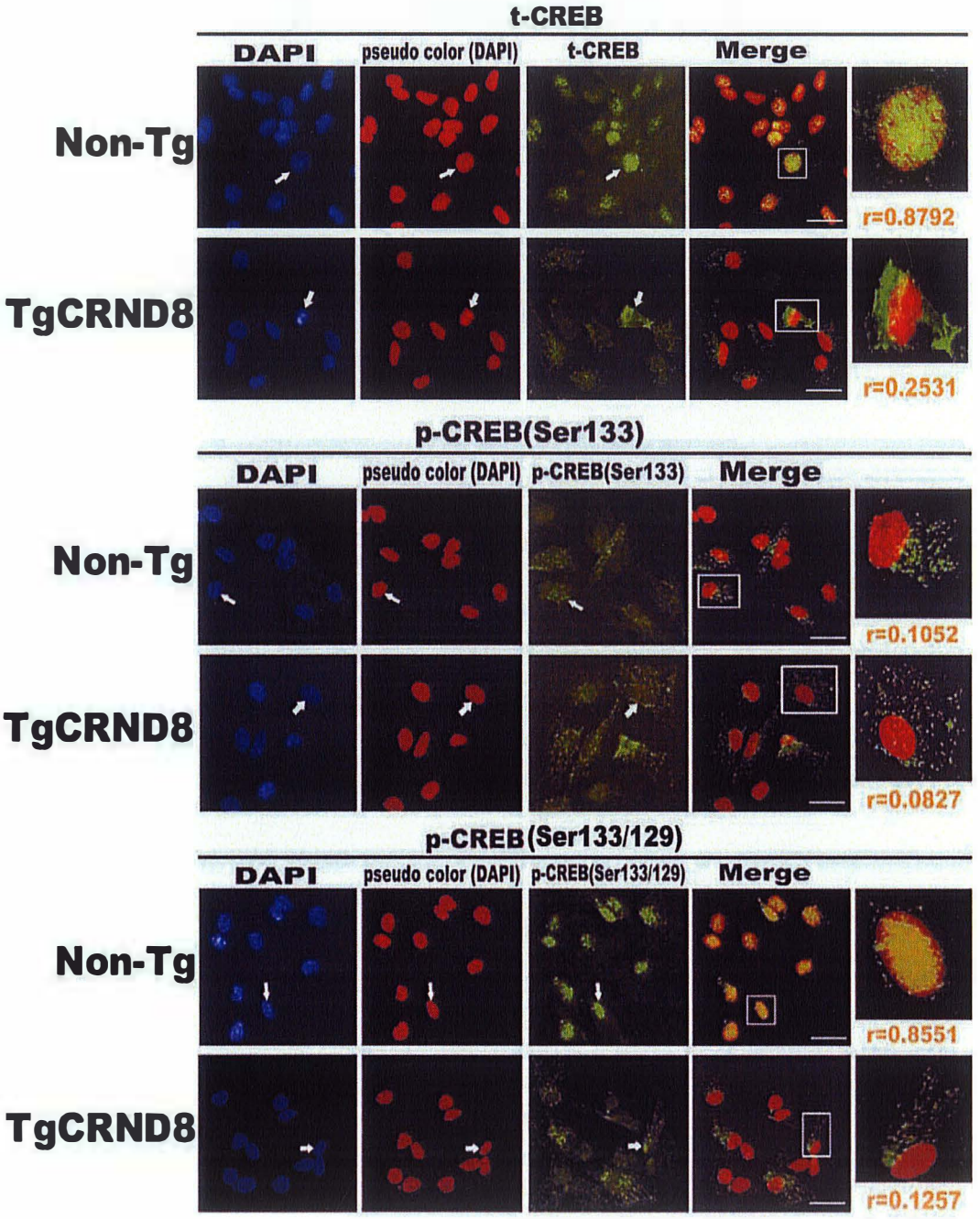

Figure 14. Immunostaining of CREBs in mouse cortical neuronal cultures. Primary mouse neuronal cell cultures (MCN) grown on poly-D-lysine-coated coverslips were fixed, washed and processed in immunocyto fluorescence staining. The blue DAPI stainings were converted to the red pseudo colors for purpose of viewing colocalized colors. Cross co-localization coefficients (r_{cc}) are measured (see Experimental Procedures 4.7). Scale bar, 50μm.

5.2. Amyloid beta deposition does not affect CREB expression and distribution

We tested the possibility that the differential localization of CREBs that we have observed is related to excess Aβ production and accumulation. Mouse cortical tissue slides from 6 and 12 months were selected. 2-(4′-Methylaminophenyl) benzothiazole (BTA-1) was used to counterstain Aβ deposits in brain tissues for multicolor fluorescence. Cells close to a plaque and cells distant from the plaque were analyzed for their expression and distribution. As expected, cortical regions in the brains of TgCRND8 mice at 6 and 12 months showed increased Aβ plaque deposition with age (Figure 15) [173]. These regions were then examined histologically for the distribution and expression of CREB immunoreactivity centered on or adjacent to Aβ deposits by morphometric analysis as described previously [178, 179]. The results showed that there was no colocalization of CREB with the Aβ deposits. However, CREB immunoreactivity was located around Aβ deposits with no significant difference in staining intensity corresponding to increased Aβ deposit size (burden). Like wise, there was no significant correlation between the proportions of volume occupied by CREB-positive cells and Aβ plaque size (Figure 15, graph). These results suggest that CREB expression is not affected directly by Aβ deposition. In addition, we also observed that the cellular distribution of CREB, which was mainly

cytoplasmic in the TgCRND8 mice, was not affected by the proximity of CREB immunoreactivity to the Aβ deposits. From this study, CREB was expressed predominantly in the cytoplasm irrespective of the age or proximity to the Aβ deposits (Figure 15).

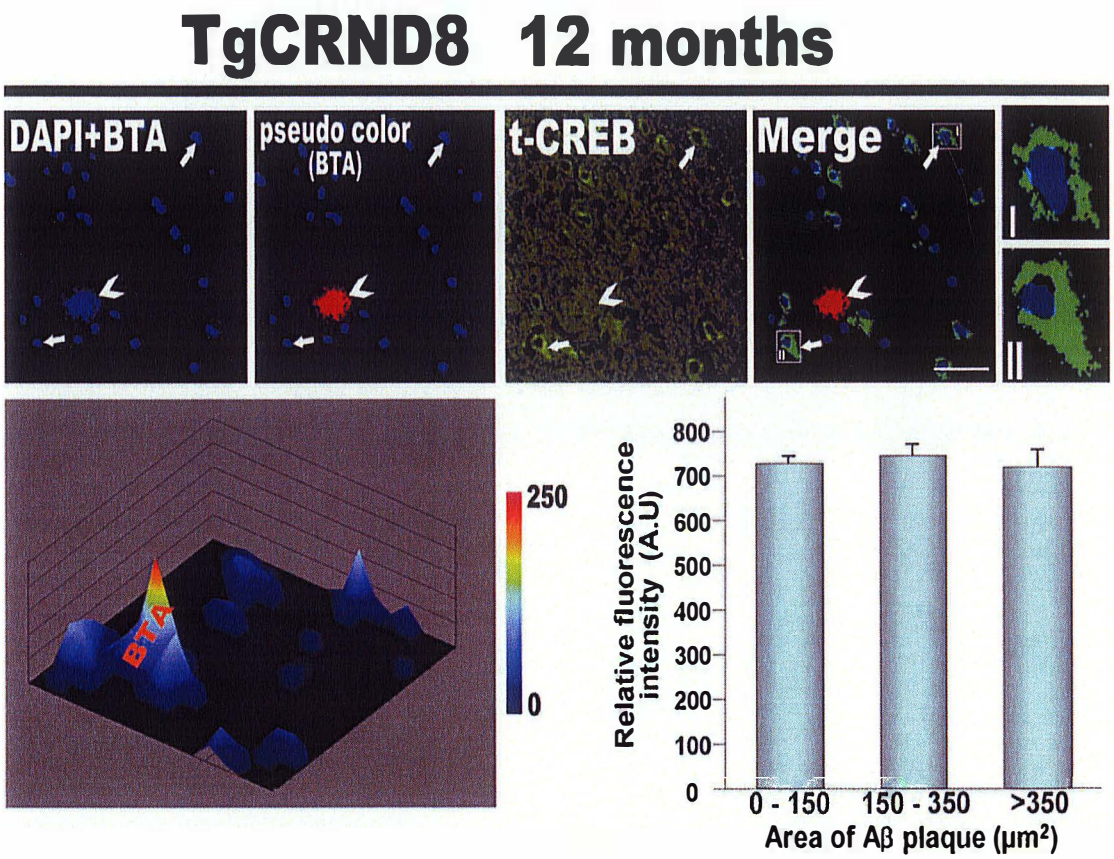

Figure 15. Immunostaining of CREB (green) and plaques (BTA, arrow head). Mouse cortical tissue slides from 12 months were selected. 2-(4′-Methylaminophenyl) benzothiazole (BTA-1) was used to counterstain Aβ deposits in brain tissues. Cells (I) close to a plaque and cells (II) distant from the plaque were analysized for their expression and distribution. Scale bar, 100μm. The 3D graph, reflecting on the "merge" panel, shows the t-CREB expressions relating to the location of a plaque (BTA). The graph shows that the expression levels of t-CREB are not significant different with the accumulation of plaques.

5.3. Protein kinase A and Glycogen synthase kinase-3 activities are not altered in the Cortex of the AD mouse model.

CREB phosphorylation at Ser133 and Ser129 depends on PKA [180] and GSK-3 [93] activities, respectively. In addition, PKA activity is inhibited by $A\beta_{42}$ [176], whereas GSK-3 activity is stimulated by $A\beta_{42}$ [181], and it has been shown that active GSK-3β is increased in dystrophic neurites adjacent to Aβ deposits in the APP_{SWE} (Tg2576)-transgenic mice brain [182]. Searching for a mechanism to explain the lack of difference in the phosphorylation status of CREB between the Non-Tg and TgCRND8 mice, we examined the activity of two prominent protein kinases that are known to phosphorylate CREB, protein kinase A (PKA) and glycogen synthase kinase-3 (GSK). Mouse cortical tissues were homogenized and then measured basal PKA activity in the presence of [γ^{-32}P] ATP. We observed that there was no significant difference in cortical PKA activity with age between the Non-Tg and TgCRND8 mice (Figure 16a). We also measured GSK-3 phosphorylation activity indirectly by Western blot analysis of phosphorylated GSK-3α/β (Tyr-216/279), because GSK-3 stimulatory activity depends on phosphorylation at tyrosine-216 residue [183]. Although there was an age dependent decrease in pGSK-3 levels, there was no significant difference in GSK-3α/β levels between the Non-Tg and TgCRND8 mice (Figure 16b).

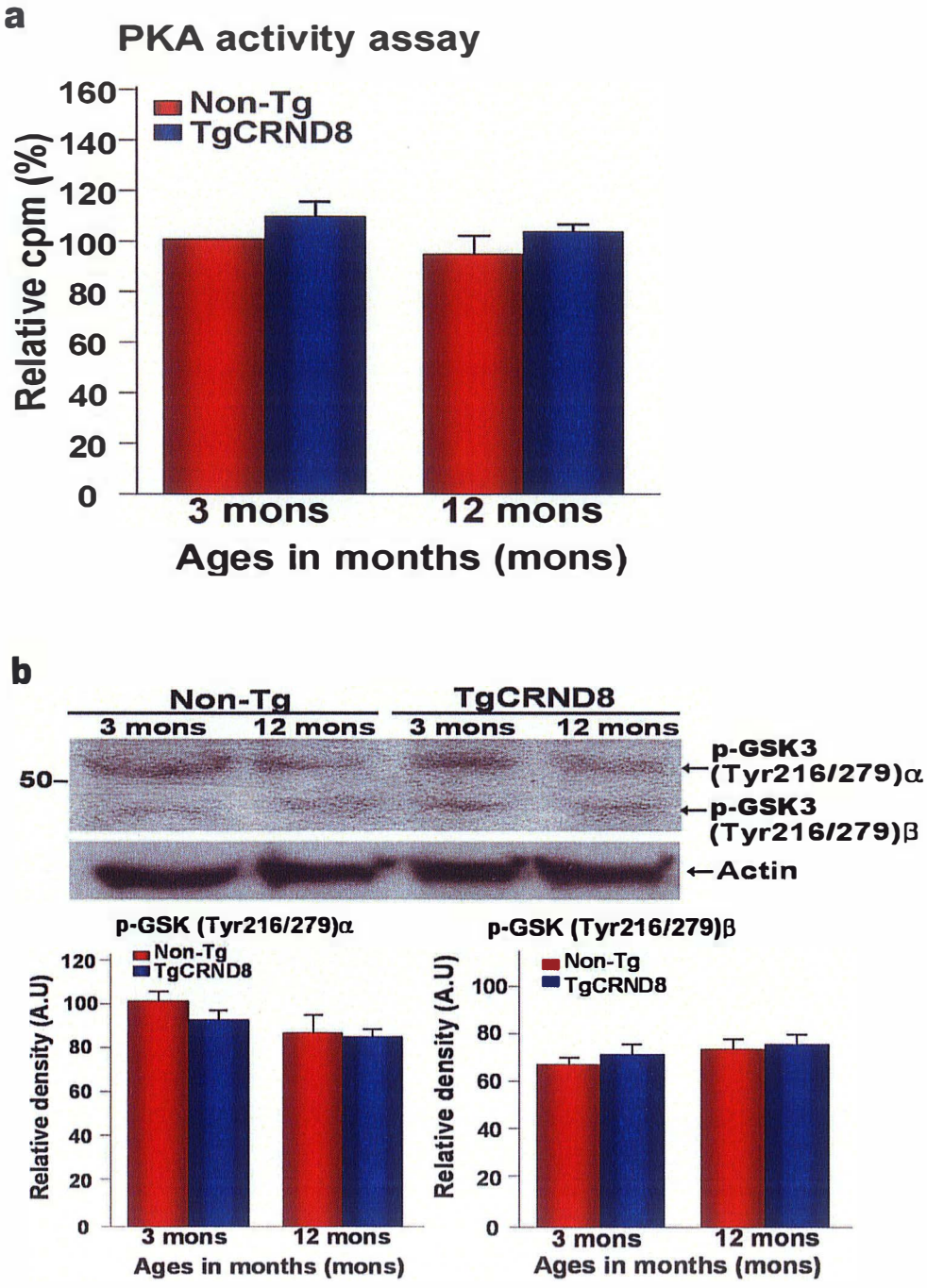

Figure 16. The activities of PKA and GSK3. Mouse cortical tissues were homogenized and then measured basal PKA activity in the presence of [γ^{-32}P] ATP. **a.** The levels of PKA activity have no significant changes, comparing the Non-Tg with TgCRND8 mice and different ages. **b.** The expression levels of pGSK3α/β(Tyr216/279) have no significant changes, analyzed by western blotting.

5.4. Phosphorylation status of CREB is not Altered in the brain of Alzheimer's Patients

We extended the examination of CREB expression and phosphorylation status to human brain tissues from ten sporadic AD cases of ten ages and sex-matched controls (Table 2). All tissue samples from patients with AD displayed a high degree of pathology (Braak score V-IV). Immunofluorescent intensities of t-CREB in cortical and hippocampal regions revealed that there was no difference between the AD cases and matched-controls (Figure 17a). Consistently, Western blotting analyses of cortical tissue extracts showed that there were no significant differences in t-CREB, p-CREBSer133, and p-CREBSer129/133 expression levels between the Non-Tg and TgCRND8 mice (Figure 17b). However, there was differential localization of CREB in the cortical and hippocampal regions between the Non-AD and AD cases (Figure 17c). As shown, t-CREB immunofluorescent signal was expressed predominantly in the nuclei of the Non-AD cortical and hippocampal cells, whereas in the AD brain, it was expressed predominantly in the cytoplasm (Figure 17c). These results were supported by Western blotting analysis, which showed significantly higher levels of nuclear t-CREB in cortical tissue extracts from the Non-AD than those of the AD cases (Figure 17d). Likewise, in the hippocampus there was a significant increase in t-CREB levels in

nuclear extracts from the Non-AD compared to the AD cases (Figure 17d). These results are in agreement with those obtained from the Non-Tg and TgCRND8 mice brain samples (Figure 9, 13).

Table 2. Human brain tissue samples

Case	Age at death	Gender	PMI[a]	Braak stage[b]	Tangle cores[c]
Control 1	89	F	10.34	II	2.50
Control 2	77	M	13.00	II	4.50
Control 3	94	F	14.65	III	3.50
Control 4	80	F	14.25	III	2.55
Control 5	91	M	13.00	II	2.25
Control 6	86	M	14.0	II	5.00
Control 7	90	F	12.75	III	6.45
Control 8	78	F	13.55	III	3.50
Control 9	82	M	15.25	III	5.50
Control 10	77	F	16.53	III	6.50
Mean	**84.4**	**6 F, 4 M**	**13.73**	**II - III**	**4.0**
AD 1	78	M	13.4	VI	10.0
AD 2	89	F	13.00	VI	13.5
AD 3	80	F	14.25	V	14.0
AD 4	92	F	12.25	V	13.0
AD 5	78	M	13.5	V	15.0
AD 6	86	M	16.17	VI	10.0
AD 7	85	F	14.65	V	13.0
AD 8	93	F	15.13	VI	14.5
AD 9	83	M	13.53	VI	12.5
AD 10	77	M	12.55	V	12.0
Mean	**84.1**	**5 F, 5 M**	**13.84**	**V-VI**	**12.70**

[a]PMI means postmortem intervals, hours

[b]Neuropathology was staged as described to (Braak and Braak, 1995)

[c] Plaque-tangle count score was a density estimate to a maximum of 15, and was defined according to the Consortium to Establish a Registry for AD (CERAD) criteria.

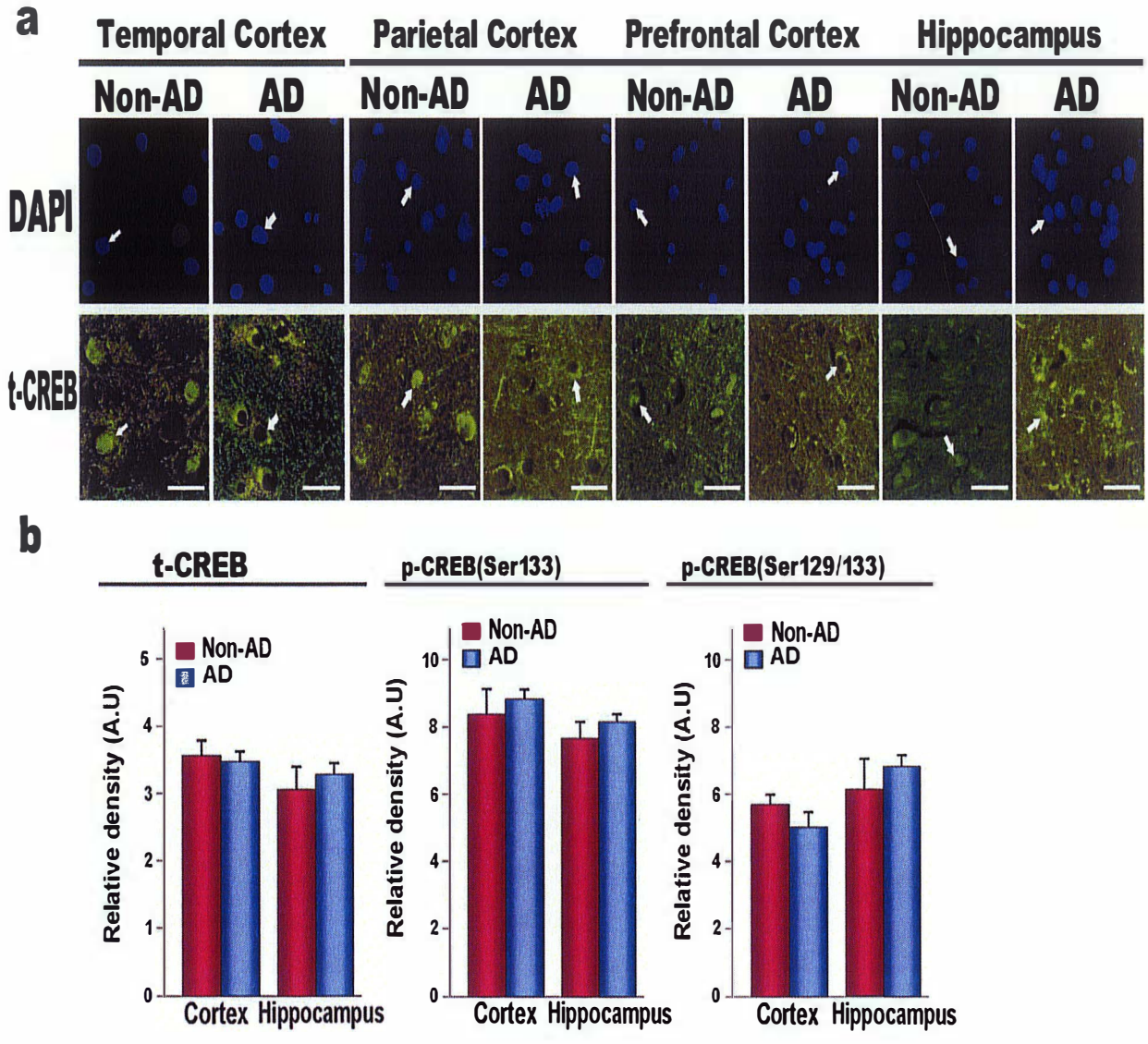

Figure 17 (a, b). a. The immunoreactivity of t-CREB (arrow) respectively in human brain regions. Human sample slides from AD and matched-contol were processed in immunofluorescence staining with t-CREB antibody. Different regions of cortex and hippocampus are presented. Scale bar, 50μm. **b**. Human tissue lysis from cortex and hippocampus were prepared for Western blot analysis. t-CREB, p-CREB(Ser133) and p-CREB(Ser129/133) were detected in those samples. No significant difference of CREB levels between the Non-AD and AD cases.

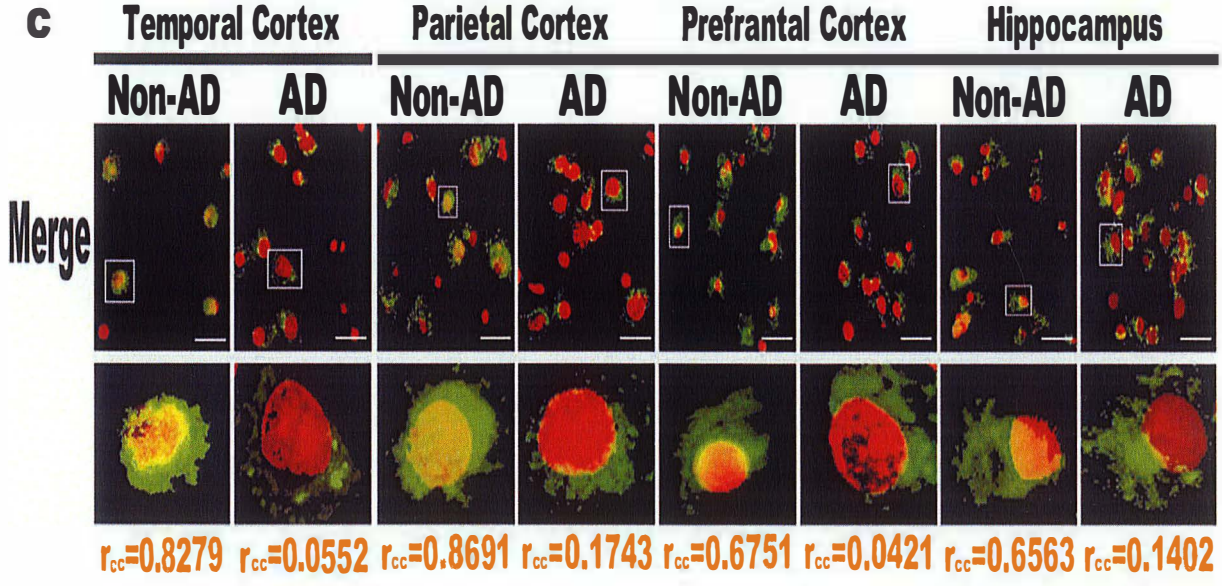

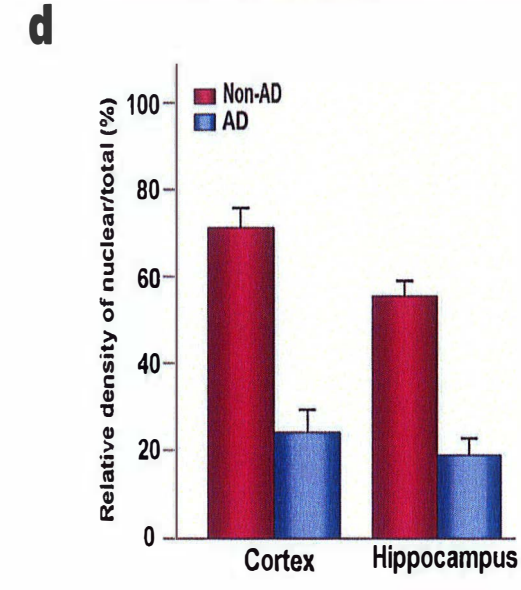

Figure 17 (c, d). c. Differential localization of CREB (green) overlayed with nuclei staining (psudo-color, red). t-CREB immunofluorescent signal was expressed predominantly in the nuclei of the Non-AD cortical and hippocampal cells, whereas in the AD brain, it was expressed predominantly in the cytoplasm. Cross co-localization coefficients (r_{cc}) are shown for this set of markers. Scale bar, 50μm. **d.** cytoplasmic and nuclear fractions from human cortex and hippocampus were analysized by Western blot. Densities of t-CREB were normalized by internal controls (actin for total lysis; histone-1 for nuclear extraction). Following calculations were performed for relative density ratio of nuclear/total protein of CREB. $p<0.05$ *vs* AD.

5.5. CREB-DNA binding activity and CRE-mediated transcription is altered in cortex and primary cortical neurons of the AD Model

Because of no significant difference in expression level and phosphorylation status of CREB on Ser133 and Ser129 between the TgCRND8 mice or AD cases compared with controls, we tested whether the differential localization of CREBs may be associated with changes in its DNA-binding activity. We analyzed DNA binding activity of endogenous CREB to the CRE by electrophoretic mobility shift assay (EMSA) on cortical nuclear extracts. We observed formation of a specific CREB-DNA-protein complex in the presence of wtCRE but not mutCRE probe. Although the CREB-DNA binding complex level decreased with age, it was significantly higher (by 2 and 3 fold at 6 and 12 months, respectively) in nuclear extracts from the Non-Tg compared with those from the TgCRND8 mice (Figure 18). Thus, we used MCN to study CRE-mediated transcription as a functional consequence of the CREB-DNA binding activity.

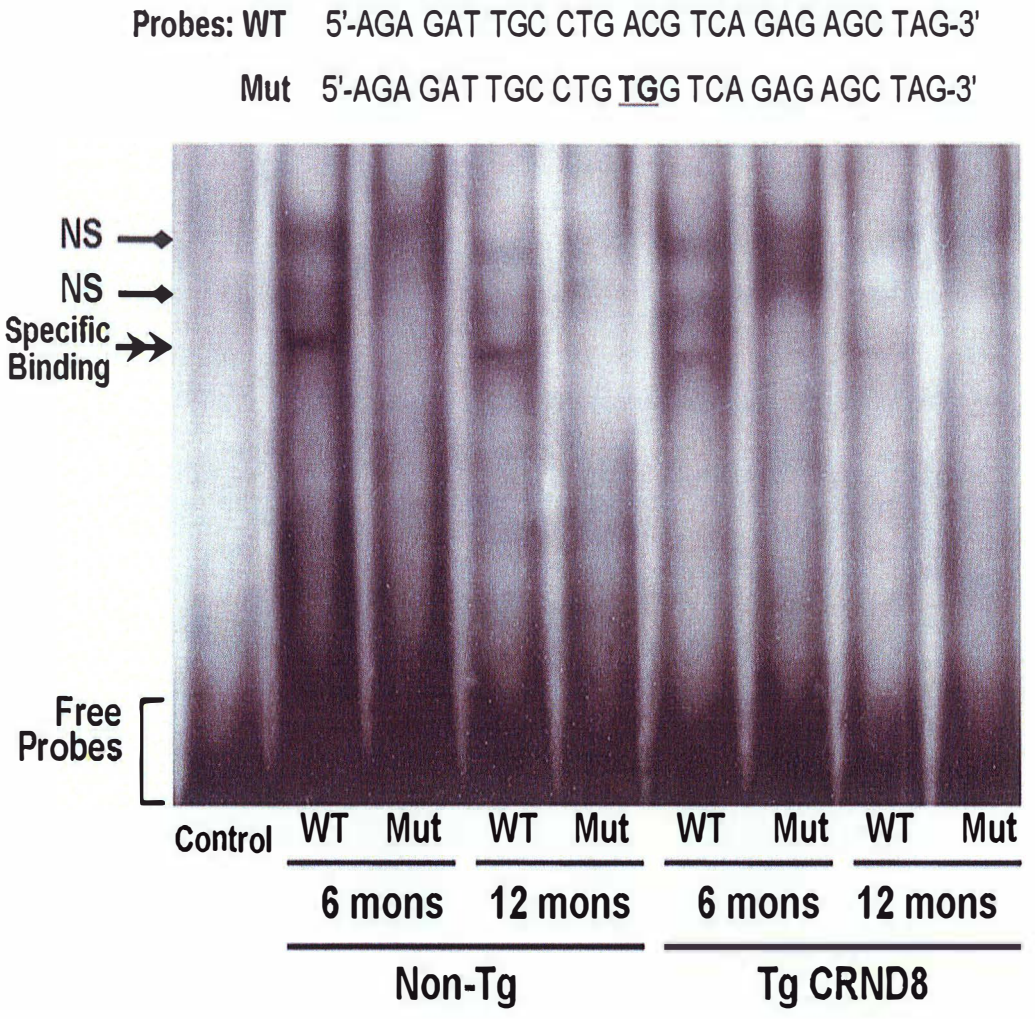

Figure 18. EMSA from nuclear extracts of the Non-Tg and TgCRND8 mice cortical tissues by using an oligonucleotide sequence corresponding to CRE wt and a mutant oligonucleotide. NS, non-specific binding. CREB-DNA binding activity level is shown decreased with age and it was significantly higher (at 6 and 12 months, respectively) in the Non-Tg compared with the TgCRND8 mice.

We also examined the possibility that the increased DNA-binding activity observed in the tissue extracts could be parallel to the increase of CRE-directed transcription in MCN from the Non-Tg compared with TgCRND8 mice. We determined if there was similar difference in DNA-binding activity in MCN from the Non-Tg and TgCRND8 mice to reflect the *in vivo* result. As measured by EMSA in MCN, the specific CREB-DNA binding complex was significantly reduced in nuclear extracts from the TgCRND8 mice compared with those from the Non-Tg mice (Figure 19a), supporting our *in vivo* observation (Figure 18). To determine the functional consequence of this DNA-binding-CREB complex, the transcriptional activity of the CREB was monitored using a transient transcritptional activity assay with luciferase reporter gene. Consistent with the DNA binding activity (Figure 19a), the relative CRE-luciferase reporter gene activity in MCN from the Non-Tg was significantly higher compared with the TgCRND8 mice (Figure 19b). These results suggest that although there is no difference in CREB phosphorylation in the TgCRND8 mice compared with control littermates, the differential localization of CREB leads to a significant reduction in nuclear CREB levels in the TgCRND8 relative to the Non-Tg mice. This reduction likely contributed to the impairment or decrease in CREB-DNA binding activity and CRE-mediated transcription observed in the TgCRND8 mice, because CREBs usually accumulate in the nucleus [132].

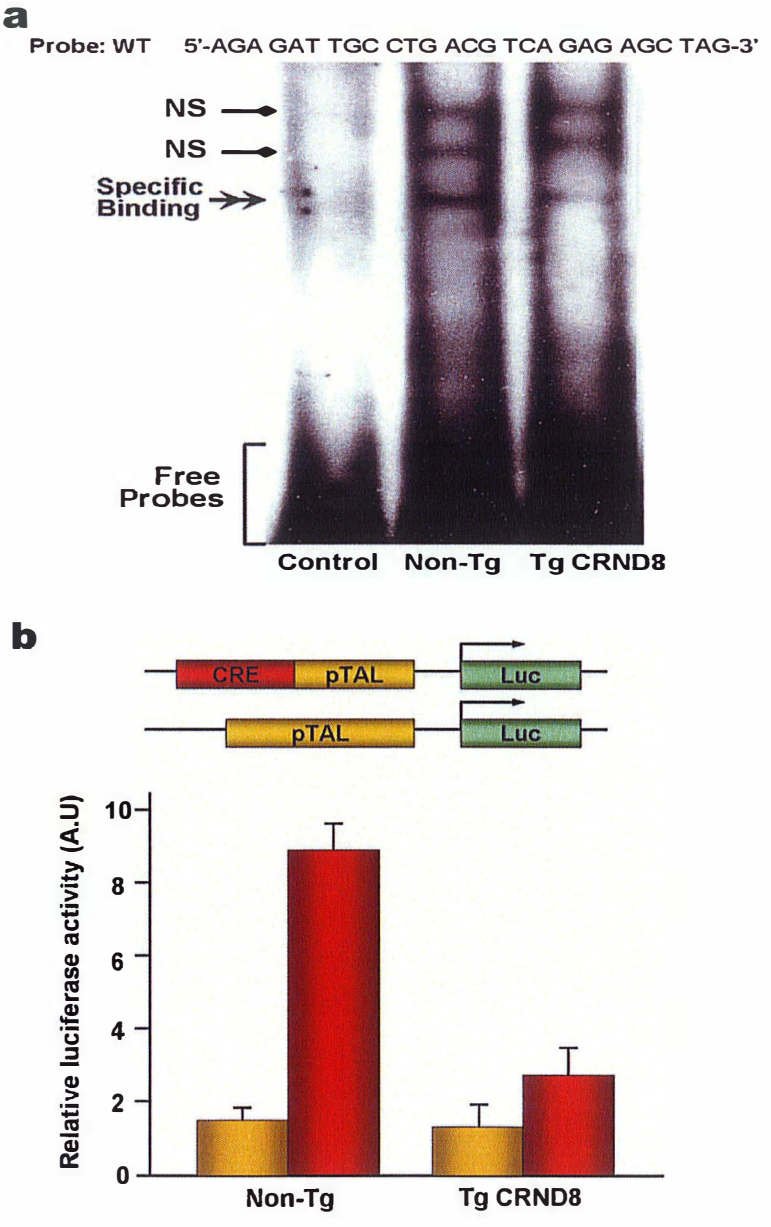

Figure 19. The transcription activity of CREB in mouse cortical neurons. **a**. EMSA of mouse cortical neurons from the Non-Tg and TgCRND8 mice by using an oligonucleotide sequence corresponding to CRE. The specific CREB-DNA binding complex was significantly reduced in nuclear extracts from the TgCRND8 compared with the Non-Tg mice. NS, non-specific binding complex. **b.** The luciferase reporter assay for CREB binding activity is shown in the cortical neurons of the Non-Tg and TgCRND8 mice. CRE-luciferase reporter gene activity in MCN from the Non-Tg was significantly higher compared with the TgCRND8 mice. $P<0.05$. Each experiment was performed at least three times in triplicate.

To test this idea, we analyzed the transcriptional activity of one of the target gene promoters for CREB, Bcl-2, which has a CRE in the promoter region along with many other transcriptional response elements. In addition, cell survival mediated by neurotrophin-induced CREB phosphorylation in neurons is associated with increased Bcl-2 level [129], it has a protective effect on Aβ-induced neuronal apoptosis [184], and plays a critical role in neuronal survival [170]. To examine the role of CRE in the expression of Bcl-2, MCN from the Non-Tg and TgCRND8 mice were transiently transfected with either the Bcl-2 wtCRE or mutCRE promoter-luciferase reporter plasmids. There was a markedly reduced luciferase activity of the Bcl-2 wtCRE-promoter in the MCN from the TgCRND8 compared with the Non-Tg mice. However, there was no significant difference in the luciferase activity of the Bcl-2 mutCRE-promoter-luciferase plasmid (Figure 20b). As determined by western blots, there was a significant decrease in Bcl-2 protein levels in the TgCRND8 compared with the Non-Tg mice (Figure 20a), indicating that the effects of CRE in the induction of the Bcl-2 promoter is associated with the difference in CREB localization and expression of CREB-dependent survival protein, Bcl-2.

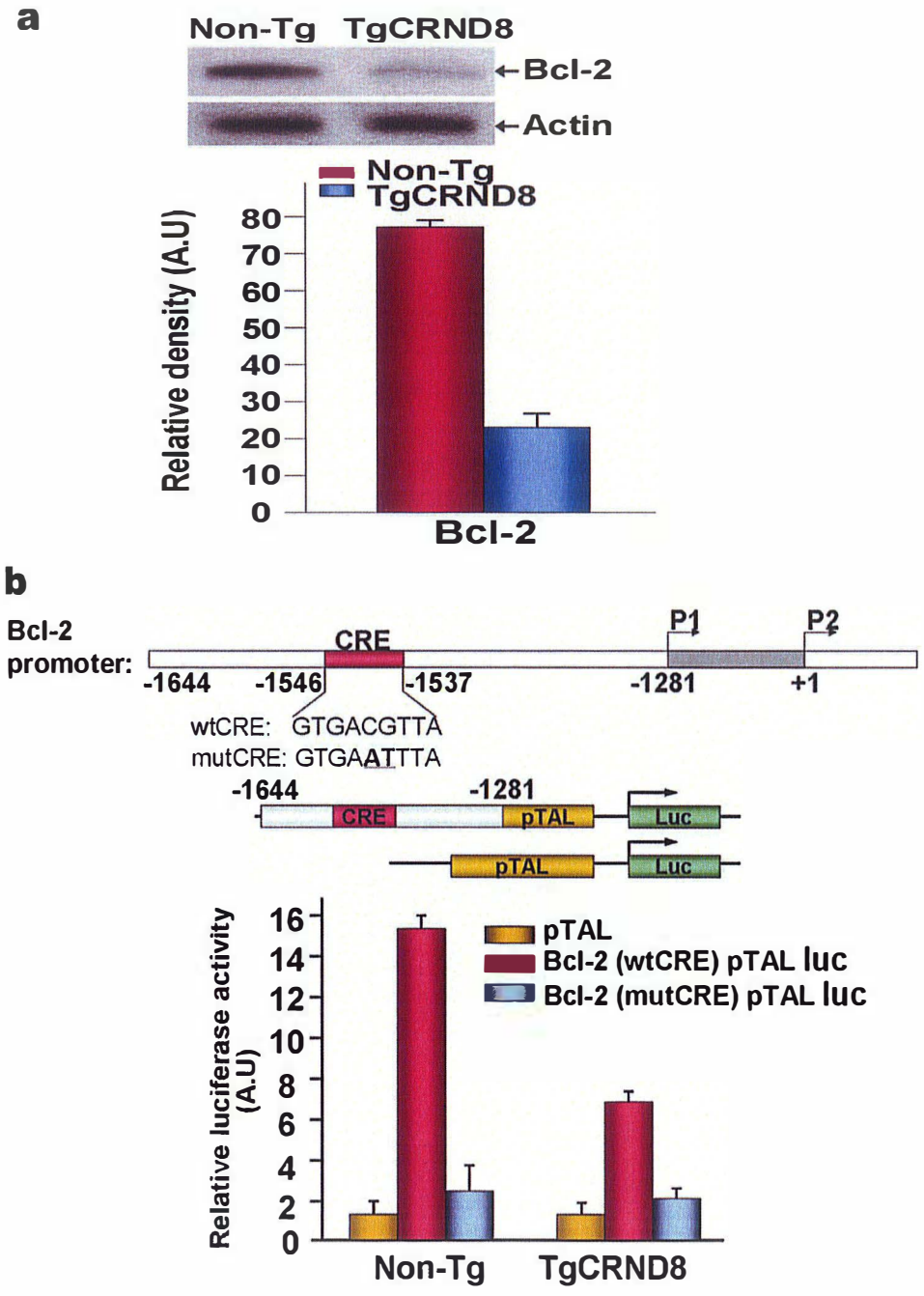

Figure 20. a, The levels of Bcl-2 are measured in the Non-Tg and TgCRND8 mice by Western blot. **b**, MCN from the Non-Tg and TgCRND8 mice were transiently transfected with either the Bcl-2 wtCRE or mutCRE promoter-luciferase reporter plasmids. The luciferase activities of Bcl-2 promoter containing wt/mut CRE have measured in mouse cortical neurons of the Non-Tg and TgCRND8 mice. There was a markedly reduced luciferase activity of the Bcl-2 wtCRE-promoter in the MCN from the TgCRND8 compared with the Non-Tg mice. However, there was no significant difference in the luciferase activity of the Bcl-2 mutCRE-promoter-luciferase plasmid. Each experiment was performed at least three times in triplicate.

5.6. APP and APP-carboxy terminal fragment interacts with CREB

Considering we have observed that the differential localization of CREB appears to be important for its functions, we sought to analyze the mechanisms underlying this localization. We reasoned that APP and/or its proteolytic fragments could function as cytosolic anchoring sites for CREB preventing its nuclear translocation, because there is overexpression of mutAPP, APP carboxy terminal fragments (APP-CTFs), and $A\beta_{42}$ in the TgCRND [173]. Likewise, in AD brain, several studies have reported expression of excess APP-CTFs [22, 185] and $A\beta_{42}$ [186] relative to non-AD. To test this possibility, we performed solid phase *in vitro* binding assays to determine if APP or its proteolytic fragments could interact with CREB. In "pull-down" assays as described [73], glutathione *S*-transferase (GST) fusion proteins of wt and mut APPs, APP-CTFs, deleted C-terminal APP (APPΔC), and deleted N-terminal APP (APPΔN) were immobilized on glutathione sepharose beads and incubated with *in vitro*-synthesized [^{35}S]-methione labeled CREB. The beads were pelleted, washed, and subjected to SDS-PAGE analysis. Autoradiograms of the gels (Figure 21a) demonstrated precipitation of labeled CREB by GST-APP_{695}, GST-APP_{717}, GST-APP_{SWE}, GST-APP-CTF_{100} and GST-APPΔN, but not by GST-APPΔC,

GST-APP-CTF$_{59}$, GST-APP-CTF$_{31}$, and GST alone.

To demonstrate physiological relevant interactions of APP or APP-CTF$_{100}$ with CREB, we performed coimmunoprecipitation analyses on cytoplasmic lysates from cortical brain tissues and primary neuronal cultures. In cortical tissues, APP and APP-CTF$_{100}$ can be found in anti-CREB precipitated complexes, and that t-CREB is present in anti-APP or anti-APP-CTF$_{100}$ precipitated complexes (Figure 21b). However, as expected because of transgene APP overexpression and that CREB is expressed predominantly in the cytoplasm of the TgCRND8 mice, there was a significant increase in t-CREB immunocomplexed with APP/APP-CTF$_{100}$ in the TgCRND8 relative to the Non-Tg mice.

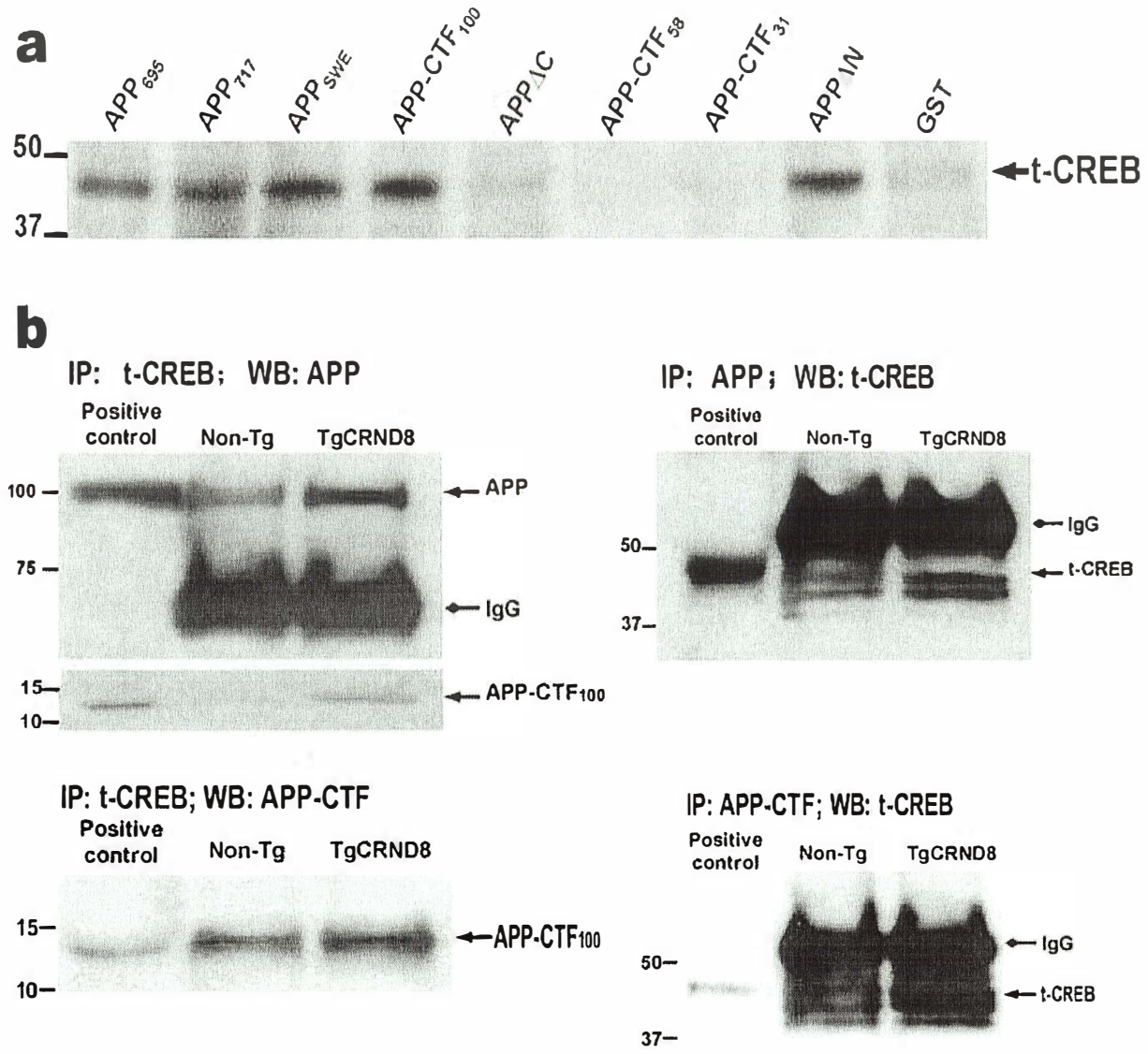

Figure 21. a, Precipitation of radiolabeled *in vitro* transcribed and translated CREB by APP and APP-CTFs glutathione *S*-transferase (GST) fusion proteins in a GST "pull-down" assay. GST fusion proteins of wt and mut APPs, APP-CTFs, deleted C-terminal APP (APPΔC), and deleted N-terminal APP (APPΔN) were immobilized on glutathione sepharose beads and incubated with *in vitro*-synthesized [^{35}S]-methione labeled CREB. The beads were pelleted, washed, and subjected to SDS-PAGE analysis.The 43 kDa CREB *in vitro* translation product is indicated. Note the absence of the 43 kDa band in the control GST lane. The results showed that CREB interacted with APP and APP-CTF$_{100}$, but not with shorter APP-CTFs. **b**, cytoplasmic lysates from cortical brain tissues were precleared with pre-immune serum and protein G agarose beads, followed by immunoprecipitated by t-CREB or APP or APP-CTF antibodies. The immunoprecipitated proteins were analysized in Westernblot by using appropriate antibodies. There was an increase in t-CREB immunocomplexed with APP/APP-CTF$_{100}$ in the TgCRND8 relative to the Non-Tg mice.

Similarly, in primary mouse cortical neuronal cultures, APP-CTF_{100} can be found in anti-t-CREB precipitated complexes, and that t-CREB is present in anti-APP-CTF_{100} precipitated complexes. As expected there was a significant increase in t-CREB that was detected in anti-APP-CTF_{100} precipitated complexes in the MCN of TgCRND8 mice relative to the Non-Tg (Figure 22a). Next, we examined the relevance of these interactions in AD by co-immunoprecipitation analyses on human brain samples from AD patients and age-sex matched controls. In both non-AD and AD cortical tissue lysates, t-CREB was detected in anti-APP-CTF_{100} precipitated complexes, and likewise APP-CTF_{100} was found in anti-t-CREB precipitated complexes (Figure 22b). Interestingly, there was a marked increase in the immunoprecipitated t-CREB complexed with APP-CTF_{100} in the AD samples compared to controls, and there was significant increase in the level of APP-CTF_{100} in the AD samples compared with the non-AD cases (Figure 22b). Together, these data suggest that CREB interacts with APP and APP-CTF_{100}.

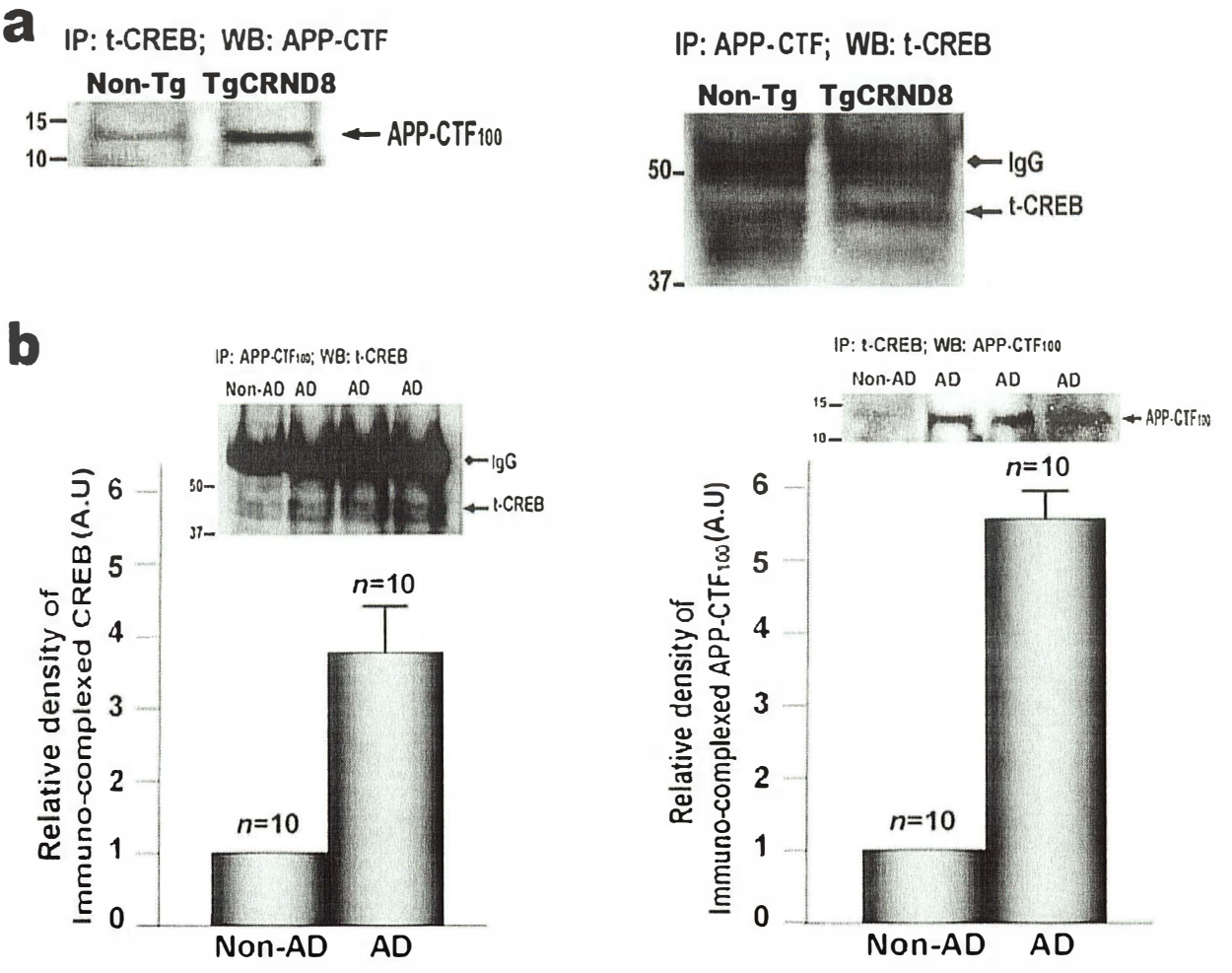

Figure 22. a, Co-immunoprecipitation analysis CREB and APP/APP-CTF$_{100}$ in MCN cell extracts from the Non-Tg and TgCRND8 mice brains. A significant (p<0.05) increase in t-CREB immuno-complexed with APP/APP-CTF in the TgCRND8 relative to the Non-Tg mice was observed. **b**, Co-immunoprecipitation analyses of CREB and APP/APP-CTF$_{100}$ in autopsied human brain samples from AD patients and age-sex matched controls. The insets show Western blotting of immunoprecipitated proteins. Quantification of the relative densities of the immunoprecipitated proteins. Estimates are the mean ± SEM for three independent experiments; p<0.05 *versus* Non-AD.

To further demonstrate our findings that APP and APP-CTF_{100} interacts with CREB and prevents its nuclear translocation, we employed differentiated rat B103 neuroblastoma cells, which do not express endogenous APP or APP-like proteins [187]. We transfected differentiated B103 cells with wt or mutAPP, and APP-CTF_{100} mammalian expression plasmids, and examined the distribution of CREB by immunofluorescent staining. The results demonstrated that both wt and mutAPP, and APP-CTF_{100} overexpression led to cytosolic anchoring of CREB that prevented its nuclear translocation (Figure 23). As expected in the controls (B103 cells and B103 cells with empty vector transfected), CREB was expressed mainly in the nuclei. Next, we also examined the distribution of CREB in MCN of the TgCRND8 mice, by manipulating endogenous APP levels. By knocking down the levels of endogenous APP by a specific small interference RNA [177], there was a significant increase in nuclear t-CREB levels compared to control siRNA (Figure 24). This result is consistent with our hypothesis that APP could influence the regulation of CREB nuclear translocation. We also examined if $A\beta_{42}$ may have effect on t-CREB localization by exposing MCN to $A\beta_{42}$, and staining for CREB. There was no difference in t-CREB distribution or expression between the $A\beta_{42}$-treated and untreated MCN (result not included), indicating that $A\beta_{42}$ may not directly contribute to the cytosolic anchoring of CREB.

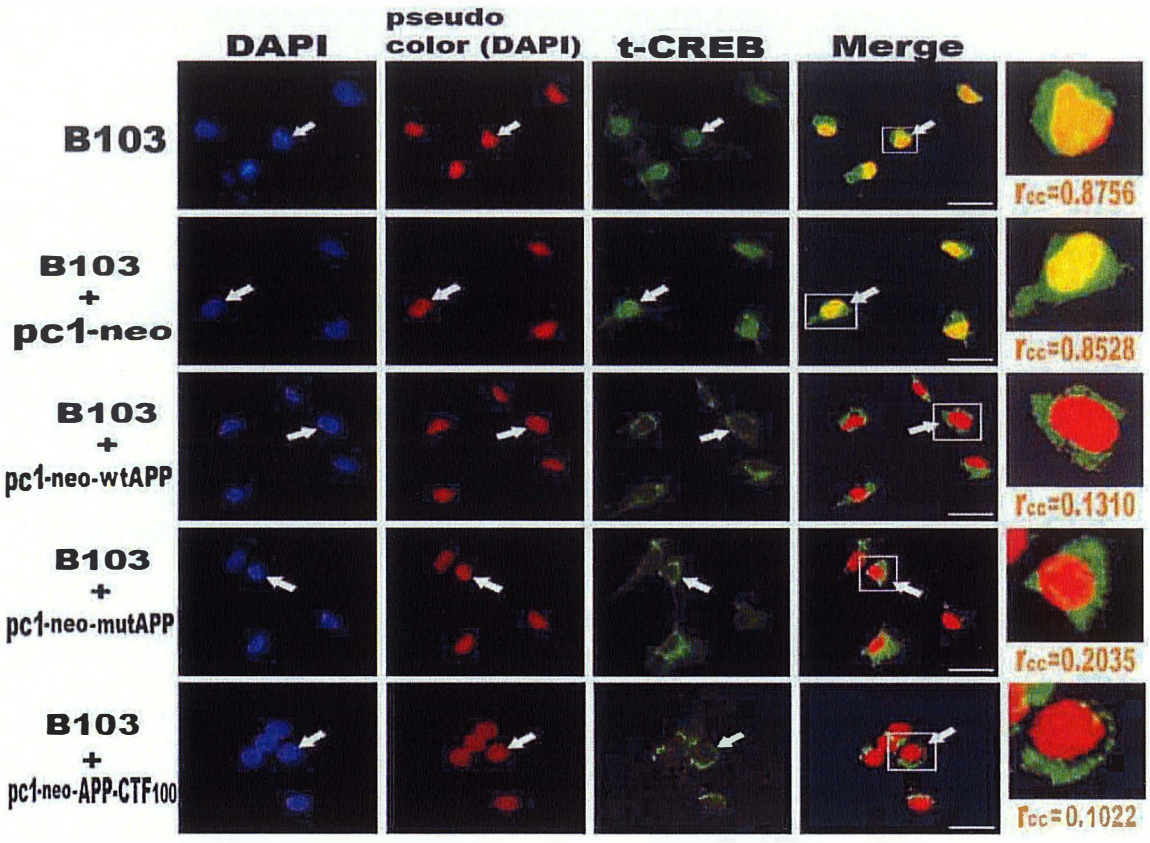

Figure 23. APP or APP-CTF_{100} acts as an anchoring site for localization of CREB in the cytoplasm. We transfected differentiated rat B103 neuroblastoma cells that do not express endogenous APP or APP-like proteins, with wt or mutAPP, and APP-CTF_{100} mammalian expression plasmids, and examined the distribution of CREB by immunofluorescent staining. CREB were expressed predominantly in cytoplasm of B103 cells that overexpress both wt and mutAPP, and APP-CTF_{100}. Nuclear CREB were detected in plain and empty vector (pc1-neo) transfected B103 cells. Cross co-localization coefficients (r_{cc}) are shown. Scale bar, 50 μm.

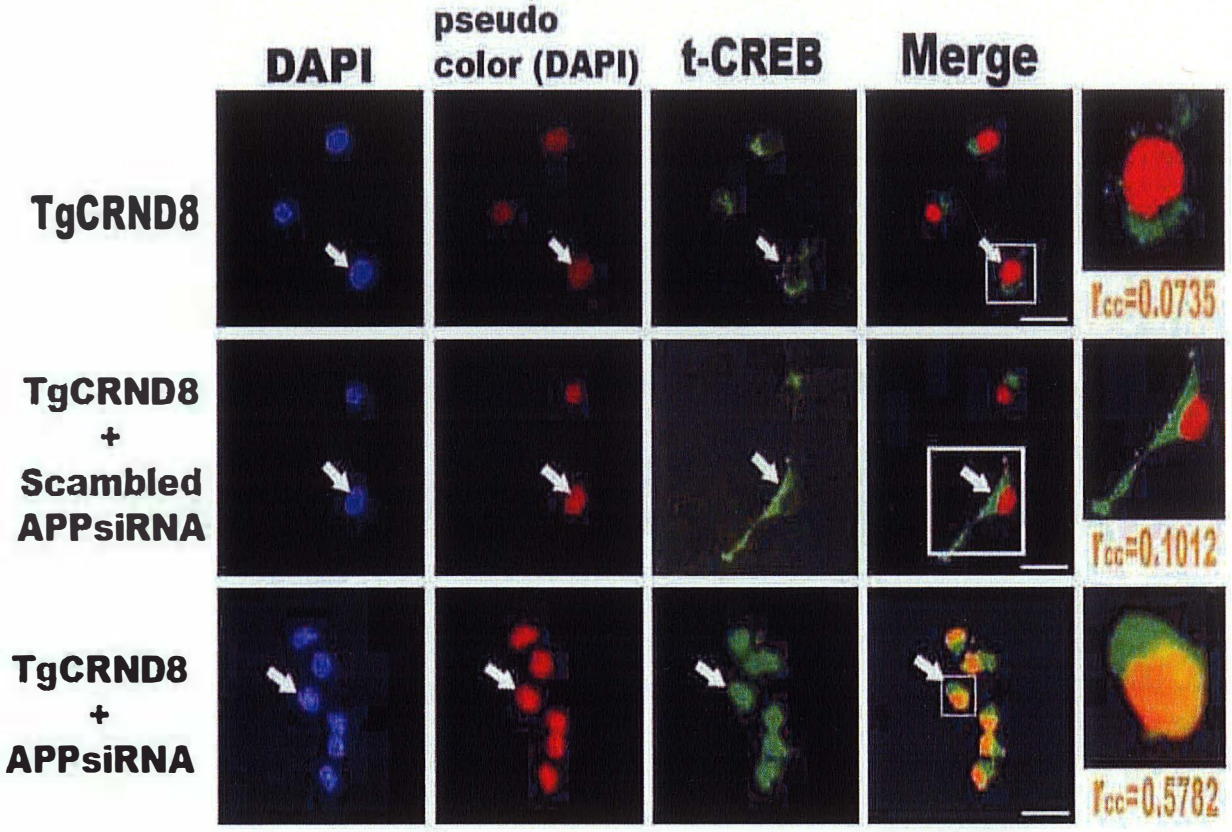

Figure 24. Total-CREB immunostaining in MCN from the TgCRND8 transfected with scambled APPsiRNA or APPsiRNA. The oligonucleotides of the APPsiRNA and scammbled APPsiRNA were duplexed, desalted, and transfected into MCN cultures from the TgCRND8 mice. Knocking down endogenous APP by siRNA led to CREB nuclear localization. Cross co-localization coefficients (r_{cc}) are shown. Scale bar, 50 μm.

Knowing that caspase-3 is the predominant caspase involved in APP- cleavage [156] and it is activated by Aβ [188], and that CREB is cleaved by caspase-3 during neuronal cell apoptosis [164], we tested whether caspase-3 interacts with t-CREB in both the TgCRND8 mice and human cortical brain samples from AD and non-AD cases. The tissue protein lysates were precleared with pre-immune serum and protein G agarose beads, followed by immunoprecipitated by t-CREB or active caspase-3 antibodies. The immunoprecipitated proteins were analysized in Westernblot by using active caspase-3 or t-CREB antibodies, respectively. As determined by co-immunoprecipitation, there was an interaction between t-CREB and active caspase-3 (Figure 25). This interaction was markedly higher in the TgCRND8 mice and AD samples, compared with the Non-Tg and non-AD cases. As APP is cleaved by casapse-3, this result raises the possibility of a multiple protein complex involving APP, CREB and caspase-3 *in vivo*.

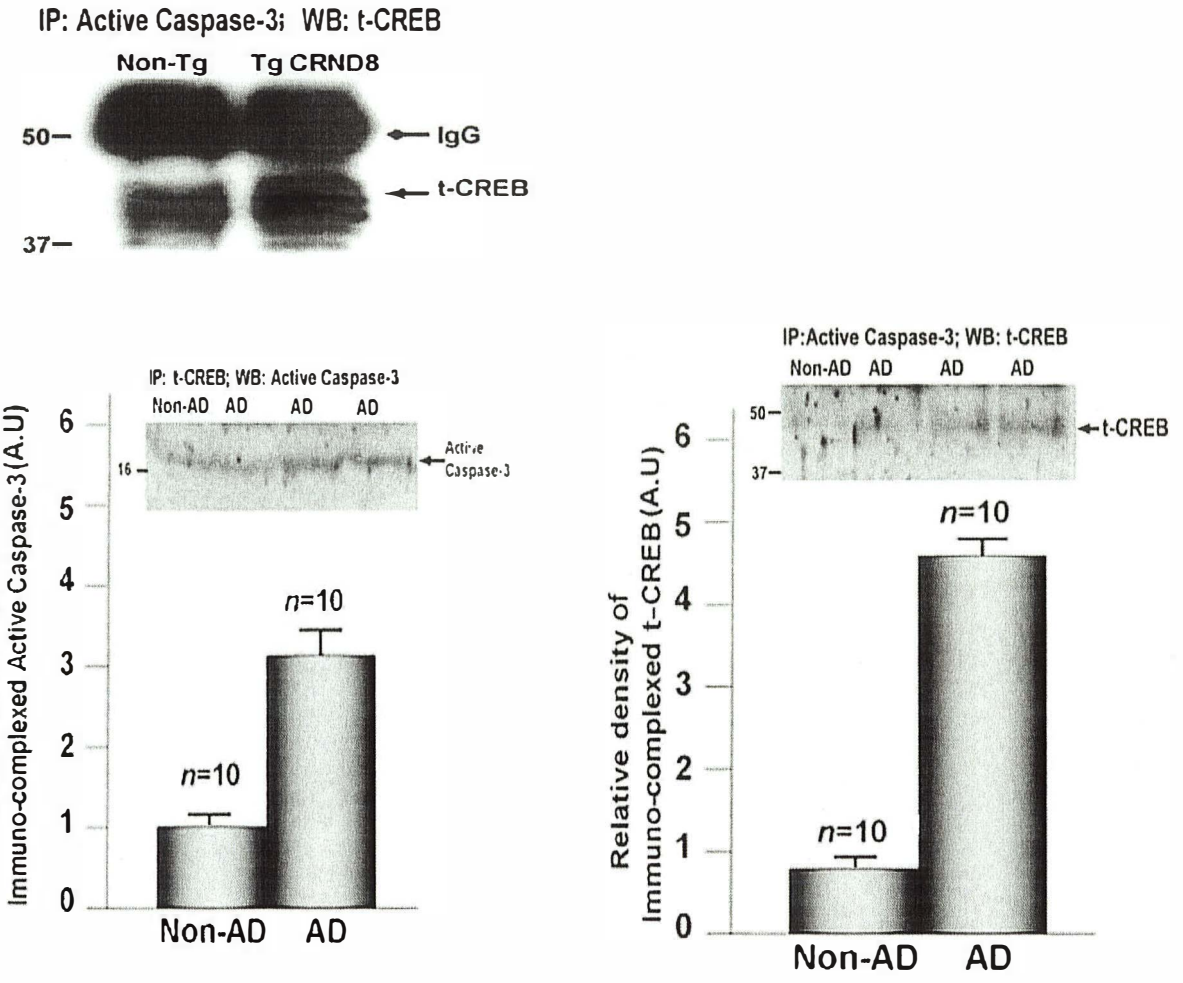

Figure 25. The tissue protein lysates were precleared with pre-immune serum and protein G agarose beads, followed by immunoprecipitated by t-CREB or active caspase-3 antibodies. The immunoprecipitated proteins were analysized in Western blot by using active caspase-3 or t-CREB antibodies, respectively. The results showed interaction between CREB and active Caspase-3 in the Non-Tg and TgCRND8 mice (top) and human brain samples; $p<0.05$ *versus* Non–Tg and Non-AD. The insets show Western blotting of immunoprecipitated proteins.

5.7. Decreased levels of Nuclear CREB is associated with apoptosis in cortical neurons from the TgCRND8 mice and Alzheimer disease brain

Considering that CREB attenuates $A\beta_{42}$-induced neurotoxicity and $A\beta_{42}$ is overexpressed in the TgCRND8 mice, we then sought to investigate the relationship between the differential localization of CREB and neuronal apoptosis (neurodegeneration) in AD. Apoptosis in fixed paraffin-embedded brain tissues (mice and human samples) was measured using TUNEL assay *In Situ cell detection Kit* reagents. The number of TUNEL positive cells in random fields was counted and normalized as percentage ratios to the total number of cells stained per field. The results showed that an age dependent increase in cortical neuronal apoptosis was observed in the TgCRND8 compared with the Non-Tg mice (Figure 26, left). Similarly, an increase in cortical neuronal apoptosis was observed in the sporadic AD over non-AD cases (Figure 26, right). These results suggest that, at least, in part, neuronal apoptosis contributes to neurodegeneration in cortical brain regions of the TgCRND8 mice and AD patients.

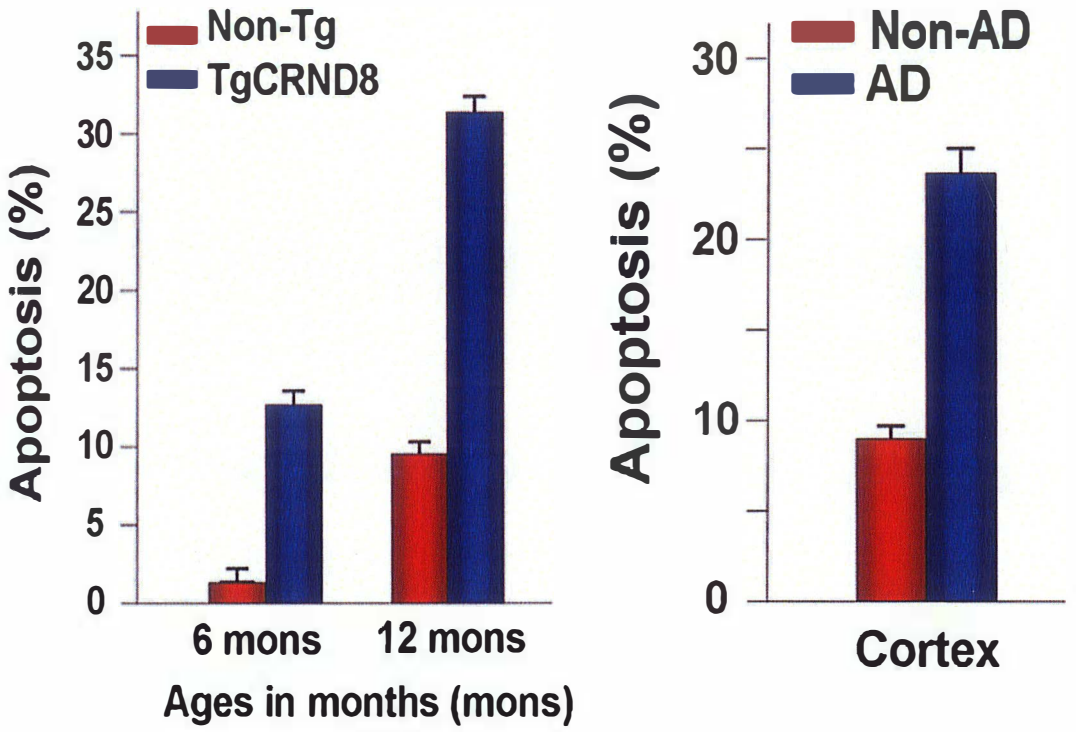

Figure 26. Quantitative analysis of apoptosis in cortical tissues from mice and autopsied human samples. Apoptosis was measured by TUNEL assay. The number of TUNEL positive cells in random fields was counted and normalized as percentage ratios to the total number of cells stained per field. An age dependent increase in cortical neuronal apoptosis was observed in the TgCRND8 compared with the Non-Tg mice (left). Similarly, an increase in cortical neuronal apoptosis was observed in the sporadic AD over non-AD cases (right), mean $\pm$SEM; $p<0.05$ *versus* Non-Tg and Non-AD.

As we have demonstrated that CREB protects neurons from $A\beta_{42}$- neurotoxity, we then tested the possibility that neurodegeneration in AD is associated with reduced nuclear CREB levels in cortical neurons. We determined neurodegeneration by measuring neuronal apoptosis. The mouse cortical slides of 12 months were performed by *in situ* Annexin V-FLUOS binding test. Cells that are undergoing apoptosis would be stained with Annexin V. Annexin positive cells (apoptotic cells) and CREB staining in cells were evaluated under the fluorescence microscope. We found that apoptotic cells have significantly less nuclear CREB immunoreactivity than non-apoptotic cells (Figure 27a). In particular, there was a significant inverse correlation between nuclear CREB levels and the number of apoptotic nuclei in cortical regions from the TgCRND8 mice (Figure 27b) and AD brains (Figure 27c), indicating that CREB neuroprotective activity is a specific response that is associated with its nuclear localization.

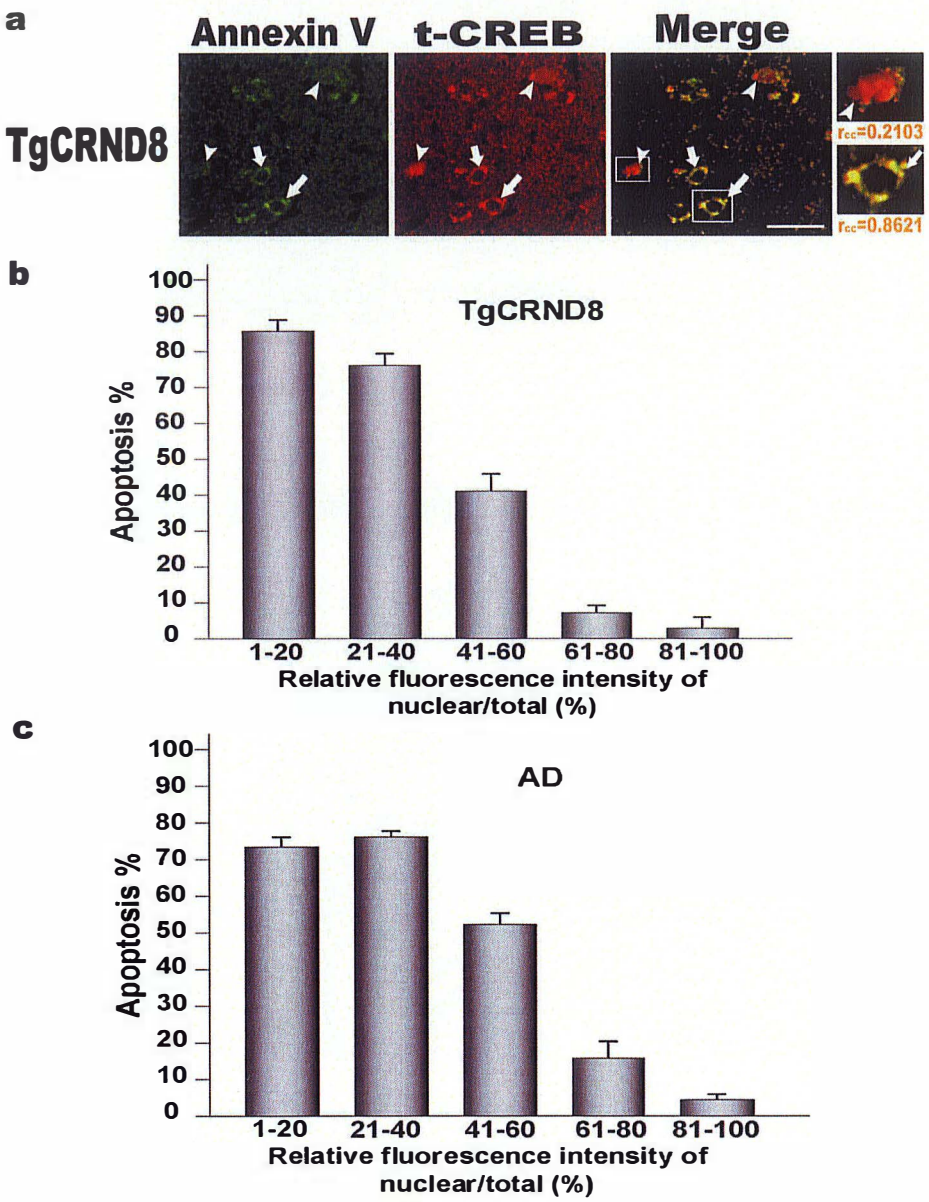

Figure 27. Apoptosis and t-CREB localization. The mouse cortical slides of 12 months and human samples were performed by Annexin V-FLUOS binding test. Annexin positive cells (apoptotic cells) and CREB staining in cells were evaluated under the fluorescence microscope.**a**, In situ labeling of apoptotic cells (Annexin V, Green) with little nuclear t-CREB expression (Texas Red) had been indicated by arrows, and non-apoptotic cells with nuclear CREB expression had been indicated by arrow heads. Apoptotic cells have less nuclear CREB immunoreactivity than non-apoptotic cells. Scale bar, 50μm. **b and c**, the number of apoptotic cells were accounted and the percentages of nuclear CREB in relative cells were analysized. The graphs present inverse correlations between cortical cell apoptosis and nuclear CREB expression in TgCRND8 and AD samples.

6. DISCUSSION

CREB regulates many aspects of neuronal function such as neuroprotection. Accumulating evidence suggests that CREB phosphorylation (presumably activation of CREB) is a protective response to neuronal damage [131]. It is expected, therefore, that neuronal loss in AD is likely to involve impairment of CREB signalling that is the prevailing hypothesis. The relevance of CREB to the pathogenesis of AD is supported by several studies *in vitro*. $A\beta_{42}$ impaired CREB phosphorylation at Ser133 in hippocampal neurons that was associated with decrease in long-term potential (LTP) [176], inhibition of neuronal activity-dependent CREB signaling [135], and induction of neuronal apoptosis [136]. Until now, no attempts have been made to examine this prevailing hypothesis in AD *in vivo*. Here, we have examined this hypothesis as it relates to neuronal apoptosis in a mouse model (TgCRND8) of FAD and in AD brains. Surprisingly, contrary to the prevailing hypothesis, there was no alteration in CREB phosphorylation in the FAD mice and AD brains. However, there was differential localization of CREB in the FAD mice and AD cases compared with controls. This differential localization (mislocalization) contributed to impairment of CREB signaling. We further demonstrate that CREB mediates downstream Bcl-2 transcription. Finally, we present evidence that degenerating neurons in AD and TgCRND8 mice have markedly reduced levels of nuclear

CREB relative to controls, and that CREB significantly interacts with APP or active caspase-3 in the TgCRND8 relative to the Non-Tg mice. The interactions could contribute to the neuronal apoptosis in the TgCRND8 mice and AD brains.

6.1. CREB phosphorylation is not impaired in AD *In vivo*

We have observed that there was no significant difference of the levels of t-CREB and p-CREBs (p-CREBSer133 and p-CREBSer129/133) between the Non-Tg and TgCRND8 mice. Similarly, no difference was observed between the Non-AD and AD brains. This finding is novel and unanticipated because it is contrary to the prevailing hypothesis. Consistently, we did not observe any difference in the PKA kinase activity and active GSK-3 levels. This observation is also in disagreement with the report that a reduction in p-CREB (Ser133) level has been observed in postmortem AD brains [189]. The discrepancy between these results could be due to several reasons: First, the difference in mean postmortem intervals, which were 37. 4 h (controls) and 42. 8 h for dementia of the Alzheimer type (DAT) [189] compared with 5.29 (Non-AD) and 5.92 h (AD) in our study. Second, heterogeneity in the stages and number of samples of the brain regions; NINCDS-ADRDA criteria and n=7 [189] versus Braak's stages and n=10 in the present study). Because of induction of

CREB phosphorylation in hippocampal and cortical neurons as a protective response after exposure to Aβ [190], and that Aβ can induce CREB phosphorylation [137], these observations indicate that in AD there may be a subpopulation of cells with increased p-CREB levels. These levels may counteract the decreased CREB levels that may be found in degenerating cells, resulting in no significant change in CREB phosphorylation. This view is consistent with our data. Our observations that t-CREB and p-CREBSer129/133 were expressed predominantly in the cytoplasm of brain cells in the TgCRND8 mice and AD cases, whereas they are expressed mainly in nuclei of brain cells in the Non-Tg mice and Non-AD cases. Surprisingly, there was no difference in the localization of p-CREB Ser133, indicating that it may require a secondary phosphorylation event to be activated [191]. These results suggest that p-CREBSer129/133 and t-CREB are mislocalized in AD and may reflect early pathological changes. This suggestion is supported by a previous report that in AD, the cytoplasm of cortical neurons was positively stained for ATF-2, one of the CREBs, but no such staining was seen in non-neurological cases [192]. The differential localization of CREBs that we have observed clearly represented an impairment of CREB signaling because phosphorylated CREBs are expected to be mainly localized in the nuclei. In support of this idea, CREB-DNA binding activity and CRE-mediated transcription were significantly higher in cortical tissues and MCN from the TgCRND8 mice compared to the Non-Tg.

6.2. What is the Role of CREB Localization and Phosphorylation in $A\beta_{42}$-Neurotoxicity?

We have altered CREB functions in several ways by overexpressing CA-CREB and K-CREB in human neuronal cells exposed to $A\beta_{42}$-neurotoxicity. When p-CREB function was negatively and positively regulated, there was an enhancement and reduction of $A\beta_{42}$-induced neurotoxicity respectively. This suggests that CREB phosphorylation may be important for survival after exposure to $A\beta_{42}$ in the excess level produced in the TgCRND8 mice. The experiment with the CRE-decoy oligonucleotide showed that CRE-mediated gene expression follows CREB phosphorylation. Evidence suggests that overexpression of Bcl-2 provides protection against neuronal apoptosis [184]. We have observed that Bcl-2 protein expression was significantly decreased in the TgCRND8 compared with the Non-Tg mice. Our results indicate that this decrease could be due to mislocalization of CREB to the cytoplasm instead of its nuclear location, resulting in decreased transcriptional activation of the Bcl-2 promoter which contains a CRE sequence. Indeed, reporter gene activity of a segment of this promoter with the CRE sequence was markedly reduced in the MCN of the TgCRND8 where CREB was localized mainly in the cytoplasm. Our findings suggest

that activation of CREB on its own is not sufficient to induce CRE-dependent transcription, but that the nuclear localization of CREB is critical in its neuroprotective role.

Moreover, decreased levels of nuclear CREB as we observed in brains tissues and cells of the TgCRND8 and AD cases may enhance sensitivity of neuronal cells to $A\beta_{42}$-toxicity. This view is consistent with our observation that cortical apoptotic neurons of the TgCRND8 mice and AD brains showed markedly reduced levels of nuclear CREB. Whether direct neuroprotection by CREB contributes to neuronal survival in the brain cannot be completely resolved by our data because in AD brain, increased levels of Bcl-2 have been reported [193]. Alternatively, this increase in Bcl-2 may not be due to CRE-mediated transcription in cells with reduced nuclear CREB, but rather from a subpopulation of non-apoptotic cells as a compensatory response in AD to protect the remaining neurons from apoptosis.

6.3. CREB Interaction with an Active Caspase-3 Complex could Contribute to Neurodegeneration in AD

There is increasing evidence to suggest that Aβ is not the only component of neurotoxicity associated with AD. There is also a role for APP to negatively

affect CREB signaling [71]. We have demonstrated that the mislocalization of t-CREB and p-CREBs to the cytoplasm instead of the nuclei of the TgCRND8 mice and AD cases may be due to overexpression of the mutAPP. APP may act as an anchoring site in the cytoplasm for CREB preventing its nuclear translocation. Since caspase-3 is involved in APP cleavage [156]and it is activated by Aβ [188], it was of interest to characterize the functional significance of the CREB/active caspase-3 complex. Studies have reported that CREB is cleaved by caspase-3 [164], and that calpain- and calcineurin-dependent proteolysis of the neuroprotective calcium/calmodulin-dependent protein kinase IV and CREB contributes to APP-induced neuronal death [194]. So our findings that formation of CREB/active caspase-3 complex need to be further investigated in its relations with neuronal death in AD. A new model of CREB regulation has been presented in the pathogenesis of AD (Figure 28). APP or its carboxy terminal fragments (APP-CTF) interacts with CREB in the cytoplasm, preventing its nuclear translocation. CREB phosphorylation on Serine 133 and 129 leads to its activation. Although CREB interacts with APP cytosolic domain, dual phosphorylated CREB translocates to nuclei and interact with the CRE binding site, resulting in transcription of CRE-dependent genes which contribute to neuro-protection, neuronal differentiation and synaptic plasticity. In AD, there is overexpression of APP-CTFs which sequester

CREB and phosphorylated CREBs. The pro-caspases are activated by $A\beta_{42}$. Active caspase-3 can also interact with CREB or phosphorylated CREBs, leading to impairment of CREB signaling. This disruption in CREB signaling sensitizes neurons to Aβ-induced toxicity and likely contributes to cell death in AD.

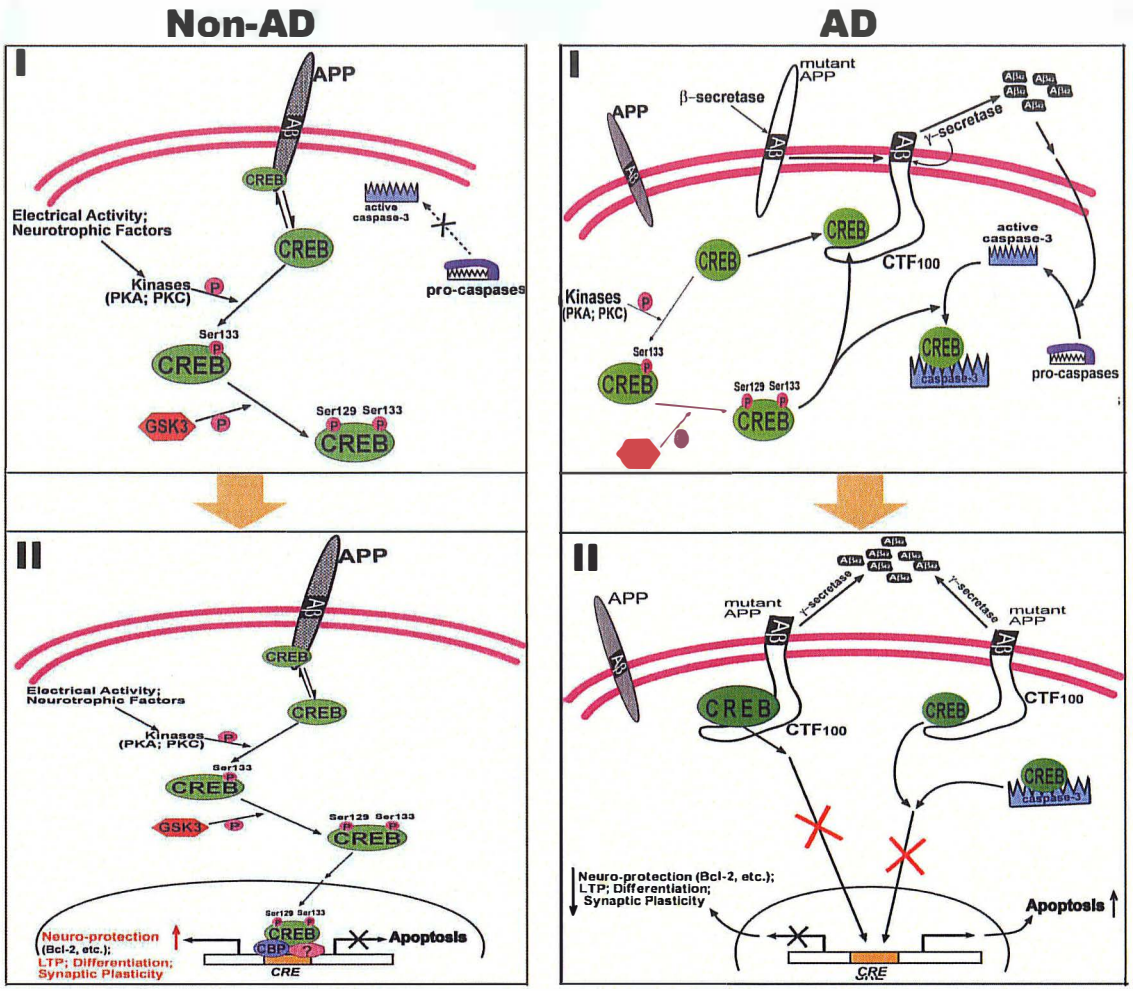

Figure 28. A model of CREB regulation in AD. APP or its carboxy terminal fragments (APP-CTF) interacts with CREB in the cytoplasm, preventing its nuclear translocation. CREB phosphorylation on Serine 133 and 129 leads to its activation. Although CREB interacts with APP cytosolic domain, dual phosphorylated CREB translocates to nuclei and interact with the CRE binding site, resulting in transcription of CRE-dependent genes which contribute to neuro-protection, neuronal differentiation and synaptic plasticity. In AD, there is overexpression of APP-CTFs which sequester CREB and phosphorylated CREBs. The pro-caspases are activated by $A\beta_{42}$. Active caspase-3 can also interact with CREB or phosphorylated CREBs, leading to impairment of CREB signaling. This disruption in CREB signaling sensitizes neurons to Aβ-induced toxicity and likely contributes to cell death in AD.

7. CONCLUSION

Regulation of CREB activation involves complex interactions among transcription factors, coactivators (CBP/p300), corepressors, kinases, acetylases, dephosphatases and histones. Our studies demonstrate for the first time that APP and its carboxyl terminal fragments could act as anchoring sites for CREB, inhibiting its nuclear translocation. This results in mislocalization of CREB to the cytoplasm. In the cytoplasm, CREB interacts with the APP and active caspase-3, which in turn affects CRE-dependent gene transcription, and ultimately contributes to neuronal apoptosis. Thus, mislocalization of CREB in the cytoplasm represents a novel finding of CREB regulation in the pathogenesis of AD. Differential localization of CREB may also help to explain the discrepancy between CREB phosphorylation and activation of CREB-dependent gene transcription. Since CREB plays a role in many diverse cellular processes, a similar mechanism involving the mislocalization of CREB may also play a role in the pathogenesis of other conditions.

8. ACKNOWLEDGEMENTS

First of all, I would like to sincerely thank my supervisor, Dr. Francis Amara, for his advice and help through my Master program. I really enjoyed all the time in our lab. I would like to thank my advisory committee, Dr. Etienne Leygue and Dr. Yuewen Gong for their advice and kind helps on my projects. They are the excellent advisors for students. I really appreciate my parents through my whole life for supporting me to study in North America. I would like to thank Mr. Pradeep Salins and Miss Kelly Olson for all of friendly helps during these two years, and thank my friends Miss Jianghong Fan and Miss Yu Sun for all the time with me. We really have spent a good time together. I also thank all my friends and professors who gave me advices and helps.

9. REFERENCES

1. Gottfries, C. G. (1988) Alzheimer's disease. A critical review. Compr Gerontol [C] **2**, 47-62
2. Gauthier, S. (2002) Advances in the pharmacotherapy of Alzheimer's disease. Cmaj **166**, 616-623
3. Turner, P. R., O'Connor, K., Tate, W. P. and Abraham, W. C. (2003) Roles of amyloid precursor protein and its fragments in regulating neural activity, plasticity and memory. Prog Neurobiol **70**, 1-32
4. Kang, J., Lemaire, H. G., Unterbeck, A., Salbaum, J. M., Masters, C. L., Grzeschik, K. H., Multhaup, G., Beyreuther, K. and Muller-Hill, B. (1987) The precursor of Alzheimer's disease amyloid A4 protein resembles a cell-surface receptor. Nature **325**, 733-736
5. Price, D. L. and Sisodia, S. S. (1998) Mutant genes in familial Alzheimer's disease and transgenic models. Annu Rev Neurosci **21**, 479-505
6. Alonso, A. C., Zaidi, T., Grundke-Iqbal, I. and Iqbal, K. (1994) Role of abnormally phosphorylated tau in the breakdown of microtubules in Alzheimer disease. Proc Natl Acad Sci U S A **91**, 5562-5566
7. Terry, R. D. (1998) The cytoskeleton in Alzheimer disease. J Neural Transm Suppl **53**, 141-145
8. Spillantini, M. G. and Goedert, M. (1998) Tau protein pathology in

neurodegenerative diseases. Trends Neurosci **21**, 428-433

9. Lee, V. M. and Trojanowski, J. Q. (1999) Neurodegenerative tauopathies: human disease and transgenic mouse models. Neuron **24**, 507-510

10. Lovestone, S. and Reynolds, C. H. (1997) The phosphorylation of tau: a critical stage in neurodevelopment and neurodegenerative processes. Neuroscience **78**, 309-324

11. Praprotnik, D., Smith, M. A., Richey, P. L., Vinters, H. V. and Perry, G. (1996) Filament heterogeneity within the dystrophic neurites of senile plaques suggests blockage of fast axonal transport in Alzheimer's disease. Acta Neuropathol (Berl) **91**, 226-235

12. Lewis, J., Dickson, D. W., Lin, W. L., Chisholm, L., Corral, A., Jones, G., Yen, S. H., Sahara, N., Skipper, L., Yager, D., Eckman, C., Hardy, J., Hutton, M. and McGowan, E. (2001) Enhanced neurofibrillary degeneration in transgenic mice expressing mutant tau and APP. Science **293**, 1487-1491

13. Zheng, W. H., Bastianetto, S., Mennicken, F., Ma, W. and Kar, S. (2002) Amyloid beta peptide induces tau phosphorylation and loss of cholinergic neurons in rat primary septal cultures. Neuroscience **115**, 201-211

14. Lemere, C. A., Maier, M., Jiang, L., Peng, Y. and Seabrook, T. J. (2006) Amyloid-beta immunotherapy for the prevention and treatment of Alzheimer disease: lessons from mice, monkeys, and humans. Rejuvenation Res **9**, 77-84

15. Zimmermann, M., Gardoni, F. and Di Luca, M. (2005) Molecular rationale for the pharmacological treatment of Alzheimer's disease. Drugs Aging **22 Suppl 1**, 27-37

16. Schmechel, D. E., Goldgaber, D., Burkhart, D. S., Gilbert, J. R., Gajdusek, D. C. and Roses, A. D. (1988) Cellular localization of messenger RNA encoding amyloid-beta-protein in normal tissue and in Alzheimer disease. Alzheimer Dis Assoc Disord **2**, 96-111

17. Ling, Y., Morgan, K. and Kalsheker, N. (2003) Amyloid precursor protein (APP) and the biology of proteolytic processing: relevance to Alzheimer's disease. Int J Biochem Cell Biol **35**, 1505-1535

18. Yamazaki, T., Selkoe, D. J. and Koo, E. H. (1995) Trafficking of cell surface beta-amyloid precursor protein: retrograde and transcytotic transport in cultured neurons. J Cell Biol **129**, 431-442

19. Selkoe, D. J. (1994) Normal and abnormal biology of the beta-amyloid precursor protein. Annu Rev Neurosci **17**, 489-517

20. Tanaka, S., Shiojiri, S., Takahashi, Y., Kitaguchi, N., Ito, H., Kameyama, M., Kimura, J., Nakamura, S. and Ueda, K. (1989) Tissue-specific expression of three types of beta-protein precursor mRNA: enhancement of protease inhibitor-harboring types in Alzheimer's disease brain. Biochem Biophys Res Commun **165**, 1406-1414

21. De Strooper, B. and Annaert, W. (2000) Proteolytic processing and cell

biological functions of the amyloid precursor protein. J Cell Sci **113 (Pt 11)**, 1857-1870

22. Chang, K. A. and Suh, Y. H. (2005) Pathophysiological roles of amyloidogenic carboxy-terminal fragments of the beta-amyloid precursor protein in Alzheimer's disease. J Pharmacol Sci **97**, 461-471

23. Citron, M., Oltersdorf, T., Haass, C., McConlogue, L., Hung, A. Y., Seubert, P., Vigo-Pelfrey, C., Lieberburg, I. and Selkoe, D. J. (1992) Mutation of the beta-amyloid precursor protein in familial Alzheimer's disease increases beta-protein production. Nature **360**, 672-674

24. Cai, X. D., Golde, T. E. and Younkin, S. G. (1993) Release of excess amyloid beta protein from a mutant amyloid beta protein precursor. Science **259**, 514-516

25. Suzuki, T., Oishi, M., Marshak, D. R., Czernik, A. J., Nairn, A. C. and Greengard, P. (1994) Cell cycle-dependent regulation of the phosphorylation and metabolism of the Alzheimer amyloid precursor protein. Embo J **13**, 1114-1122

26. Fraser, P. E., Levesque, L. and McLachlan, D. R. (1993) Biochemistry of Alzheimer's disease amyloid plaques. Clin Biochem **26**, 339-349

27. Higgins, G. A. and Jacobsen, H. (2003) Transgenic mouse models of Alzheimer's disease: phenotype and application. Behav Pharmacol **14**, 419-438

28. Yankner, B. A. (1996) Mechanisms of neuronal degeneration in Alzheimer's disease. Neuron **16**, 921-932

29. Geula, C., Wu, C. K., Saroff, D., Lorenzo, A., Yuan, M. and Yankner, B. A. (1998) Aging renders the brain vulnerable to amyloid beta-protein neurotoxicity. Nat Med **4**, 827-831

30. Behl, C., Davis, J. B., Lesley, R. and Schubert, D. (1994) Hydrogen peroxide mediates amyloid beta protein toxicity. Cell **77**, 817-827

31. Mattson MP, Tomaselli KJ and RE., R. (1993) Calcium-destabilizing and neurodegenerative effects of aggregated beta-amyloid peptide are attenuated by basic FGF. Brain Res. **621**, 35

32. Yan, S. D., Chen, X., Fu, J., Chen, M., Zhu, H., Roher, A., Slattery, T., Zhao, L., Nagashima, M., Morser, J., Migheli, A., Nawroth, P., Stern, D. and Schmidt, A. M. (1996) RAGE and amyloid-beta peptide neurotoxicity in Alzheimer's disease. Nature **382**, 685-691

33. Yaar, M., Zhai, S., Pilch, P. F., Doyle, S. M., Eisenhauer, P. B., Fine, R. E. and Gilchrest, B. A. (1997) Binding of beta-amyloid to the p75 neurotrophin receptor induces apoptosis. A possible mechanism for Alzheimer's disease. J Clin Invest **100**, 2333-2340

34. Nakagawa, T., Zhu, H., Morishima, N., Li, E., Xu, J., Yankner, B. A. and Yuan, J. (2000) Caspase-12 mediates endoplasmic-reticulum-specific apoptosis and cytotoxicity by amyloid-beta. Nature **403**, 98-103

35. Troy, C. M., Rabacchi, S. A., Friedman, W. J., Frappier, T. F., Brown, K. and Shelanski, M. L. (2000) Caspase-2 mediates neuronal cell death induced by beta-amyloid. J Neurosci **20**, 1386-1392

36. Giulian, D., Haverkamp, L. J., Yu, J. H., Karshin, W., Tom, D., Li, J., Kirkpatrick, J., Kuo, L. M. and Roher, A. E. (1996) Specific domains of beta-amyloid from Alzheimer plaque elicit neuron killing in human microglia. J Neurosci **16**, 6021-6037

37. Tan, J., Town, T., Paris, D., Mori, T., Suo, Z., Crawford, F., Mattson, M. P., Flavell, R. A. and Mullan, M. (1999) Microglial activation resulting from CD40-CD40L interaction after beta-amyloid stimulation. Science **286**, 2352-2355

38. Brown, D. R., Schmidt, B. and Kretzschmar, H. A. (1996) Role of microglia and host prion protein in neurotoxicity of a prion protein fragment. Nature **380**, 345-347

39. Cao, X. and Sudhof, T. C. (2004) Dissection of amyloid-beta precursor protein-dependent transcriptional transactivation. J Biol Chem **279**, 24601-24611

40. Breen, K. C., Bruce, M. and Anderton, B. H. (1991) Beta amyloid precursor protein mediates neuronal cell-cell and cell-surface adhesion. J Neurosci Res **28**, 90-100

41. Chen, M. and Yankner, B. A. (1991) An antibody to beta amyloid and the

amyloid precursor protein inhibits cell-substratum adhesion in many mammalian cell types. Neurosci Lett **125**, 223-226

42. Yankner, B. A., Caceres, A. and Duffy, L. K. (1990) Nerve growth factor potentiates the neurotoxicity of beta amyloid. Proc Natl Acad Sci U S A **87**, 9020-9023

43. Sabo, S. L., Ikin, A. F., Buxbaum, J. D. and Greengard, P. (2001) The Alzheimer amyloid precursor protein (APP) and FE65, an APP-binding protein, regulate cell movement. J Cell Biol **153**, 1403-1414

44. Mok, S. S., Sberna, G., Heffernan, D., Cappai, R., Galatis, D., Clarris, H. J., Sawyer, W. H., Beyreuther, K., Masters, C. L. and Small, D. H. (1997) Expression and analysis of heparin-binding regions of the amyloid precursor protein of Alzheimer's disease. FEBS Lett **415**, 303-307

45. Beher, D., Hesse, L., Masters, C. L. and Multhaup, G. (1996) Regulation of amyloid protein precursor (APP) binding to collagen and mapping of the binding sites on APP and collagen type I. J Biol Chem **271**, 1613-1620

46. Kibbey, M. C., Jucker, M., Weeks, B. S., Neve, R. L., Van Nostrand, W. E. and Kleinman, H. K. (1993) beta-Amyloid precursor protein binds to the neurite-promoting IKVAV site of laminin. Proc Natl Acad Sci U S A **90**, 10150-10153

47. Storey, E., Beyreuther, K. and Masters, C. L. (1996) Alzheimer's disease amyloid precursor protein on the surface of cortical neurons in primary

culture co-localizes with adhesion patch components. Brain Res **735**, 217-231

48. Annaert, W. G., Esselens, C., Baert, V., Boeve, C., Snellings, G., Cupers, P., Craessaerts, K. and De Strooper, B. (2001) Interaction with telencephalin and the amyloid precursor protein predicts a ring structure for presenilins. Neuron **32**, 579-589

49. Okamoto, T., Takeda, S., Murayama, Y., Ogata, E. and Nishimoto, I. (1995) Ligand-dependent G protein coupling function of amyloid transmembrane precursor. J Biol Chem **270**, 4205-4208

50. Lorenzo, A., Yuan, M., Zhang, Z., Paganetti, P. A., Sturchler-Pierrat, C., Staufenbiel, M., Mautino, J., Vigo, F. S., Sommer, B. and Yankner, B. A. (2000) Amyloid beta interacts with the amyloid precursor protein: a potential toxic mechanism in Alzheimer's disease. Nat Neurosci **3**, 460-464

51. White, A. R., Maher, F., Brazier, M. W., Jobling, M. F., Thyer, J., Stewart, L. R., Thompson, A., Gibson, R., Masters, C. L., Multhaup, G., Beyreuther, K., Barrow, C. J., Collins, S. J. and Cappai, R. (2003) Diverse fibrillar peptides directly bind the Alzheimer's amyloid precursor protein and amyloid precursor-like protein 2 resulting in cellular accumulation. Brain Res **966**, 231-244

52. da Cruz e Silva, E. F. and da Cruz e Silva, O. A. (2003) Protein phosphorylation and APP metabolism. Neurochem Res **28**, 1553-1561

53. Esposito, F., Ammendola, R., Duilio, A., Costanzo, F., Giordano, M., Zambrano, N., D'Agostino, P., Russo, T. and Cimino, F. (1990) Isolation of cDNA fragments hybridizing to rat brain-specific mRNAs. Dev Neurosci **12**, 373-381

54. Duilio, A., Zambrano, N., Mogavero, A. R., Ammendola, R., Cimino, F. and Russo, T. (1991) A rat brain mRNA encoding a transcriptional activator homologous to the DNA binding domain of retroviral integrases. Nucleic Acids Res **19**, 5269-5274

55. Simeone, A., Duilio, A., Fiore, F., Acampora, D., De Felice, C., Faraonio, R., Paolocci, F., Cimino, F. and Russo, T. (1994) Expression of the neuron-specific FE65 gene marks the development of embryo ganglionic derivatives. Dev Neurosci **16**, 53-60

56. Bressler, S. L., Gray, M. D., Sopher, B. L., Hu, Q., Hearn, M. G., Pham, D. G., Dinulos, M. B., Fukuchi, K., Sisodia, S. S., Miller, M. A., Disteche, C. M. and Martin, G. M. (1996) cDNA cloning and chromosome mapping of the human Fe65 gene: interaction of the conserved cytoplasmic domains of the human beta-amyloid precursor protein and its homologues with the mouse Fe65 protein. Hum Mol Genet **5**, 1589-1598

57. Russo, T., Faraonio, R., Minopoli, G., De Candia, P., De Renzis, S. and Zambrano, N. (1998) Fe65 and the protein network centered around the cytosolic domain of the Alzheimer's beta-amyloid precursor protein. FEBS

Lett **434**, 1-7

58. Fiore, F., Zambrano, N., Minopoli, G., Donini, V., Duilio, A. and Russo, T. (1995) The regions of the Fe65 protein homologous to the phosphotyrosine interaction/phosphotyrosine binding domain of Shc bind the intracellular domain of the Alzheimer's amyloid precursor protein. J Biol Chem **270**, 30853-30856

59. Zambrano, N., Buxbaum, J. D., Minopoli, G., Fiore, F., De Candia, P., De Renzis, S., Faraonio, R., Sabo, S., Cheetham, J., Sudol, M. and Russo, T. (1997) Interaction of the phosphotyrosine interaction/phosphotyrosine binding-related domains of Fe65 with wild-type and mutant Alzheimer's beta-amyloid precursor proteins. J Biol Chem **272**, 6399-6405

60. Kashour, T., Burton, T., Dibrov, A. and Amara, F. M. (2003) Late Simian virus 40 transcription factor is a target of the phosphoinositide 3-kinase/Akt pathway in anti-apoptotic Alzheimer's amyloid precursor protein signalling. Biochem J **370**, 1063-1075

61. Kim, H. S., Kim, E. M., Lee, J. P., Park, C. H., Kim, S., Seo, J. H., Chang, K. A., Yu, E., Jeong, S. J., Chong, Y. H. and Suh, Y. H. (2003) C-terminal fragments of amyloid precursor protein exert neurotoxicity by inducing glycogen synthase kinase-3beta expression. Faseb J **17**, 1951-1953

62. Lanier, L. M., Gates, M. A., Witke, W., Menzies, A. S., Wehman, A. M., Macklis, J. D., Kwiatkowski, D., Soriano, P. and Gertler, F. B. (1999) Mena

is required for neurulation and commissure formation. Neuron **22**, 313-325

63. Ermekova, K. S., Zambrano, N., Linn, H., Minopoli, G., Gertler, F., Russo, T. and Sudol, M. (1997) The WW domain of neural protein FE65 interacts with proline-rich motifs in Mena, the mammalian homolog of Drosophila enabled. J Biol Chem **272**, 32869-32877

64. Nishimoto, I., Okamoto, T., Matsuura, Y., Takahashi, S., Okamoto, T., Murayama, Y. and Ogata, E. (1993) Alzheimer amyloid protein precursor complexes with brain GTP-binding protein G(o). Nature **362**, 75-79

65. Schuch, U., Lohse, M. J. and Schachner, M. (1989) Neural cell adhesion molecules influence second messenger systems. Neuron **3**, 13-20

66. Strittmatter, S. M., Fishman, M. C. and Zhu, X. P. (1994) Activated mutants of the alpha subunit of G(o) promote an increased number of neurites per cell. J Neurosci **14**, 2327-2338

67. Sebok, K., Woodside, D., al-Aoukaty, A., Ho, A. D., Gluck, S. and Maghazachi, A. A. (1993) IL-8 induces the locomotion of human IL-2-activated natural killer cells. Involvement of a guanine nucleotide binding (Go) protein. J Immunol **150**, 1524-1534

68. Giambarella, U., Yamatsuji, T., Okamoto, T., Matsui, T., Ikezu, T., Murayama, Y., Levine, M. A., Katz, A., Gautam, N. and Nishimoto, I. (1997) G protein betagamma complex-mediated apoptosis by familial Alzheimer's disease mutant of APP. Embo J **16**, 4897-4907

69. Yamatsuji, T., Matsui, T., Okamoto, T., Komatsuzaki, K., Takeda, S., Fukumoto, H., Iwatsubo, T., Suzuki, N., Asami-Odaka, A., Ireland, S., Kinane, T. B., Giambarella, U. and Nishimoto, I. (1996) G protein-mediated neuronal DNA fragmentation induced by familial Alzheimer's disease-associated mutants of APP. Science **272**, 1349-1352

70. Yamatsuji, T., Okamoto, T., Takeda, S., Murayama, Y., Tanaka, N. and Nishimoto, I. (1996) Expression of V642 APP mutant causes cellular apoptosis as Alzheimer trait-linked phenotype. Embo J **15**, 498-509

71. Ikezu, T., Okamoto, T., Komatsuzaki, K., Matsui, T., Martyn, J. A. and Nishimoto, I. (1996) Negative transactivation of cAMP response element by familial Alzheimer's mutants of APP. Embo J **15**, 2468-2475

72. Zheng, P., Eastman, J., Vande Pol, S. and Pimplikar, S. W. (1998) PAT1, a microtubule-interacting protein, recognizes the basolateral sorting signal of amyloid precursor protein. Proc Natl Acad Sci U S A **95**, 14745-14750

73. Chow, N., Korenberg, J. R., Chen, X. N. and Neve, R. L. (1996) APP-BP1, a novel protein that binds to the carboxyl-terminal region of the amyloid precursor protein. J Biol Chem **271**, 11339-11346

74. Montminy, M. R. and Bilezikjian, L. M. (1987) Binding of a nuclear protein to the cyclic-AMP response element of the somatostatin gene. Nature **328**, 175-178

75. Brindle, P. K. and Montminy, M. R. (1992) The CREB family of

transcription activators. Curr Opin Genet Dev **2**, 199-204

76. Sassone-Corsi, P. (1995) Transcription factors responsive to cAMP. Annu Rev Cell Dev Biol **11**, 355-377

77. Haus-Seuffert, P. and Meisterernst, M. (2000) Mechanisms of transcriptional activation of cAMP-responsive element-binding protein CREB. Mol Cell Biochem **212**, 5-9

78. Hai, T. and Hartman, M. G. (2001) The molecular biology and nomenclature of the activating transcription factor/cAMP responsive element binding family of transcription factors: activating transcription factor proteins and homeostasis. Gene **273**, 1-11

79. Nakajima, T., Uchida, C., Anderson, S. F., Parvin, J. D. and Montminy, M. (1997) Analysis of a cAMP-responsive activator reveals a two-component mechanism for transcriptional induction via signal-dependent factors. Genes Dev **11**, 738-747

80. Rehfuss, R. P., Walton, K. M., Loriaux, M. M. and Goodman, R. H. (1991) The cAMP-regulated enhancer-binding protein ATF-1 activates transcription in response to cAMP-dependent protein kinase A. J Biol Chem **266**, 18431-18434

81. Laoide, B. M., Foulkes, N. S., Schlotter, F. and Sassone-Corsi, P. (1993) The functional versatility of CREM is determined by its modular structure. Embo J **12**, 1179-1191

82. Carlezon, W. A., Jr., Duman, R. S. and Nestler, E. J. (2005) The many faces of CREB. Trends Neurosci **28**, 436-445

83. Cha-Molstad, H., Keller, D. M., Yochum, G. S., Impey, S. and Goodman, R. H. (2004) Cell-type-specific binding of the transcription factor CREB to the cAMP-response element. Proc Natl Acad Sci U S A **101**, 13572-13577

84. Gonzalez, G. A. and Montminy, M. R. (1989) Cyclic AMP stimulates somatostatin gene transcription by phosphorylation of CREB at serine 133. Cell **59**, 675-680

85. Bonni, A., Ginty, D. D., Dudek, H. and Greenberg, M. E. (1995) Serine 133-phosphorylated CREB induces transcription via a cooperative mechanism that may confer specificity to neurotrophin signals. Mol Cell Neurosci **6**, 168-183

86. Wu, X. and McMurray, C. T. (2001) Calmodulin kinase II attenuation of gene transcription by preventing cAMP response element-binding protein (CREB) dimerization and binding of the CREB-binding protein. J Biol Chem **276**, 1735-1741

87. Matthews, R. P., Guthrie, C. R., Wailes, L. M., Zhao, X., Means, A. R. and McKnight, G. S. (1994) Calcium/calmodulin-dependent protein kinase types II and IV differentially regulate CREB-dependent gene expression. Mol Cell Biol **14**, 6107-6116

88. Alberts, A. S., Montminy, M., Shenolikar, S. and Feramisco, J. R. (1994)

Expression of a peptide inhibitor of protein phosphatase 1 increases phosphorylation and activity of CREB in NIH 3T3 fibroblasts. Mol Cell Biol **14**, 4398-4407

89. Hagiwara, M., Alberts, A., Brindle, P., Meinkoth, J., Feramisco, J., Deng, T., Karin, M., Shenolikar, S. and Montminy, M. (1992) Transcriptional attenuation following cAMP induction requires PP-1-mediated dephosphorylation of CREB. Cell **70**, 105-113

90. Wadzinski, B. E., Wheat, W. H., Jaspers, S., Peruski, L. F., Jr., Lickteig, R. L., Johnson, G. L. and Klemm, D. J. (1993) Nuclear protein phosphatase 2A dephosphorylates protein kinase A-phosphorylated CREB and regulates CREB transcriptional stimulation. Mol Cell Biol **13**, 2822-2834

91. Hongpaisan, J., Winters, C. A. and Andrews, S. B. (2003) Calcium-dependent mitochondrial superoxide modulates nuclear CREB phosphorylation in hippocampal neurons. Mol Cell Neurosci **24**, 1103-1115

92. Huang, H., Cheville, J. C., Pan, Y., Roche, P. C., Schmidt, L. J. and Tindall, D. J. (2001) PTEN induces chemosensitivity in PTEN-mutated prostate cancer cells by suppression of Bcl-2 expression. J Biol Chem **276**, 38830-38836

93. Fiol, C. J., Williams, J. S., Chou, C. H., Wang, Q. M., Roach, P. J. and Andrisani, O. M. (1994) A secondary phosphorylation of CREB341 at Ser129 is required for the cAMP-mediated control of gene expression. A role

for glycogen synthase kinase-3 in the control of gene expression. J Biol Chem **269**, 32187-32193

94. Johannessen, M., Delghandi, M. P., Seternes, O. M., Johansen, B. and Moens, U. (2004) Synergistic activation of CREB-mediated transcription by forskolin and phorbol ester requires PKC and depends on the glutamine-rich Q2 transactivation domain. Cell Signal **16**, 1187-1199

95. De Cesare, D., Jacquot, S., Hanauer, A. and Sassone-Corsi, P. (1998) Rsk-2 activity is necessary for epidermal growth factor-induced phosphorylation of CREB protein and transcription of c-fos gene. Proc Natl Acad Sci U S A **95**, 12202-12207

96. Xing, J., Kornhauser, J. M., Xia, Z., Thiele, E. A. and Greenberg, M. E. (1998) Nerve growth factor activates extracellular signal-regulated kinase and p38 mitogen-activated protein kinase pathways to stimulate CREB serine 133 phosphorylation. Mol Cell Biol **18**, 1946-1955

97. Lin, C. H., Yeh, S. H., Lin, C. H., Lu, K. T., Leu, T. H., Chang, W. C. and Gean, P. W. (2001) A role for the PI-3 kinase signaling pathway in fear conditioning and synaptic plasticity in the amygdala. Neuron **31**, 841-851

98. Perkinton, M. S., Ip, J. K., Wood, G. L., Crossthwaite, A. J. and Williams, R. J. (2002) Phosphatidylinositol 3-kinase is a central mediator of NMDA receptor signalling to MAP kinase (Erk1/2), Akt/PKB and CREB in striatal neurones. J Neurochem **80**, 239-254

99. Dash, P. K., Karl, K. A., Colicos, M. A., Prywes, R. and Kandel, E. R. (1991) cAMP response element-binding protein is activated by Ca2+/calmodulin- as well as cAMP-dependent protein kinase. Proc Natl Acad Sci U S A **88**, 5061-5065

100. Sheng, M., Thompson, M. A. and Greenberg, M. E. (1991) CREB: a Ca(2+)-regulated transcription factor phosphorylated by calmodulin-dependent kinases. Science **252**, 1427-1430

101. Shaywitz, A. J. and Greenberg, M. E. (1999) CREB: a stimulus-induced transcription factor activated by a diverse array of extracellular signals. Annu Rev Biochem **68**, 821-861

102. West, A. E., Chen, W. G., Dalva, M. B., Dolmetsch, R. E., Kornhauser, J. M., Shaywitz, A. J., Takasu, M. A., Tao, X. and Greenberg, M. E. (2001) Calcium regulation of neuronal gene expression. Proc Natl Acad Sci U S A **98**, 11024-11031

103. Anderson, K. A. and Means, A. R. (2002) Defective signaling in a subpopulation of CD4(+) T cells in the absence of Ca(2+)/calmodulin-dependent protein kinase IV. Mol Cell Biol **22**, 23-29

104. Ho, N., Liauw, J. A., Blaeser, F., Wei, F., Hanissian, S., Muglia, L. M., Wozniak, D. F., Nardi, A., Arvin, K. L., Holtzman, D. M., Linden, D. J., Zhuo, M., Muglia, L. J. and Chatila, T. A. (2000) Impaired synaptic plasticity and cAMP response element-binding protein activation in

Ca2+/calmodulin-dependent protein kinase type IV/Gr-deficient mice. J Neurosci **20**, 6459-6472

105. Kang, H., Sun, L. D., Atkins, C. M., Soderling, T. R., Wilson, M. A. and Tonegawa, S. (2001) An important role of neural activity-dependent CaMKIV signaling in the consolidation of long-term memory. Cell **106**, 771-783

106. Ribar, T. J., Rodriguiz, R. M., Khiroug, L., Wetsel, W. C., Augustine, G. J. and Means, A. R. (2000) Cerebellar defects in Ca2+/calmodulin kinase IV-deficient mice. J Neurosci **20**, RC107

107. Wei, F., Qiu, C. S., Liauw, J., Robinson, D. A., Ho, N., Chatila, T. and Zhuo, M. (2002) Calcium calmodulin-dependent protein kinase IV is required for fear memory. Nat Neurosci **5**, 573-579

108. Ferrer, I., Marin, C., Rey, M. J., Ribalta, T., Goutan, E., Blanco, R., Tolosa, E. and Marti, E. (1999) BDNF and full-length and truncated TrkB expression in Alzheimer disease. Implications in therapeutic strategies. J Neuropathol Exp Neurol **58**, 729-739

109. Connor, B., Young, D., Yan, Q., Faull, R. L., Synek, B. and Dragunow, M. (1997) Brain-derived neurotrophic factor is reduced in Alzheimer's disease. Brain Res Mol Brain Res **49**, 71-81

110. Bading, H., Ginty, D. D. and Greenberg, M. E. (1993) Regulation of gene expression in hippocampal neurons by distinct calcium signaling pathways.

Science **260**, 181-186

111. Davis, S., Vanhoutte, P., Pages, C., Caboche, J. and Laroche, S. (2000) The MAPK/ERK cascade targets both Elk-1 and cAMP response element-binding protein to control long-term potentiation-dependent gene expression in the dentate gyrus in vivo. J Neurosci **20**, 4563-4572

112. Dolmetsch, R. E., Pajvani, U., Fife, K., Spotts, J. M. and Greenberg, M. E. (2001) Signaling to the nucleus by an L-type calcium channel-calmodulin complex through the MAP kinase pathway. Science **294**, 333-339

113. Silva, A. J., Kogan, J. H., Frankland, P. W. and Kida, S. (1998) CREB and memory. Annu Rev Neurosci **21**, 127-148

114. Hsia, A. Y., Masliah, E., McConlogue, L., Yu, G. Q., Tatsuno, G., Hu, K., Kholodenko, D., Malenka, R. C., Nicoll, R. A. and Mucke, L. (1999) Plaque-independent disruption of neural circuits in Alzheimer's disease mouse models. Proc Natl Acad Sci U S A **96**, 3228-3233

115. Yin, J. C., Del Vecchio, M., Zhou, H. and Tully, T. (1995) CREB as a memory modulator: induced expression of a dCREB2 activator isoform enhances long-term memory in Drosophila. Cell **81**, 107-115

116. Josselyn, S. A., Shi, C., Carlezon, W. A., Jr., Neve, R. L., Nestler, E. J. and Davis, M. (2001) Long-term memory is facilitated by cAMP response element-binding protein overexpression in the amygdala. J Neurosci **21**, 2404-2412

117. Muller, D., Nikonenko, I., Jourdain, P. and Alberi, S. (2002) LTP, memory and structural plasticity. Curr Mol Med **2**, 605-611

118. Holscher, C. (1999) Synaptic plasticity and learning and memory: LTP and beyond. J Neurosci Res **58**, 62-75

119. Hummler, E., Cole, T. J., Blendy, J. A., Ganss, R., Aguzzi, A., Schmid, W., Beermann, F. and Schutz, G. (1994) Targeted mutation of the CREB gene: compensation within the CREB/ATF family of transcription factors. Proc Natl Acad Sci U S A **91**, 5647-5651

120. Bourtchuladze, R., Frenguelli, B., Blendy, J., Cioffi, D., Schutz, G. and Silva, A. J. (1994) Deficient long-term memory in mice with a targeted mutation of the cAMP-responsive element-binding protein. Cell **79**, 59-68

121. Kogan, J. H., Frankland, P. W., Blendy, J. A., Coblentz, J., Marowitz, Z., Schutz, G. and Silva, A. J. (1997) Spaced training induces normal long-term memory in CREB mutant mice. Curr Biol **7**, 1-11

122. Pham, T. A., Impey, S., Storm, D. R. and Stryker, M. P. (1999) CRE-mediated gene transcription in neocortical neuronal plasticity during the developmental critical period. Neuron **22**, 63-72

123. Deisseroth, K., Heist, E. K. and Tsien, R. W. (1998) Translocation of calmodulin to the nucleus supports CREB phosphorylation in hippocampal neurons. Nature **392**, 198-202

124. Schulz, S., Siemer, H., Krug, M. and Hollt, V. (1999) Direct evidence for

biphasic cAMP responsive element-binding protein phosphorylation during long-term potentiation in the rat dentate gyrus in vivo. J Neurosci **19**, 5683-5692

125. Taubenfeld, S. M., Wiig, K. A., Monti, B., Dolan, B., Pollonini, G. and Alberini, C. M. (2001) Fornix-dependent induction of hippocampal CCAAT enhancer-binding protein [beta] and [delta] Co-localizes with phosphorylated cAMP response element-binding protein and accompanies long-term memory consolidation. J Neurosci **21**, 84-91

126. Stanciu, M., Radulovic, J. and Spiess, J. (2001) Phosphorylated cAMP response element binding protein in the mouse brain after fear conditioning: relationship to Fos production. Brain Res Mol Brain Res **94**, 15-24

127. Guzowski, J. F. and McGaugh, J. L. (1997) Antisense oligodeoxynucleotide-mediated disruption of hippocampal cAMP response element binding protein levels impairs consolidation of memory for water maze training. Proc Natl Acad Sci U S A **94**, 2693-2698

128. Bonni, A., Brunet, A., West, A. E., Datta, S. R., Takasu, M. A. and Greenberg, M. E. (1999) Cell survival promoted by the Ras-MAPK signaling pathway by transcription-dependent and -independent mechanisms. Science **286**, 1358-1362

129. Riccio, A., Ahn, S., Davenport, C. M., Blendy, J. A. and Ginty, D. D. (1999) Mediation by a CREB family transcription factor of NGF-dependent

survival of sympathetic neurons. Science **286**, 2358-2361

130. Walton, M., Woodgate, A. M., Muravlev, A., Xu, R., During, M. J. and Dragunow, M. (1999) CREB phosphorylation promotes nerve cell survival. J Neurochem **73**, 1836-1842

131. Mabuchi, T., Kitagawa, K., Kuwabara, K., Takasawa, K., Ohtsuki, T., Xia, Z., Storm, D., Yanagihara, T., Hori, M. and Matsumoto, M. (2001) Phosphorylation of cAMP response element-binding protein in hippocampal neurons as a protective response after exposure to glutamate in vitro and ischemia in vivo. J Neurosci **21**, 9204-9213

132. Riccio, A., Pierchala, B. A., Ciarallo, C. L. and Ginty, D. D. (1997) An NGF-TrkA-mediated retrograde signal to transcription factor CREB in sympathetic neurons. Science **277**, 1097-1100

133. Glover, C. P., Heywood, D. J., Bienemann, A. S., Deuschle, U., Kew, J. N. and Uney, J. B. (2004) Adenoviral expression of CREB protects neurons from apoptotic and excitotoxic stress. Neuroreport **15**, 1171-1175

134. Freeland, K., Boxer, L. M. and Latchman, D. S. (2001) The cyclic AMP response element in the Bcl-2 promoter confers inducibility by hypoxia in neuronal cells. Brain Res Mol Brain Res **92**, 98-106

135. Tong, L., Thornton, P. L., Balazs, R. and Cotman, C. W. (2001) Beta -amyloid-(1-42) impairs activity-dependent cAMP-response element-binding protein signaling in neurons at concentrations in which cell

survival Is not compromised. J Biol Chem **276**, 17301-17306

136. Watson, K. and Fan, G. H. (2005) Macrophage inflammatory protein 2 inhibits beta-amyloid peptide (1-42)-mediated hippocampal neuronal apoptosis through activation of mitogen-activated protein kinase and phosphatidylinositol 3-kinase signaling pathways. Mol Pharmacol **67**, 757-765

137. Sato, N., Kamino, K., Tateishi, K., Satoh, T., Nishiwaki, Y., Yoshiiwa, A., Miki, T. and Ogihara, T. (1997) Elevated amyloid beta protein(1-40) level induces CREB phosphorylation at serine-133 via p44/42 MAP kinase (Erk1/2)-dependent pathway in rat pheochromocytoma PC12 cells. Biochem Biophys Res Commun **232**, 637-642

138. Echeverria, V., Ducatenzeiler, A., Chen, C. H. and Cuello, A. C. (2005) Endogenous beta-amyloid peptide synthesis modulates cAMP response element-regulated gene expression in PC12 cells. Neuroscience **135**, 1193-1202

139. Sheng, M. and Greenberg, M. E. (1990) The regulation and function of c-fos and other immediate early genes in the nervous system. Neuron **4**, 477-485

140. Greenberg, M. E. and Ziff, E. B. (1984) Stimulation of 3T3 cells induces transcription of the c-fos proto-oncogene. Nature **311**, 433-438

141. Sheng, M., McFadden, G. and Greenberg, M. E. (1990) Membrane depolarization and calcium induce c-fos transcription via phosphorylation of

transcription factor CREB. Neuron **4**, 571-582

142. Ginty, D. D., Bonni, A. and Greenberg, M. E. (1994) Nerve growth factor activates a Ras-dependent protein kinase that stimulates c-fos transcription via phosphorylation of CREB. Cell **77**, 713-725

143. Fisch, T. M., Prywes, R., Simon, M. C. and Roeder, R. G. (1989) Multiple sequence elements in the c-fos promoter mediate induction by cAMP. Genes Dev **3**, 198-211

144. Berkowitz, L. A., Riabowol, K. T. and Gilman, M. Z. (1989) Multiple sequence elements of a single functional class are required for cyclic AMP responsiveness of the mouse c-fos promoter. Mol Cell Biol **9**, 4272-4281

145. Patterson, S. L., Grover, L. M., Schwartzkroin, P. A. and Bothwell, M. (1992) Neurotrophin expression in rat hippocampal slices: a stimulus paradigm inducing LTP in CA1 evokes increases in BDNF and NT-3 mRNAs. Neuron **9**, 1081-1088

146. Zafra, F., Hengerer, B., Leibrock, J., Thoenen, H. and Lindholm, D. (1990) Activity dependent regulation of BDNF and NGF mRNAs in the rat hippocampus is mediated by non-NMDA glutamate receptors. Embo J **9**, 3545-3550

147. Loo, D. T., Copani, A., Pike, C. J., Whittemore, E. R., Walencewicz, A. J. and Cotman, C. W. (1993) Apoptosis is induced by beta-amyloid in cultured central nervous system neurons. Proc Natl Acad Sci U S A **90**, 7951-7955

148. Ivins, K. J., Ivins, J. K., Sharp, J. P. and Cotman, C. W. (1999) Multiple pathways of apoptosis in PC12 cells. CrmA inhibits apoptosis induced by beta-amyloid. J Biol Chem **274**, 2107-2112

149. Ivins, K. J., Thornton, P. L., Rohn, T. T. and Cotman, C. W. (1999) Neuronal apoptosis induced by beta-amyloid is mediated by caspase-8. Neurobiol Dis **6**, 440-449

150. Gamblin, T. C., Chen, F., Zambrano, A., Abraha, A., Lagalwar, S., Guillozet, A. L., Lu, M., Fu, Y., Garcia-Sierra, F., LaPointe, N., Miller, R., Berry, R. W., Binder, L. I. and Cryns, V. L. (2003) Caspase cleavage of tau: linking amyloid and neurofibrillary tangles in Alzheimer's disease. Proc Natl Acad Sci U S A **100**, 10032-10037

151. Rissman, R. A., Poon, W. W., Blurton-Jones, M., Oddo, S., Torp, R., Vitek, M. P., LaFerla, F. M., Rohn, T. T. and Cotman, C. W. (2004) Caspase-cleavage of tau is an early event in Alzheimer disease tangle pathology. J Clin Invest **114**, 121-130

152. Canu, N., Dus, L., Barbato, C., Ciotti, M. T., Brancolini, C., Rinaldi, A. M., Novak, M., Cattaneo, A., Bradbury, A. and Calissano, P. (1998) Tau cleavage and dephosphorylation in cerebellar granule neurons undergoing apoptosis. J Neurosci **18**, 7061-7074

153. Chung, C. W., Song, Y. H., Kim, I. K., Yoon, W. J., Ryu, B. R., Jo, D. G., Woo, H. N., Kwon, Y. K., Kim, H. H., Gwag, B. J., Mook-Jung, I. H. and

Jung, Y. K. (2001) Proapoptotic effects of tau cleavage product generated by caspase-3. Neurobiol Dis **8**, 162-172

154. Guo, H., Albrecht, S., Bourdeau, M., Petzke, T., Bergeron, C. and LeBlanc, A. C. (2004) Active caspase-6 and caspase-6-cleaved tau in neuropil threads, neuritic plaques, and neurofibrillary tangles of Alzheimer's disease. Am J Pathol **165**, 523-531

155. Horowitz, P. M., Patterson, K. R., Guillozet-Bongaarts, A. L., Reynolds, M. R., Carroll, C. A., Weintraub, S. T., Bennett, D. A., Cryns, V. L., Berry, R. W. and Binder, L. I. (2004) Early N-terminal changes and caspase-6 cleavage of tau in Alzheimer's disease. J Neurosci **24**, 7895-7902

156. Gervais, F. G., Xu, D., Robertson, G. S., Vaillancourt, J. P., Zhu, Y., Huang, J., LeBlanc, A., Smith, D., Rigby, M., Shearman, M. S., Clarke, E. E., Zheng, H., Van Der Ploeg, L. H., Ruffolo, S. C., Thornberry, N. A., Xanthoudakis, S., Zamboni, R. J., Roy, S. and Nicholson, D. W. (1999) Involvement of caspases in proteolytic cleavage of Alzheimer's amyloid-beta precursor protein and amyloidogenic A beta peptide formation. Cell **97**, 395-406

157. Pellegrini, L., Passer, B. J., Tabaton, M., Ganjei, J. K. and D'Adamio, L. (1999) Alternative, non-secretase processing of Alzheimer's beta-amyloid precursor protein during apoptosis by caspase-6 and -8. J Biol Chem **274**, 21011-21016

158. LeBlanc, A., Liu, H., Goodyer, C., Bergeron, C. and Hammond, J. (1999)

Caspase-6 role in apoptosis of human neurons, amyloidogenesis, and Alzheimer's disease. J Biol Chem **274**, 23426-23436

159. Weidemann, A., Paliga, K., Durrwang, U., Reinhard, F. B., Schuckert, O., Evin, G. and Masters, C. L. (1999) Proteolytic processing of the Alzheimer's disease amyloid precursor protein within its cytoplasmic domain by caspase-like proteases. J Biol Chem **274**, 5823-5829

160. Lazebnik, Y. A., Kaufmann, S. H., Desnoyers, S., Poirier, G. G. and Earnshaw, W. C. (1994) Cleavage of poly(ADP-ribose) polymerase by a proteinase with properties like ICE. Nature **371**, 346-347

161. Kothakota, S., Azuma, T., Reinhard, C., Klippel, A., Tang, J., Chu, K., McGarry, T. J., Kirschner, M. W., Koths, K., Kwiatkowski, D. J. and Williams, L. T. (1997) Caspase-3-generated fragment of gelsolin: effector of morphological change in apoptosis. Science **278**, 294-298

162. Widmann, C., Gibson, S. and Johnson, G. L. (1998) Caspase-dependent cleavage of signaling proteins during apoptosis. A turn-off mechanism for anti-apoptotic signals. J Biol Chem **273**, 7141-7147

163. Francois, F. and Grimes, M. L. (1999) Phosphorylation-dependent Akt cleavage in neural cell in vitro reconstitution of apoptosis. J Neurochem **73**, 1773-1776

164. Francois, F., Godinho, M. J. and Grimes, M. L. (2000) CREB is cleaved by caspases during neural cell apoptosis. FEBS Lett **486**, 281-284

165. Korsmeyer, S. J. (1999) BCL-2 gene family and the regulation of programmed cell death. Cancer Res **59**, 1693s-1700s

166. Mah, S. P., Zhong, L. T., Liu, Y., Roghani, A., Edwards, R. H. and Bredesen, D. E. (1993) The protooncogene bcl-2 inhibits apoptosis in PC12 cells. J Neurochem **60**, 1183-1186

167. Farlie, P. G., Dringen, R., Rees, S. M., Kannourakis, G. and Bernard, O. (1995) bcl-2 transgene expression can protect neurons against developmental and induced cell death. Proc Natl Acad Sci U S A **92**, 4397-4401

168. Allsopp, T. E., Wyatt, S., Paterson, H. F. and Davies, A. M. (1993) The proto-oncogene bcl-2 can selectively rescue neurotrophic factor-dependent neurons from apoptosis. Cell **73**, 295-307

169. Garcia, I., Martinou, I., Tsujimoto, Y. and Martinou, J. C. (1992) Prevention of programmed cell death of sympathetic neurons by the bcl-2 proto-oncogene. Science **258**, 302-304

170. Martinou, J. C., Dubois-Dauphin, M., Staple, J. K., Rodriguez, I., Frankowski, H., Missotten, M., Albertini, P., Talabot, D., Catsicas, S., Pietra, C. and et al. (1994) Overexpression of BCL-2 in transgenic mice protects neurons from naturally occurring cell death and experimental ischemia. Neuron **13**, 1017-1030

171. Krajewski, S., Tanaka, S., Takayama, S., Schibler, M. J., Fenton, W. and

Reed, J. C. (1993) Investigation of the subcellular distribution of the bcl-2 oncoprotein: residence in the nuclear envelope, endoplasmic reticulum, and outer mitochondrial membranes. Cancer Res **53**, 4701-4714

172. Davies, A. M. (1995) The Bcl-2 family of proteins, and the regulation of neuronal survival. Trends Neurosci **18**, 355-358

173. Chishti, M. A., Yang, D. S., Janus, C., Phinney, A. L., Horne, P., Pearson, J., Strome, R., Zuker, N., Loukides, J., French, J., Turner, S., Lozza, G., Grilli, M., Kunicki, S., Morissette, C., Paquette, J., Gervais, F., Bergeron, C., Fraser, P. E., Carlson, G. A., George-Hyslop, P. S. and Westaway, D. (2001) Early-onset amyloid deposition and cognitive deficits in transgenic mice expressing a double mutant form of amyloid precursor protein 695. J Biol Chem **276**, 21562-21570

174. Pike, C. J. and Cotman, C. W. (1993) Cultured GABA-immunoreactive neurons are resistant to toxicity induced by beta-amyloid. Neuroscience **56**, 269-274

175. Sun, A., Liu, M., Nguyen, X. V. and Bing, G. (2003) P38 MAP kinase is activated at early stages in Alzheimer's disease brain. Exp Neurol **183**, 394-405

176. Vitolo, O. V., Sant'Angelo, A., Costanzo, V., Battaglia, F., Arancio, O. and Shelanski, M. (2002) Amyloid beta -peptide inhibition of the PKA/CREB pathway and long-term potentiation: reversibility by drugs that enhance

cAMP signaling. Proc Natl Acad Sci U S A **99**, 13217-13221

177. Herard, A. S., Besret, L., Dubois, A., Dauguet, J., Delzescaux, T., Hantraye, P., Bonvento, G. and Moya, K. L. (2005) siRNA targeted against amyloid precursor protein impairs synaptic activity in vivo. Neurobiol Aging

178. Delatour, B., Mercken, L., El Hachimi, K. H., Colle, M. A., Pradier, L. and Duyckaerts, C. (2001) FE65 in Alzheimer's disease: neuronal distribution and association with neurofibrillary tangles. Am J Pathol **158**, 1585-1591

179. Apkarian, A. V., Sosa, Y., Sonty, S., Levy, R. M., Harden, R. N., Parrish, T. B. and Gitelman, D. R. (2004) Chronic back pain is associated with decreased prefrontal and thalamic gray matter density. J Neurosci **24**, 10410-10415

180. Wu, J., Su, G., Ma, L., Zhang, X., Lei, Y., Li, J., Lin, Q. and Fang, L. (2005) Protein kinases mediate increment of the phosphorylation of cyclic AMP-responsive element binding protein in spinal cord of rats following capsaicin injection. Mol Pain **1**, 26

181. Hoshi, M., Sato, M., Matsumoto, S., Noguchi, A., Yasutake, K., Yoshida, N. and Sato, K. (2003) Spherical aggregates of beta-amyloid (amylospheroid) show high neurotoxicity and activate tau protein kinase I/glycogen synthase kinase-3beta. Proc Natl Acad Sci U S A **100**, 6370-6375

182. Tomidokoro, Y., Ishiguro, K., Harigaya, Y., Matsubara, E., Ikeda, M., Park, J. M., Yasutake, K., Kawarabayashi, T., Okamoto, K. and Shoji, M. (2001)

Abeta amyloidosis induces the initial stage of tau accumulation in APP(Sw) mice. Neurosci Lett **299**, 169-172

183. Chen, G., Bower, K. A., Ma, C., Fang, S., Thiele, C. J. and Luo, J. (2004) Glycogen synthase kinase 3beta (GSK3beta) mediates 6-hydroxydopamine-induced neuronal death. Faseb J **18**, 1162-1164

184. Song, Y. S., Park, H. J., Kim, S. Y., Lee, S. H., Yoo, H. S., Lee, H. S., Lee, M. K., Oh, K. W., Kang, S. K., Lee, S. E. and Hong, J. T. (2004) Protective role of Bcl-2 on beta-amyloid-induced cell death of differentiated PC12 cells: reduction of NF-kappaB and p38 MAP kinase activation. Neurosci Res **49**, 69-80

185. Lu, D. C., Rabizadeh, S., Chandra, S., Shayya, R. F., Ellerby, L. M., Ye, X., Salvesen, G. S., Koo, E. H. and Bredesen, D. E. (2000) A second cytotoxic proteolytic peptide derived from amyloid beta-protein precursor. Nat Med **6**, 397-404

186. Cuello, A. C. (2005) Intracellular and extracellular Abeta, a tale of two neuropathologies. Brain Pathol **15**, 66-71

187. Schubert, D. and Behl, C. (1993) The expression of amyloid beta protein precursor protects nerve cells from beta-amyloid and glutamate toxicity and alters their interaction with the extracellular matrix. Brain Res **629**, 275-282

188. Marin, N., Romero, B., Bosch-Morell, F., Llansola, M., Felipo, V., Roma, J. and Romero, F. J. (2000) Beta-amyloid-induced activation of caspase-3 in

primary cultures of rat neurons. Mech Ageing Dev **119**, 63-67

189. Yamamoto-Sasaki, M., Ozawa, H., Saito, T., Rosler, M. and Riederer, P. (1999) Impaired phosphorylation of cyclic AMP response element binding protein in the hippocampus of dementia of the Alzheimer type. Brain Res **824**, 300-303

190. Bayatti, N., Zschocke, J. and Behl, C. (2003) Brain region-specific neuroprotective action and signaling of corticotropin-releasing hormone in primary neurons. Endocrinology **144**, 4051-4060

191. Salas, T. R., Reddy, S. A., Clifford, J. L., Davis, R. J., Kikuchi, A., Lippman, S. M. and Menter, D. G. (2003) Alleviating the suppression of glycogen synthase kinase-3beta by Akt leads to the phosphorylation of cAMP-response element-binding protein and its transactivation in intact cell nuclei. J Biol Chem **278**, 41338-41346

192. Yamada, T., Yoshiyama, Y. and Kawaguchi, N. (1997) Expression of activating transcription factor-2 (ATF-2), one of the cyclic AMP response element (CRE) binding proteins, in Alzheimer disease and non-neurological brain tissues. Brain Res **749**, 329-334

193. Masliah, E., Mallory, M., Alford, M., Tanaka, S. and Hansen, L. A. (1998) Caspase dependent DNA fragmentation might be associated with excitotoxicity in Alzheimer disease. J Neuropathol Exp Neurol **57**, 1041-1052

194. Mbebi, C., See, V., Mercken, L., Pradier, L., Muller, U. and Loeffler, J. P. (2002) Amyloid precursor protein family-induced neuronal death is mediated by impairment of the neuroprotective calcium/calmodulin protein kinase IV-dependent signaling pathway. J Biol Chem **277**, 20979-20990